EXPERIEMENTAL INVESTIGATION OF POOL BOILING AND BOILING UNDER SUBMERGED IMPINGING JET OF NANOFLUIDS

EXPERIEMENTAL INVESTIGATION OF POOL BOILING AND BOILING UNDER SUBMERGED IMPINGING JET OF NANOFLUIDS

By: Ahmed Abdelhady, B. Sc.

A Thesis

Submitted to the School of Graduate Studies

in Partial Fulfilment of the Requirements

for the Degree

Master of Applied Sciences

McMaster University

Hamilton, Ontario, Canada

MASTERS OF APPLIED SCIENCES (2013) McMaster University

(Mechanical Engineering) Hamilton, Ontario, Canada

TITLE: Experimental Investigation of Pool Boiling and Boiling under Submerged Impinging Jet of Nanofluids

AUTHOR: Ahmed Abdelhady, B.Sc. (Alexandria University)

SUPERVISOR: Dr. Mohamed S. Hamed

NUMBER OF PAGES: 131

Abstract

Heat transfer is an important parameter that defines the process performance in many industrial applications. Past research has been focused on pool boiling, flow boiling and until recently few studies have been conducted on jet impingement boiling of nanofluids.

For pool boiling, several parameters have been investigated such as nanofluid concentration, stability, particles sizes and the preparation method of nanofluids. The effect of surface initial conditions, low concentrations, nanoparticles material, nanoparticles sizes and deposition patterns have not been thoroughly investigated.

An experimental investigation has been carried out in order to investigate the effect of surface initial conditions, concentration, nanoparticles size and deposition pattern on pool boiling and jet impingement boiling of nanofluids. A flat copper surface with initial conditions of Ra = 420 nm, Ra = 80 nm and Ra = 20 nm has been used as the boiling surface. Al_2O_3 and CuO nanoparticles have been used with de-ionized water to prepare the nanofluids. At 0.01 vol. % concentration of Al_2O_3, the rate of heat transfer enhanced by 41% and 34% for the Ra = 80 nm and Ra = 20 nm, respectively. While, in the case of Ra = 420 nm, the rate of heat transfer deteriorated by 49%. At 0.005 vol. % concentration the rate of heat transfer deteriorated for all three surfaces. It is believed that the deterioration was due to the uniformity of the deposition. Using 0.01 vol. % concentration of CuO nanofluids resulted in the same trend, however, the rate of heat transfer is less

compared to using Al_2O_3 nanofluids. For example, in the case of Ra = 80 nm, the rate of heat transfer was reduced by 14%.

The effect of nanoparticles size has been investigated by changing the nanoparticles size from 50 nm to 10 nm. The change in nanoparticles size resulted in a significant deterioration in the rate of heat transfer for all three surfaces. It is believed that the deterioration was due to the deposition uniformity. As the deposition uniformity has been found to be a major factor that affects the rate of heat transfer, new approach was introduced to quantify the effect of the rate of deposition on the pool boiling of nanofluids.

An experimental investigation has been carried out in order to investigate using submerged impingement jet on the rate of heat transfer using nanofluids. At of 0.005 vol. % concentration of Al_2O_3, surface with Ra = 80 nm, jet to surface vertical distance of 3 mm and Reynolds number of 101311, the rate of heat transfer deteriorated by 19%.

Comparing the pool boiling and jet impingement boiling of nanofluids showed that, in the case of jet impingement boiling, the rate of heat transfer was enhanced compared to the case of pool boiling and the deposition was less. However, jet impingent boiling experiments showed deterioration in the rate of heat transfer by 19% compared with pure water.

Acknowledgement

I would like to express my deepest gratitude to my advisor, Dr. M.Hamed, who has supported me thoughout my Masters with his patience and knowledge whilst allowing me the room to work in my own way.

I would also loke to thank the department technichians for their advice and experties. Joe, Ron, Jim, Mark and Micheal,thanks for your help.

Finally, i am grateful to my family and all my friends for their support. I am so lucky to have you all. I would not habe made it without your support and encourgement.

Table of Contents

List of Figures

List of Tables

Nomenclature

SYMBOL	DESCRIPTION	UNITS
C_p	Specific heat	J/Kg ^oC
C_{sf}	Surface factor	-
d_p	Particle diameter	m
g	Gravitational acceleration	m/s^2
h	Heat transfer coefficient (HTC)	$W/m^2\ ^oC$
h_{lv}	Latent heat of vaporization	J/Kg
k	Thermal conductivity	W/m ^oC
L	Length	m
q"	Heat flux	W/m^2
Ra	Average surface-roughness	nm
R_q	Root mean square -roughness	nm
R_{sk}	Surface Skewness	-
SPIP	Surface particles interaction parameter	-
T	Temperature	^oC
x	Displacement	m
Z	Orthogonal position	nm
D	Nozzle diameter	mm
Re	Reynolds number	-
Nu	Nusselt number	-
Pr	Prandtl number	-
Φm	Volumetric concentration	%
Φv	Mass concentration	%

Greek Symbols

μ	Viscosity	Ns/m^2
ρ_l	Liquid density	Kg/m^3
ρ_v	Vapour density	Kg/m^3
σ	Surface tension	N/m
Y	The sphericity	-
α	Thermal diffusivity	m^2/s
ε	Surface Roughness	m

Subscripts

L	Liquid
v	Vapour
nf	Nanofluid
p	Particle
w	Water
s	Surface
sat	Saturation
n	Nozzle
bf	Base fluids

Chapter 1
Introduction

Heat transfer is an important parameter that defines the process performance in many industrial applications such metal processing, power generation and electronics cooling. Advances in many current and new technologies depend on the ability to dissipate large quantities of heat from relatively small surface areas such as microchips. The trend for current technology application is leading towards increasing heat fluxes and lowering surface temperature. For this reason boiling and convection heat transfer phenomena have been investigated for many decades and continue to be investigated to be utilized in the most efficient way.

One of the aspects that still under study is using nanometer size particles – referred to as nanoparticles- to enhance the heat transfer performance. Nanofluids have the potential to be the possible next generation of working heat transfer fluids due to their superior enhanced thermal conductivity. For the last decade; research concerned with nanofluids applicability and effects on different heat transfer applications has significantly increased. Figure 1.1 shows the rate of increase in nanofluids related publications over the past decade.

Past research has been focused on pool boiling, flow boiling and until recently few studies have been conducted on jet impingement boiling of nanofluids. Pool boiling is the process in which the heating surface is submerged in a large body of stagnant liquid.

Flow boiling is boiling of a liquid whose flow over a heater surface is imposed by external means. Jet impingement boiling refers to a condition where a single-phase liquid jet impinges on a heated surface and liquid undergoes phase change on the surface.

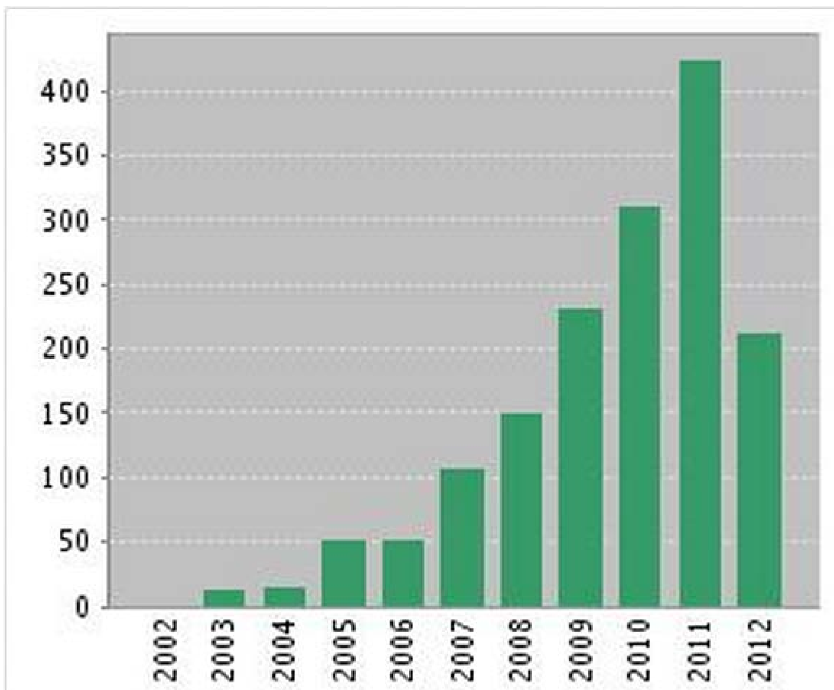

Figure 1.1 Web of Knowledge record of nanofluids related publications

Chapter 2
Literature Review

This chapter presents a review of the previous research that has been carried on pool boiling. The regimes of pool boiling and synthesis of nanofluids are briefly explained in section 2.1 and section 2.2, respectively. Section 2.3 includes a discussion of the parameters affecting pool boiling of nanofluids. Studies investigating pool boiling of nanofluids are then presented in section 2.4. Section 2.5 presents a summary of the main findings in the literature. The research objectives and plan of the present study is discussed in section 2.6 and a description of the thesis structure will conclude this chapter in section 2.7.

2.1. Pool Boiling

Pool boiling is the process in which the heating surface is submerged in a large body of stagnant liquid. The relative motion of the vapor produced and the surrounding liquid near the heated surface is due primarily to the buoyancy effect of the produced vapor. Nevertheless, the body of the liquid as a whole is essentially at rest.

Figure 2.1 shows the classical pool boiling curve as a plot of the heat flux, q", versus the degree of surface superheat, ($\Delta T = T_w - T_{sat}$). As the value of the degree of surface superheat increases, the curve goes through four different regimes: (I) natural or free convection, (II) nucleate boiling, (III) transition boiling, and (IV) film boiling.

Region (I) is called the natural convection regime. Where the degree of surface superheat is less than 5 °C, no bubbles form and heat is transferred from the solid surface to the bulk liquid via natural convection.

When the degree of surface superheat exceeds 5 °C, the system enters the nucleate boiling regime, where vapor bubbles are generated at certain locations on the heater surface called nucleation sites. Nucleation sites are microscopic cavities or cracks on the solid surface. Small cavities and surface cracks act as sites for bubble generation for two reasons: The first reason is the contact area between the liquid and heating surface increases, so liquid trapped in these areas vaporizes first; and the second reason is that as trapped gases in such cracks creates liquid-vapor interfaces, which serve as sites where the transfer of energy in the form of latent heat from the liquid to the vapor phase takes place. Once a vapor bubble has been initiated at a nucleation site, the bubble grows to a certain diameter, and rapidly detaches from the heating surface, and rises to the liquid free surface.

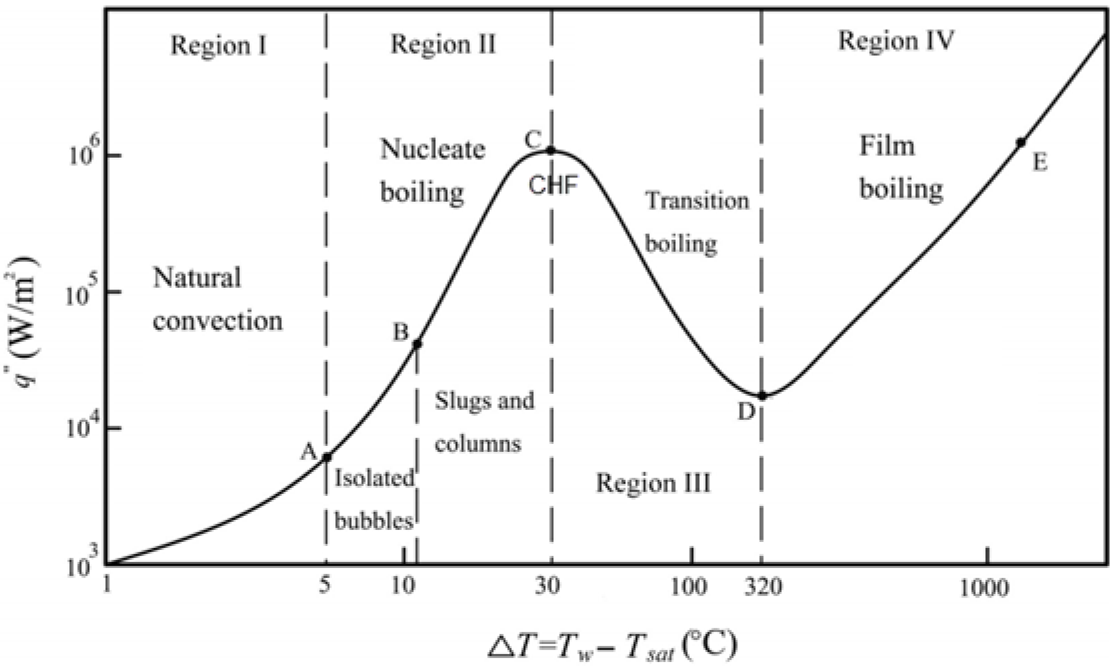

Figure 2.1: Pool boiling curve of saturated water [www.thermalfluidscentral.org]

When the degree of surface superheat remains at the low end of the nucleate boiling region, shown between points A and B of Figure 2.1, each bubble generated can grow and detach from the surface independently. As the degree of surface superheat increases beyond point B in Figure 2.1, additional nucleation sites become active and more bubbles are generated. The higher density of bubbles leads to their interaction with each other. Bubbles from different sites now merge to form columns and slugs of vapor, thus decreasing the overall contact area between the heating surface and the saturated liquid. The heat flux increases with superheat temperature to reach the critical heat flux (CHF), point C. The critical heat flux, which marks the upper limit of the nucleate boiling regime, reaches a value of approximately 10^6 W/m^2 for water at a superheat temperature of about ΔT_c = 30 °C.

Up on reaching the CHF, the surface is mostly covered by vapour and this reduces the contact between the surface and the liquid. Increasing the superheat temperature beyond point C, leads to a severe reduction in the heat transfer as more regions of the surface are covered by vapour. This region of the boiling curve between points C and D is called transition boiling.

So, as can be seen from Figure 2.1 the nucleate boiling regime is the most favorable operating regime for any heat transfer application. This is due to the high heat transfer rate that can be achieved in this regime.

2.2. Nanofluids

A nanofluid is a suspension of nanometer-sized particles, called nanoparticles in a base fluid. The nanoparticles used in nanofluids are typically made of metals or metal oxides. Common base fluids include water, ethylene glycol and oil.

Nanofluids are potentially useful in many heat transfer applications because of their enhanced thermal conductivity and convective heat transfer rate compared to the base fluid. However, nanoparticles have a high tendency to agglomerate together. There are several ways to break down these agglomerates. Common ways of breaking up the agglomerates are ultrasonic vibration and high speed homogenizers.

2.3. Parameters Affecting Pool Boiling of Nanofluids

There are many parameters that affect the heat transfer rate in pool boiling of nanofluids. There are some parameters that are related to the heated surface [1]; and other parameters that are related to the nanofluid itself [2].

Parameters that are related to the heated surface are its initial surface condition represented by the average surface roughness (Ra), material, geometry, and orientation (i.e. horizontal, inclined or vertical), [3].

Surface roughness is a major factor affecting heat transfer in pool boiling. Rougher surfaces tend to have higher heat transfer rate as they tend to have more cavities, which act as nucleation sites, and therefore higher heat fluxes can be reached for the same surface degree superheat, [4]. Surface material is another factor that affects the wettability of the surface which in turn affects the rate of heat transfer in pool boiling. Wettability, affects different behaviour of the bubbles deposition patterns [5].

Surface geometry could affect the pool boiling rate of heat transfer as it affects bubble dynamics and nanoparticles deposition on the surface. In the case of using tubes as a boiling surface, the bubble growth and departure mechanism is most likely associated with bubble sliding , while in the case of flat surfaces, bubbles tend to grow and depart the surface; sliding is not likely to occur.

Surface orientation is another important factor that could affect the rate of heat transfer. The surface could be horizontal, inclined or vertical. The bubble sliding mechanism is the main difference between different orientations. Bubble sliding is more likely to occur for an inclined and vertical surface than for horizontal surfaces. The different mechanisms affect the time when the bubbles are in contact with the surface which affects the heat transfer rate.

As mentioned previously, there are other parameters affecting the pool boiling rate of heat transfer which are related to the fluid. The type of base fluid is a major parameter to be considered as different fluids have different thermal properties and will have different contact angles with the surface which represents the wettability, [1].

Regarding the nanoparticle material will play a role as nanoparticles could be made of different materials, which in turn have different properties which will affect the nanofluid properties such as thermal conductivity. Nanoparticle materials that have high density are more likely to be less stable which would result in a higher deposition rate.

Also, the nanoparticle concentration affects the nanofluid properties. The deposition rate depends also on the nanofluids stability. Previous research has shown that lowering nanofluids pH level enhances its stability and hence reduces the deposition rate on the heated surface, [6] [7].

Finally, the duration of the boiling experiments was found to have an effect on the rate of deposition and hence the rate of heat transfers of pool boiling of nanofluids, [8] .

2.4. Investigations Carried out on Pool Boiling of Various Liquids and Nanofluids

Rohsenow [9] was the first to introduce the effect of surface condition/fluid combination on pool boiling of water. His correlation for the nucleate boiling heat flux of water is one of the most widely used correlations. He introduced the surface/fluid effect through an empirical constant which depends on the surface material, finish and the type of fluid in contact.

Berenson [10] performed experiments to study the surface finish effect on pool boiling heat transfer using copper and pentane. The heated surface was a flat horizontal surface made of Ni; Cu and Inconel. The surface roughness value was not reported. However, it was mentioned that the surface finish was mirror finish and emery polished in one direction using emery paper with different grit numbers (i.e. 60,120,160,320) .His conclusion indicated that the rougher surface gave a higher heat transfer coefficient, at lower wall superheat, as the active cavity size was bigger on the rougher surface regardless the surface material.

Chowdhury et al [11] performed experiments to examine the effect of surface roughness and contact angle on pool boiling heat transfer on cylindrical surfaces. The cylindrical surface was 18 mm diameter and 40 mm long. Two surfaces made of copper and aluminum was used in this study. The aluminum cylinder had surface roughness value ranged between 1.2 -5 µm, while the copper cylinder had surface roughness value ranged between

0.25-4.75 μm .Heated surfaces were immersed into deionized water or methanol. They concluded that the nucleate boiling heat transfer rate increases with surface roughness. Also, they concluded that surface material and surface roughness affected the wettability. Surfaces with low contact angle had higher heat flux values at the same superheat.

Myeong [12] carried out an experimental study to investigate the effect of surface roughness on pool boiling heat transfer using water at atmospheric pressure with different orientations of the heater. Two stainless steel tubes with average surface roughness of 60 and 15 nm were used as heated surface. Three different tube lengths (100,300 and 530 mm) and three different orientations of the tubes (horizontal: $\theta = 0^{o}$, inclined: $\theta = 45^{o}$, and vertical: $\theta = 90^{o}$).The experimental results showed that increased surface roughness enhances the heat transfer. An enhancement up to 71% in the heat transfer rate was reported for horizontal orientation when the surface roughness increased from 15 to 60 nm and tube diameter 19 mm. For vertical orientation under the same conditions an enhancement up to 230% in the heat transfer rate was reported. Also ,they concluded that the effect of surface roughness is magnified as the orientation of the heater changes from horizontal to vertical and its effect increases with the increase in the heater length to its diameter ratio,($H = \frac{L}{D}$).

Bang and Chang [13] investigated the heat transfer performance in pool boiling of Al_2O_3–water nanofluids over a flat surface. The heated surface was a rectangular block. They reported that the heater surface roughness was smaller than the particle size (few tenth of nm). Alumina particles with 47 nm nominal size were used with two different volume concentrations, 0.5% and 4%. A highly smooth flat surface was used as the heating surface. Deterioration in the heat transfer coefficient was observed with nanoparticles compared to pure water. Nucleate boiling occurred at a higher surface superheat in the case of nanofluids. . Both horizontal and vertical orientations were used to investigate the effect of using nanofluids on the critical heat flux (CHF). Using nanofluids resulted in enhancement in the CHF, 32% increase in the CHF was reported for horizontal surface and 13% for the vertical surface. They concluded that, the use of nanofluids changed surface characteristics which caused the observed changes in the rate of heat transfer. On the other hand, changes in liquid properties had insignificant effect on the rate of heat transfer.

Narayan et al [14] carried out an experimental investigation of the mechanism of enhancement / deterioration of the pool boiling of nanofluids over vertical tubes. They used two different sizes of aluminum oxide nanoparticles, 150 nm and 47 nm diameter. They prepared three different surfaces with an average surface roughness of 48 nm, 98 nm and 524 nm. They observed both enhancement and deterioration in boiling heat transfer using electro-stabilized nanofluids and introduced a parameter called surface particle interaction parameter (SPIP) , which is the ratio of the average surface roughness to the average particle diameter. Depending on the SPIP value there can be an enhancement in the rate of heat transfer due to the multiplication of nucleation sites or deterioration due to the reduction in number of nucleation sites. They reported that the maximum deterioration in pool boiling performance occurred when the SPIP value is near unity.

Das et al [15] investigated the effect of particle size relative to surface roughness and particles concentration on pool boiling of nanofluids. They used Al_2O_3 –water nanofluids (20-50 nm) on a cylindrical stainless steel cartridge heater of 20 mm diameter and surface roughness of 0.38-1.12µm.They conducted their experiments using particle concentrations range of 0.3-16 wt. %. They reported both enhancement and deterioration in the rate of heat transfer. They observed that deterioration in the heat transfer coefficient was mainly at higher particles concentration (4-16 % wt.) and enhancement in the rate of heat transfer was observed at lower particles concentration (0.32-1.25 % wt.). Considering the fact that the particles size is one to two orders of magnitude smaller than the surface roughness , they concluded that the higher the concentration the greater the rate of deposition and hence the boiling heat transfer deteriorated , which supports the theory of SPIP that was introduced by [14].

Hassan et al [4]investigated the effect of surface conditions on pool boiling of nanofluids on a horizontal flat surface. They used Al_2O_3 nanoparticles with an average diameter of 50 nm. Only one volume concentration of 0.1% was examined in this study. The heated surface was copper flat surface with average surface roughness of 20, 80 and 425 nm.

It was found that for both pure water and alumina-water nanofluids, the rougher the surface, the higher the heat flux obtained at the same surface superheat. However, they reported deterioration in the heat flux for the nanofluids experiments. It was observed that regardless of the SPIP value in this study, there was only deterioration in the rate of the heat transfer which indicates that the SPIP parameter has minor effect in the case of flat surface.

Osama and Hamed [6]investigated the effect of particle deposition on pool boiling of nanofluids on a horizontal flat copper surface. They used aluminum oxide nanoparticles with a diameter of 40-50nm. Three different concentrations were used in this study, 0.01 vol. %, 0.1 vol. % and 0.5 vol. %. It was reported that the higher nanoparticle concentration the more the deterioration in the heat transfer. For the case of 0.5 vol. % and average surface roughness range of 50-150 nm, they reported a deterioration of 45% at 15^{o}C superheat.

Osama and Hamed [8] investigated the effect of the nanofluid preparation method and the pH level on the pool boiling of nanofluids. Alumina oxide nanoparticles with an average particle diameter of 45 nm were used to prepare the nanofluids. In order to investigate the effect of the preparation method they prepared their nanofluids from dry particles and ready-made suspensions. The heating surface was a horizontal flat surface with an average surface roughness in the range of 100-150 nm. The effect of the pH value was investigated using acidic and neutral nanofluids. They concluded that the preparation method has no effect on the pool boiling of nanofluids. It was also noticed that by adding acid to the base fluid an enhancement in the pool boiling heat transfer coefficient was observed. Also, the deposition rate was reduced in the case of the acidic nanofluids compared to the neutral nanofluids.

Harish et al [16] investigated the effect of surface particle interactions during pool boiling of nanofluids. They used electro stabilized Al_2O_3 water nanofluids, less than 50 nm particle diameter. The heated surface was an aluminum disk having a central boiling region with an area of 314 mm^2. Two surface roughness values, 308 nm and 53 nm were used in this study. They observed heat transfer deterioration in the case of the smooth heater, which increased by increasing the concentration of nanoparticles. A deterioration of approximately 20%, 26% and 30% was observed at volume concentration of 0.5%, 1% and 2% respectively. They also reported enhancement in the rate of heat transfer in the case of the rougher heater. An enhancement of 121%, 94% and 61% was observed at volume concentration of 2%, 1% and 0.5% respectively.

The roughness of the heater surface after boiling was altered due to the nanoparticle deposition on the surface of the heater, so the SPIP is essentially the main reason for the enhancement in the heat transfer performance in the case of rough surface.

Vassallo et al [17] used Silica nanoparticles to investigate the pool boiling phenomena. The heating surface was a 0.4 mm Ni-Cr wire horizontally suspended in a Pyrex dish. Three different particles sizes were used in their experiments 15 nm, 50 nm and 3 µm, at a constant 0.5 % volume concentration. They reported a higher heat flux the

50nm particles than for the 15nm particles. Silica coating of 0.15-0.2 mm found on the wire after the experiments carried out using the 15 and 50 nm particles. The 3µm particles settled out at the bottom of the tray. A 0.05-0.25 mm coating was observed on the wire after the experiments with the 3µm particles. They concluded that, the rougher wire showed higher heat flux for nucleate boiling as well as a higher CHF. Also, in the case of using 50nm silica solutions a heat flux 3 times that of water was reported, and twice in the case of the 3µm silica solution. As the surface roughness values were not reported, the effect of SPIP can't be quantified for this study.

Yong et al [5] investigated the effect of surface wettability on the rate of heat transfer in pool boiling. They used Tri-sodium Phosphate (TSP) surfactant solutions with Alumina nanofluids having average particle size of 47 nm. Different concentrations were used. In case of TSP, they used 0.01%-0.8% mass concentration while in the case of Alumina nanofluids, the concentrations used were 0.5% – 4% volume concentration. Stainless steel strips (30 x 30 x 3mm) were heated to 400°C by an alcohol lamp and quenched in the prepared solutions and water. Samples were removed before complete quenching at surface temperature of about 150°C, where boiling was still in the nucleate boiling regime. Surface contact angles were measured and interpreted as a factor of surface wettability. They found out that contact angles on a surface quenched in pure water in the range of 5°-25°, which were much smaller than those measured on the unquenched surface 65°-70°. Contact angles on surfaces quenched in TSP solutions and nanofluids were the smallest 5°-15°. They also calculated the CHF based on a theoretical model that considered the surface orientation and the contact angle. They concluded that the CHF enhancement was due to the increased wettability of the surface due to the deposition of nanoparticles and TSP on the surface. They also reported that the deposition of nanoparticles on the surface increased with increasing concentrations.

Wen and Ding [18] carried out an experimental investigation of nanoparticles concentration on the pool boiling of nanofluids. Alumina oxide nanoparticles with an average diameter range of 10-50 nm were used with de-ionized water as the base fluid. Two different concentrations were mentioned in this study; 0.32 % and 1.25 % by weight. The nanofluid pH value was about 7. The heated surface was a 3 mm thick polished stainless steel disc with 150 mm diameter. It was mentioned that the heated surface average surface roughness was of micron-scale size.

They concluded that boiling heat transfer coefficient increased along with increasing the concentrations of the nanofluids 40% enhancement in heat transfer obtained with 1.25 wt. % concentration .The effect of thermal conductivity seems to be the key factor in enhancing the heat transfer, and nanoparticle migration may also be playing a role in the enhancement as indicated in a convection study on nanofluids by the same authors.

Das et al [19] investigated the effect of using Al_2O_3 nanofluids on the rate of heat of pool boiling on horizontal narrow tubes. Tubes of 4 , 6.5 and 20 mm in diameter were used as the heater surfaces Surface roughness of the heaters was between 0.37 – 0.45 μm. Three concentrations were investigated 1%, 2% and 4% by volume. The particle average size was 58 nm. They concluded that the boiling heat transfer of nanofluids is less than that for pure water and the heat transfer was deteriorated with increasing concentration of the nanofluids. They also reported that due to the fact that the tubes have relatively small radii of curvature, large bubbles were directly departure from the surface. However, small bubbles were slide to relatively small distances.

Sang et al [20] investigated the effect of low concentration on the pool boiling heat transfer rate. Three different types of nanoparticles were used in this study, Alumina Oxide (139 nm), Copper oxide (143 nm) and diamond (86 nm). The concentration range was between 0.27 % -0.00027 % by volume. The heated surface was a copper block. The surface roughness value was not specified in this paper. The pH level of the nanofluids used was 6.35. When checking the thermal properties of the nanofluids, no change in surface tension, viscosity or thermal conductivity was found with respect to water. CHF matches that predicted by Zuber's correlation [21]. They concluded that CHF increases with nanoparticle concentration; the pool boiling heat transfer coefficient was almost the same for concentrations below 0.0007 vol. %. For concentrations above 0.0007 vol. %, deterioration in the pool boiling heat transfer coefficient and the CHF was observed. Deterioration in boiling performance was attributed to a layer of particle deposited on the surface, whereas the CHF enhancement was attributed to the enhanced wettability of the surface, regardless of the thickness of the nanoparticle layer. It was confirmed that boiling was the mechanism responsible for the nanoparticle deposition. An experiment was conducted in which a single nucleation site was activated and left active for a while, and a clear nanoparticle deposition pattern was observed at this location. As the surface roughness values were not reported, the effect of SPIP can't be quantified for this study.

Robert et al [22] carried out an experimental study using the hot wire method to investigate the effect of using nanofluids on the boiling incipience and the rate of heat transfer of pool boiling .A 20 nm Alumina oxide nanoparticle were used. The heated surface was a Ni-Cr wire with 0.255 mm diameter and 5 cm length. They observed that compared to pure water experiment, boiling incipience occurred 2 – 3 °C earlier for nanofluids. An enhancement in the pool boiling heat transfer coefficient of 25-40% was recorded at concentrations between 0.5 and 1 % by volume. Increasing the concentration, resulted in a deterioration in the pool boiling heat transfer coefficient. They also noticed that the nanoparticle coating of the wire crumbled off when the wire was dry indicating that the deposition was weak.

Sven et al [23] reviewed the available work concerning pool boiling of nanofluids. Two main effects of adding nanoparticles to a base liquid were concluded by all research groups. The first effect was a change in thermo-physical properties of the base liquid and the second was the deposition of particles on the heated surface. Some research groups reported a significant increase in the pool boiling heat transfer coefficient using carbon nanotubes (CNTS) with water and halogenated refrigerants. Viscosity was reported to increase with increasing concentrations of the CNTS and nanoparticles. Specific heat capacity was not regarded important in nanofluids boiling studies as its variation at low concentrations was negligible. The cause of the enhanced wettability is not clear. It might be the deposition of nanoparticles on the surface. Enhanced thermal conductivity seems to be the most significant effect of nanoparticles on the base fluid thermo-physical properties.

Osama [24] carried out an experimental study to investigate the effect of a group of parameters to explain the reported contradictions in the rate of heat transfer in pool boiling of nanofluids. He investigated the effect of the pH value, nanofluids preparation method and duration of the boiling experiment. Osama used a copper flat surface with an average surface roughness of 50-150 nm as a heated surface. Alumina-water nanofluid with 0.01, 0.1 and 0.5 % by volume were used. The average particle size was 50nm. Nanofluids prepared from dry particles and ready-made suspensions have been used, and pH values of 6.5 and 5.

He found out that making the nanofluid more acidic by reducing its pH level had positive effects on the pool boiling of nanofluids. By reducing the pH level, the nanoparticles became more stable, which helped reducing the deposition rate. Also, reducing the pH level had an effect on surface tension of the base fluid, which causes a reduction in the heat transfer rate. In general, more stable nanofluids had higher pool boiling heat transfer coefficient.

Considering two different methods to prepare the nanofluids, Osama prepared his nanofluids from a ready-made suspensions and dry particles. He concluded that this parameter is not a critical parameter to be considered to explain the reported contradictions in the literature review.

Regarding the concentration effect, he concluded that higher concentration showed more deterioration in the rate of heat transfer. The maximum recorded deterioration in the heat transfer coefficient was 45% in the case of 0.5% concentration.

The final parameter that was considered by Osama [24] is the effect of the experiment duration; he found out that the heating surface usually needs 1-2 minutes to reach steady state. However, he performed experiments by leaving the surface exposed to steady-state conditions for 15 minutes. He showed that the duration of the experiment has an effect on the deposition rate that occurred on the heating surface. Osama introduced a transient surface coefficient in to the Rohsenow equation to accommodate the change in the surface conditions during the experiment. Finally, he concluded from his study that the contradictions found among the researchers; as some studies showed enhancement and others showed deterioration in the rate of heat transfer of pool boiling of nanofluids are due to differences in the experimental setups.

Suriyawong et al [25] investigated the effect of using nanofluids at low concentrations on the heat transfer rate in pool boiling of nanofluids. They used TiO_2 –water nanofluids with average particle diameter of 21nm. They investigated five different concentration levels of 0.00005 vol. %, 0.0001 vol. %, 0.0005 vol. %, 0.005 vol. %, and 0.01 vol. %. Two horizontal circular plates made from copper and aluminum with surface roughness values of 0.2μm and 4μm were used. They concluded that for copper surface at a0.0001% concentration, 15% increase in the heat transfer coefficient was obtained for the surface roughness of 0.2 μm and a 4% increase is obtained for roughness of 4 μm. For higher concentrations, the heat transfer rate was deteriorated. For aluminum heated surface, the corresponding heat transfer coefficients are higher compared to copper surface by around 30% with a roughness of 0.2 μm and around 27% with a roughness of 4 μm.

They proposed a modified correlation for nucleate boiling heat transfer of nanofluids. Their correlation is based on the Rohsenow's correlation, given here in equation (2.1).

$$Nu_{nf} = a\left(Pr_{nf}\right)^{b} \left(\frac{q''\,\varepsilon}{\mu_{nf}\,h_{fg}}\right)^{c} \left(\frac{\varepsilon^2 g\,(\rho_{nf}-\rho_v)}{\sigma}\right)^{d} \left(\frac{L_c}{\varepsilon\,(\emptyset+m)^{e}}\right) \qquad (2.1)$$

$$Nu_{nf} = \frac{h_{b,nf}\,L_c}{K_{nf}} \qquad Pr_{nf} = \frac{\mu_{nf}\,C_{p,nf}}{K_{nf}} \qquad L_c = \frac{A}{P}$$

Where, Lc is a characteristic length scale, and a, b, c, d, e, and m are the correlation coefficients given in Table 2.1

Table 2.1 Coefficients of the correlation proposed by [26]

Coefficient for copper surface						Coefficient for aluminum surface					
a	b	c	d	e	m	a	b	c	d	e	m
28.85	0.59	0.70	0.16	0.12	0.001	46.63	0.55	0.74	0.15	0.05	0.00001

Table 2.2 Thermo-physical property models of nanofluids

Investigator	Correlation	Remarks
Pak and Cho [26]	$\rho_{nf} = \emptyset\rho_{np} + (1-\emptyset)\rho_{bf}$	For Al_2O_3 and TiO_2 water nanofluids.
Pak and Cho [26]	$C_{p,nf} = \emptyset c_{np} + (1-\emptyset)c_{p,bf}$	For Al_2O_3 and TiO_2 water nanofluids.
Wang et al [2]	$\mu_{nf} = (1 + 7.3\emptyset + 123\emptyset^2)\mu_{bf}$	For Al_2O_3 water nanofluids, volume fractions less than 6 %.
Hamilton and Crosser [27]	$k_{nf} = \left(\frac{k_{np} + (n-1)k_{bf} - (n-1)\emptyset(k_{bf}-k_{np})}{k_{np} + (n-1)k_{bf} + \emptyset(k_{bf}-k_{np})}\right)$	Empirical shape factor (n=3/ψ) where ψ the sphericity, defined as the ratio of the surface area of a sphere per surface area of the particle. For spherical particles ψ=1

As can be noticed , contradicting trends have been reported in the literature .In this study we will carry out further investigation in the pool boiling of nanofluids to better understand the effect of heated surface initial conditions, nanoparticles concentration, nanoparticles size, electrostatic stability and nanoparticles type on the heat transfer performance and the nanoparticles deposition. Also we will look at using nanofluids with submerged impingement jet and how it would affect the heat transfer and the nanoparticles deposition pattern on the heated surface.

2.5. Summary

Reading through the literature review, it is clearly noticed that there are contradictions in the reported findings. Some research groups reported deterioration in the heat transfer with the use of nanofluids [4, 6, 13 and 19], while others found enhancement [8, 16, 17 and 18]. Few research groups reported both enhancement and deterioration in the same study [14, 15, 20, 22, 24, and 25] .Also, it worth noting that some researchers reported that nanofluids concentration has a positive effect on the enhancement of the rate of heat transfer of pool boiling of nanofluids, while others found the opposite. Although, many different experimental techniques have been used among the research groups, they indicated that the enhancement or deterioration of the heat transfer of pool boiling of nanofluids can be attributed to the following reasons:

- Improving the nanofluid stability, which prevents excessive particles deposition on the heater surface
- Increasing or decreasing the number of active nucleation sites, depending on the ratio between the particle size and the void size.
- Enhanced thermal conductivity of the nanofluids due to the addition of the nanoparticles to the base fluid.
- Creating a thermal insulation layer due to the position of the nanoparticles on the heater surface.

2.6. Research Objectives

The objective of this research is to investigate different parameters in order to obtain more explanations of the contrary findings in the literature, and to gain a better understanding of the heat transfer phenomena of pool boiling of nanofluids. The research team at the McMaster's Thermal Processing Lab (TPL) has investigated many parameters that affect the pool boiling of nanofluids during the last few years; this study aims to continue expanding the research scope. Previously, the TPL team investigated the effect of nanofluids stability, preparation method, experiment duration and finally nanofluid concentration. The main parameter that has been considered in this study is the effect of the initial surface condition on the heat transfer phenomena of pool boiling of nanofluids. Nanofluids concentration has been a major parameter that has been considered in the majority of the nanofluids research. However, the focus in this study is on low concentrations in the range of 0.005 – 0.01 % by volume. Different nanoparticle materials have different heat transfer behavior, as its thermal conductivity changes. In order to evaluate the effect of nanoparticle materials, two nanoparticle materials have been used in this study, namely Al_2O_3 and CuO. Some researchers [14] attributed the change in the pool boiling heat transfer coefficient to the SPIP. In order to investigate the validity of the proposed SPIP criteria, two particles sizes for Al_2O_3 with 10 and 50 nm diameter have been considered in this study. Finally, the effect of using submerged impingement jet on the boiling phenomena using nanofluids has been investigated in this study.

2.7. Thesis Structure

Chapter 3 contains the details of the experimental facility, methodology and the experimental procedure; as well as validation of the experimental setup using the Rohsenow's correlation. Chapter 4 presents all experimental results. Chapter 5 includes results of the jet impingement boiling experiments. The conclusions and recommendations for future work are presented in Chapter 6.

Chapter 3
Experimental Setup and Methodology

In this chapter the experimental setup and methodology that was used during the present experimental investigation of the pool boiling of nanofluids will be illustrate. The details and specification of the hardware are provided in detail in section 3.1. The surface and nanofluids preparation is discussed in sections 3.2. and 3.3. followed by a detailed discussion of the experimental and post experiment procedures in sections 3.4. and 3.5. Section 3.6. presents the calculations of the heat flux (q”) and the surface temperature (T_s). Section 3.13. represents the uncertainty in the experimental results followed by the validation procedure of the experimental setup in section 3.8.

3.1. The Experimental Setup

The boiling vessel used in this study is shown in Figure 3.1. The main body of the vessel is a 20 cm diameter made of stainless steel. A stainless steel skirt is fixed to support the liquid within the pipe. A 25.4 mm diameter and 71 mm length copper block is installed at the center of the skirt to serve as the boiling surface. Three $1/_4$ inch diameter and $1 1/_2$ inch length cartridge heaters are fixed inside the bottom of the copper block to provide the heat flux to the liquid, referred to as the Main Heaters .The maximum power of the main heaters is 750 W which is capable of providing a maximum heat flux of 1480 kW/m^2.

Three 1.0 mm diameter type-E thermocouples are installed in the copper block at different axial distances from the top of the block to determine the axial temperature profile of the copper block. The locations of the thermocouples in the copper block are shown in Figure 3.2.

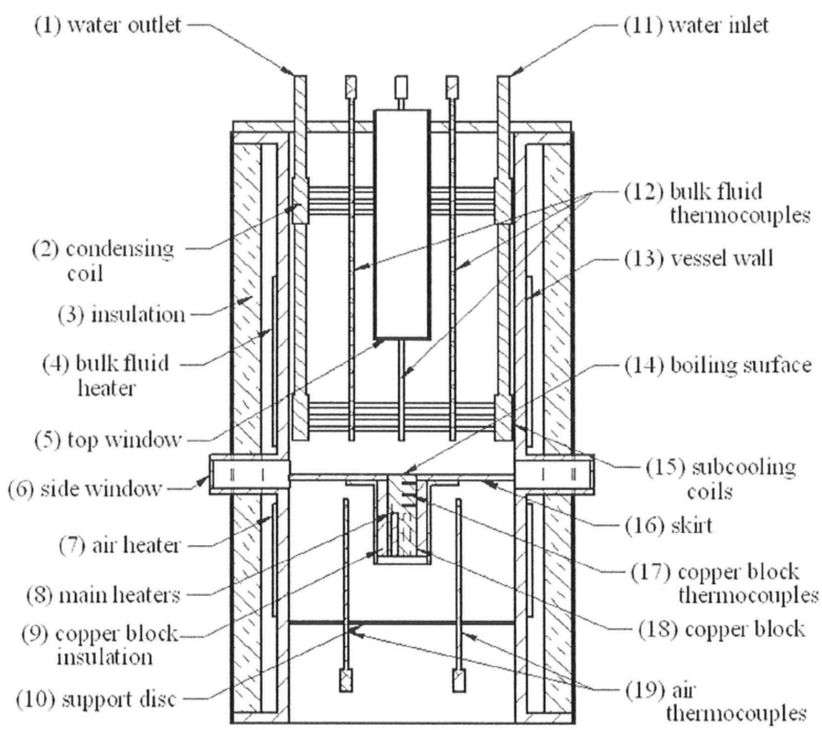

Figure 3.1 Experimental setup schematic [24]

The copper block is surrounded by insulation in order to reduce the radial heat losses which mean that we are dealing with unidirectional heat transfer. Also a heater referred to as Air Heater is installed around the vessel wall below the skirt to heat up the air surrounded the copper block and to maintain the air temperature around the copper block as close as possible to that of the copper block to reduce radial heat losses from the copper block and to prevent liquid sub-cooling. To heat up the liquid to saturation temperature, two heaters, referred to as Bulk Fluid Heater with total power of 3000W are installed around the vessel wall.

Two 3.2 mm diameter type-E thermocouples were immersed in the bulk fluid to record its temperature. A condensing coil is used to minimize the loss of liquid level during the experiment. This important feature helped maintain a constant concentration throughout the experiment time when boiling nanofluids. The water flow rate through the condensing coil is regulated through a needle valve. The inlet condensing water is too cold during the winter season, and causes some liquid sub-cooling during the experiment because the condensed droplets are too cold. A heater is installed in the inlet condensing water pipe to heat up the inlet condensing water and prevent this sub-cooling from taking place.

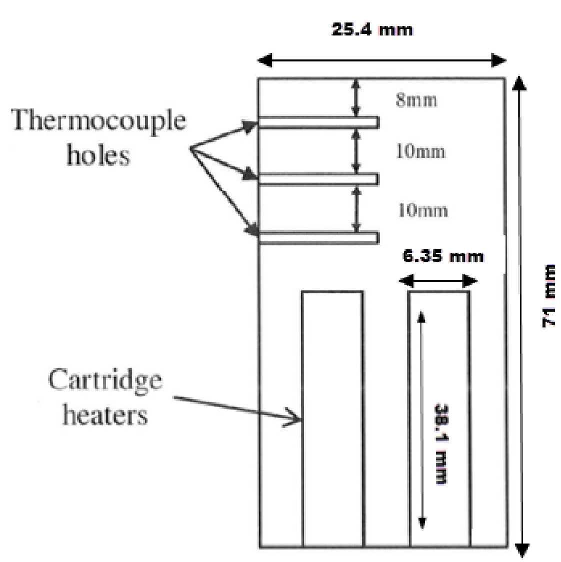

Figure 3.2 Locations of the thermocouples placed in the copper blocks

A thermocouple is installed to monitor the temperature of the inlet condensing water, as well as a flow meter to measure its flow rate. A sub-cooling coil is used to lower the liquid temperature before it was drained out of the vessel. Two opposing glass side windows allow visual observation of the boiling phenomenon on the surface from the side. The whole vessel is wrapped with an aluminum cover to protect the user from contacting the heaters. Insulation is attached between the cover and the vessel to reduce heat losses from the vessel.

3.1.1. The Data Acquisition System

A Kiethley data acquisition system Model 2700 was used to collect the thermocouples readings. The data acquisition was connected to a computer. ExceLinx software was installed into Microsoft Excel to record the temperatures from the thermocouples. The temperatures were scanned every 5 seconds. As mentioned before, nine thermocouples were used to record the following temperatures:

- The copper block temperature in three different axial locations
- The bulk liquid temperature at two different locations
- The air heater
- The water heater
- The air around the copper block
- The inlet temperature of the condensing water

3.1.2. Determination of Average Surface Roughness

The average surface roughness of the copper block was examined using a Zygo White Light Interferometer. The interferometer was used with MetroPro 8.15 software to scan an area of 1.09 x 1.45 mm of the surface and to capture the image of the surface. The software generated a 3D image of the surface and determined the average surface roughness (Ra) of the scanned area. Figure 3.3 shows the 3D image of the scanned surface under the interferometer. The average surface roughness of the scanned area is evaluated in both the x and y directions.

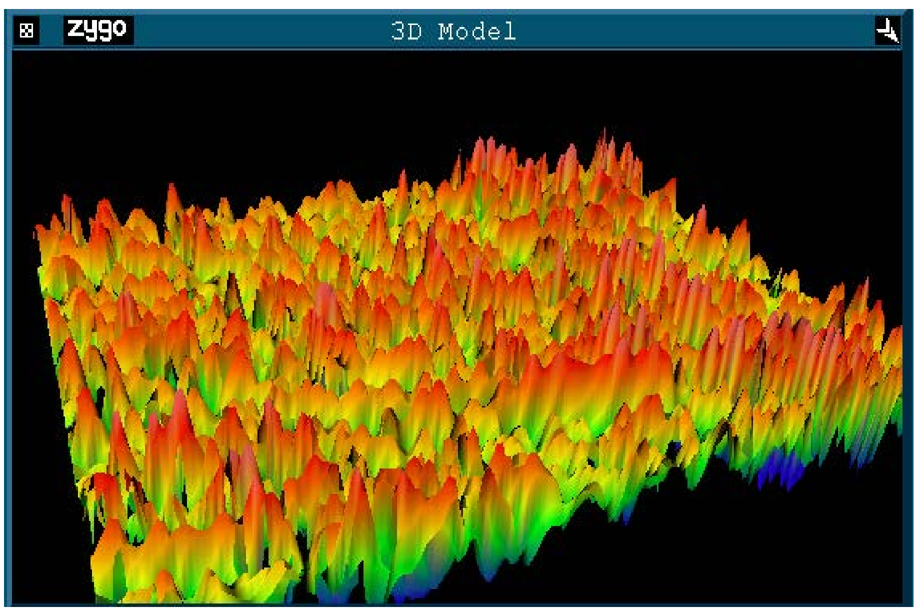

Figure 3.3 Heater Surface 3D Image

The average surface roughness (Ra) was not the only parameter returned by the software. The software also returned the values for the root mean square (Rq), maximum profile peak height (Rp) and the maximum profile valley depth (Rv). As the scanned area was 1.09 x 1.45 mm, so it is obviously that one area is not enough to evaluate the average surface roughness of the heater surface. The interferometer was used to scan 9 different areas on the heater block. The locations of surface roughness scans are illustrated in Figure **3.4**.

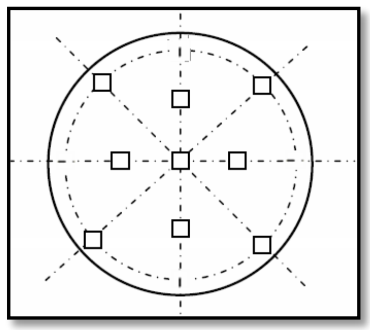

Figure 3.4 locations of the surface roughness scans

To quantify the surface finish and geometry, the Skewness (Rsk) was calculated for each surface roughness value (i.e. 420 nm, 80 nm and 20 nm) to measure the asymmetry of the profile according to Equation 3.1. Skewness is a function of number of data points, the root mean square and the height.

$$R_{sk} = \frac{1}{n\, R_q^3} \sum_{i=1}^{n} Z_i^3 \qquad (3.1)$$

Where, R_{sk} is the Skewness which is a measure of the asymmetry of the profile about the mean line. R_q is the root mean square (rms) roughness; it represents the stander deviation of the profile heights. Z is the surface height and n is number of data points.

Figures 3.5 and 3.6 represent the surface profile and the surface Skewness. The surface profile was digitized to get the values of the height for many data points. This procedure was carried out for each area of the nine areas scanned by the interferometer and the Skewness was calculated for each scanned area. Both of Ra and Rq were calculated for each scanned area and then the average value was used to represent the average surface roughness and the average surface Skewness.

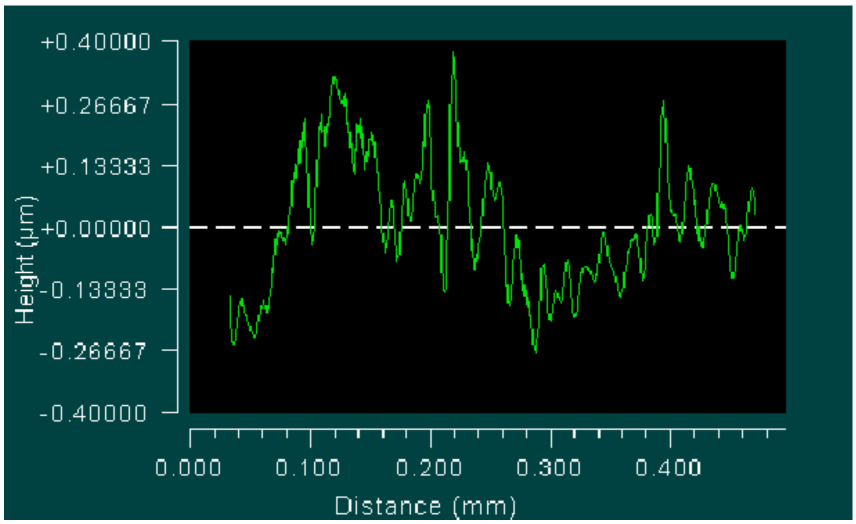

Figure 3.5 Surface Profile

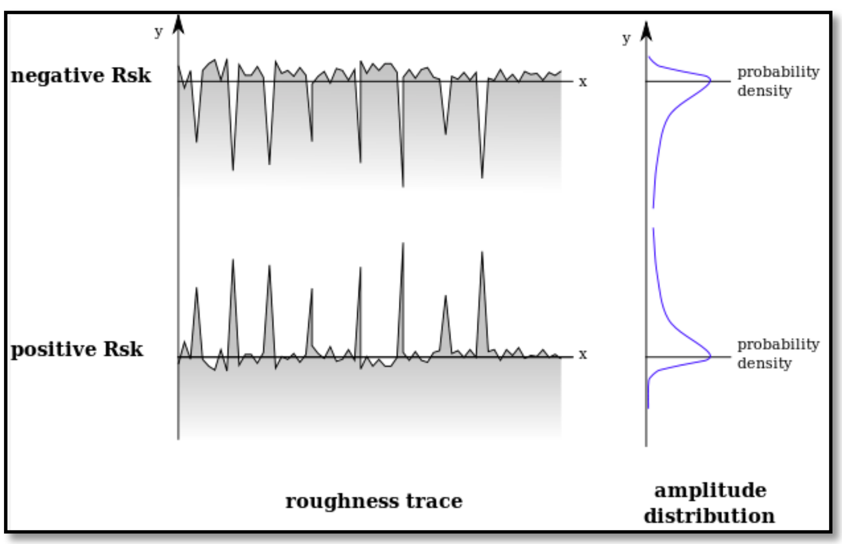

Figure 3.6 Surface Skewness

3.1.3. High-Speed Imaging

A Fastec imagining high speed camera model TSHRMS was used to record the boiling phenomenon. The camera settings were optimized for the best conditions to observe the bubbles clearly. The images were recorded at a rate of 1000 frames per second and the resolution was optimized to 1024 x 1024 pixels. A Lower Pro light source was used to illuminate the heater surface. The light source was placed at one of the two side windows while the camera was placed at the opposite side window. The light intensity was adjusted according to the light conditions inside the laboratory. A sample of the recorded images during the experiment are shown in Figure 3.7.

Figure 3.7 High Speed Imaging of vapour bubbles off the heated surface

3.2. Surface Preparation

In order to perform an experiment, the boiling surface had to be prepared first to obtain the targeted average surface roughness values (Ra). The boiling surface was polished before each experiment using emery sand papers with different grit sizes to reach the required average surface roughness of 420, 80 and 20 nm. The polishing procedure is to hold down the copper block –referred to as the boiling surface- in a 2.5 inch diameter steel collet on the polishing rotating disk. Using the collet prevented the copper block from rotating during the polishing process. It also helped keeping the copper block surface perfectly horizontal on the polishing disk to produce a flat surface.

After polishing, the surface was cleaned with a water jet and any excess water was removed using a cotton ball. After that the average surface roughness was measured using a Zygo white Light Interferometer. The heater surface after polishing is showed in Figure 3.8. The above procedure was repeated till the targeted value of the average surface roughness was reached.

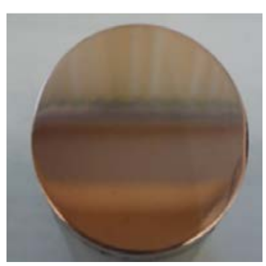

Figure 3.8 Photographs of the heater surface after polishing

3.3. Nanofluids Preparation

Alumina Oxide and Copper oxide nanoparticles of 40-50 nm nominal particle size were obtained in dry form from Nanophase Technologies Incorporation. In order to obtain the required volumetric concentration, a conversion from mass to volumetric concentrations was carried out using Equation 3.2. The particles were weighted carefully then the weighted particles were added to de-ionized water to obtain the required concentration.

$$\emptyset_v = \frac{1}{1 + \left(\frac{1 - \emptyset_m}{\emptyset_m}\right)\frac{\rho_P}{\rho_f}} \tag{3.2}$$

Where, $\emptyset_v$ is the volumetric concentration, $\emptyset_m$ is the mass concentration, ρ_P is the density of the nanoparticles and ρ_f is the base fluid density.

For health and safety reasons, the dry particles had to be handled in a fume hood. After preparing the nanofluid at the required concentration, the nanofluid was then poured into an ultrasonic bath and kept at 40 kHz for five hours before each experiment. The reason of using the ultrasonic bath is to break down particles agglomeration which occurs due to strong Van der Waals forces. In order to consider the effect of particles agglomeration on the actual particle size during the experiment, a sample from each prepared nanofluid sample (i.e. Al_2O_3 and CuO) was examined using Dynamic Light Scattering (DLS). This test measures the average particle size in motion. A laser beam was directed through the suspension, where laser would scatter upon impact with the moving particles. The laser scattering would change as the particles move down. Scattering of the laser is then fed to a correlation which gives the average particle size in the suspension.

The results of the DLS tests are shown in Figure 3.9 and Figure 3.10 for Al_2O_3 and CuO nanofluid samples respectively. The effective particle size of the Al_2O_3 nanofluid sample is 193.6 nm, which is about 4 times larger than the nominal initial particle size provided by the supplier. While the effective particle size of the CuO nanofluid sample is 550.7 nm, which is about 10 times larger than the nominal initial particle size provided by the supplier.

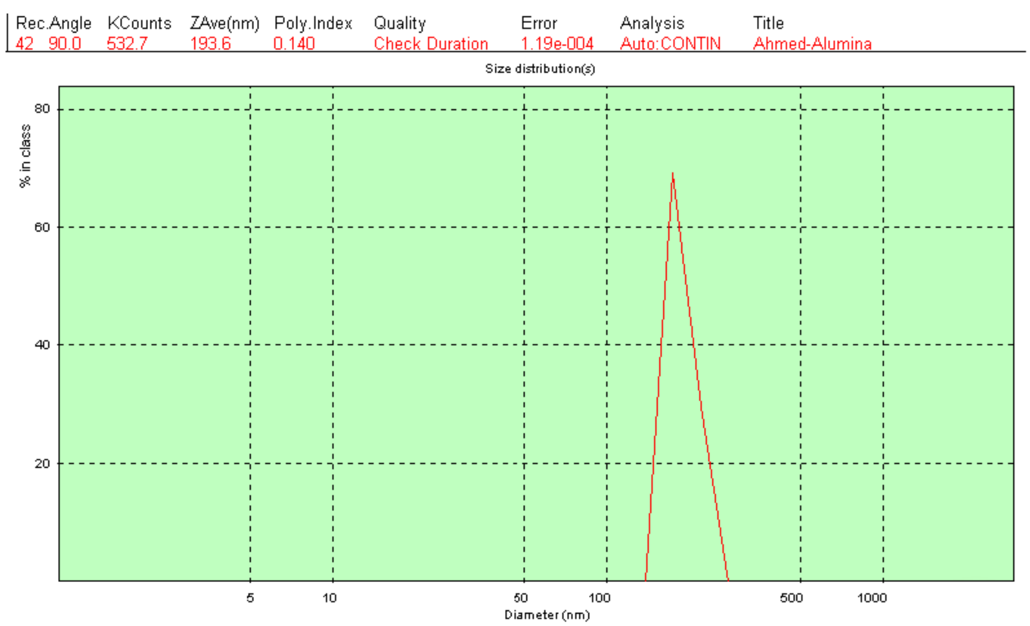

Figure 3.9 Distribution of Al_2O_3 measured particle size

For both nanofluids the particles agglomeration was very hard to break up and get the nominal particle size under ultrasonic vibration. All the nanofluids were exposed to 5 hours of ultrasonic vibration before each experiment.

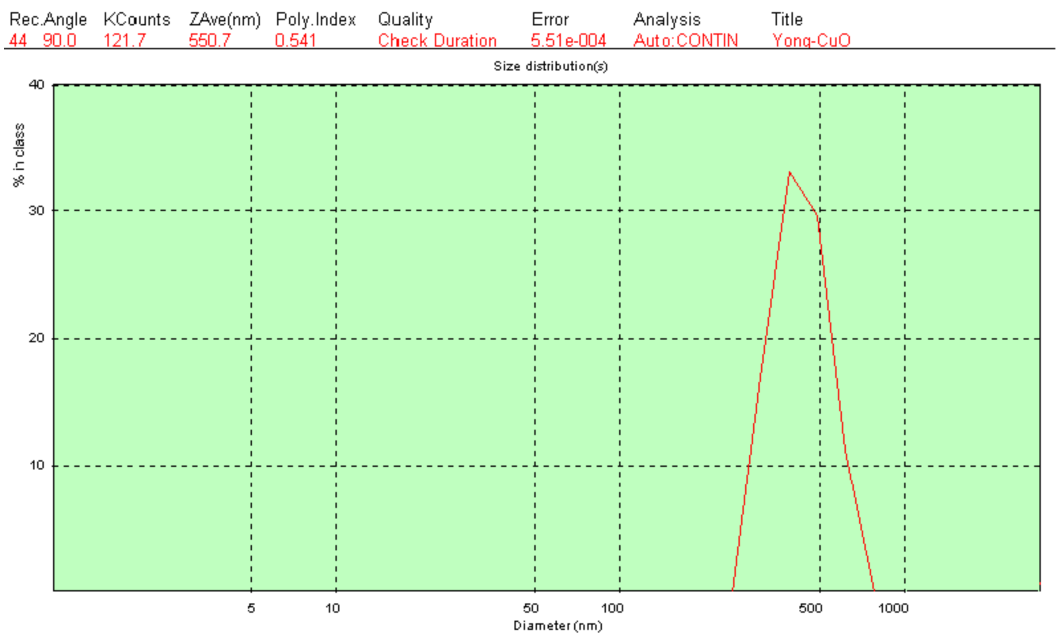

Figure 3.10 Distribution of CuO measured particle size

Alumina Oxide nanoparticles of 10 nm nominal particle size was used to investigate the effect of particle size on the pool boiling of nanofluids. As the particle size was really small, the DLS test was not suitable to measure the actual size of the particles after agglomeration. Another way of testing called Scanning Electron Microscope (SEM) was used to get the average particle size. It is basically imaging of the particles after the ultrasonic vibration. The particle diameter was then measured from the pictures and an average diameter of 30.58 nm was used as the actual particle size. Figure 3.11 shows the SEM image of the nanoparticles sample.

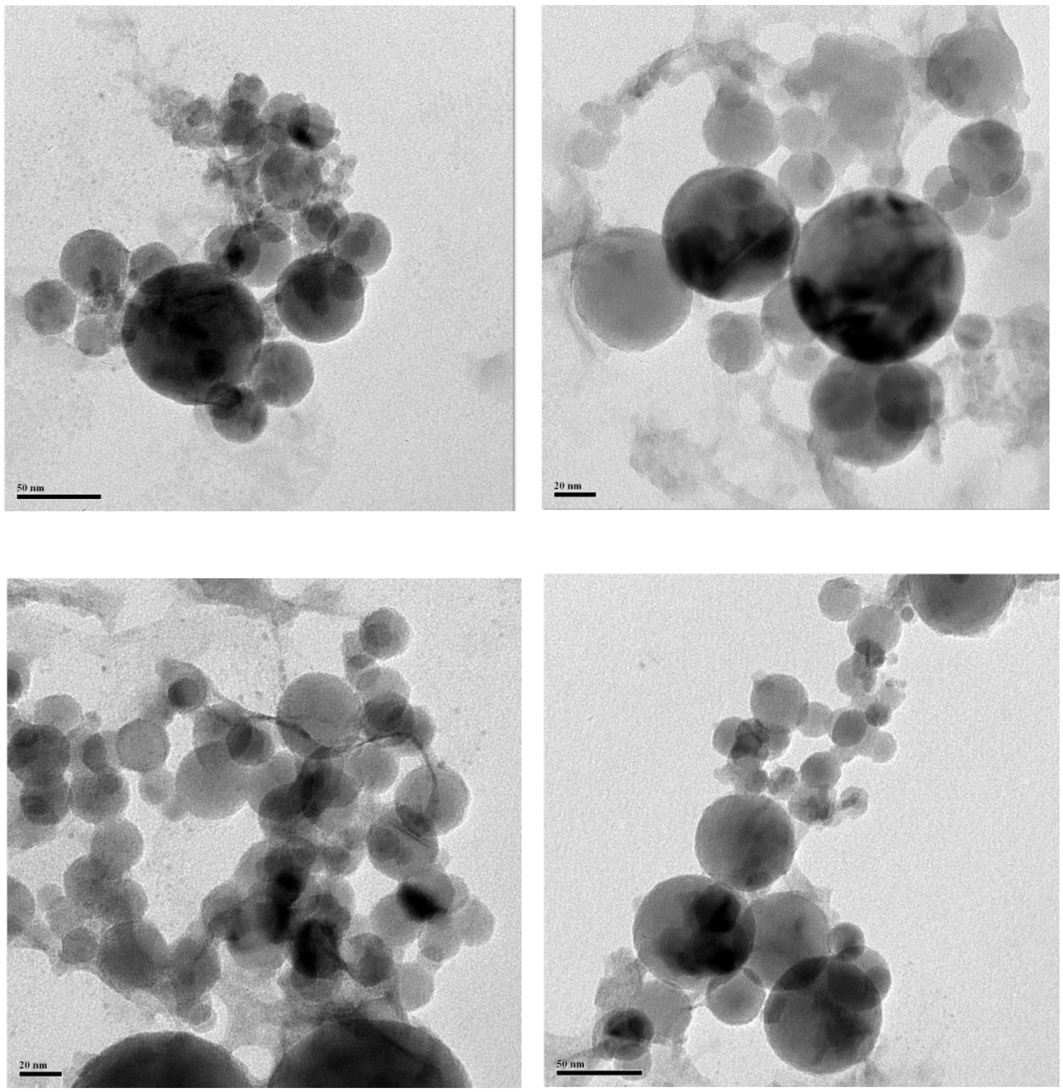

Figure 3.11 SEM images of the Al_2O_3 finer nanoparticles sample

3.4. The Experimental Procedure

Before each experiment, the boiling vessel was washed down from any nanoparticles remained from the previous experiment. The boiling vessel was then assembled by connecting all the heaters and thermocouples. Depending on the experiment, the vessel was then filled with 5 litter of pure water or nanofluid. The insulation cover was installed as a final step to get ready to start the experiment.

After configuring the data acquisition system and confirm that all the thermocouples connections are plugged in, the bulk fluid and air heaters would be switched on. The set points for the bulk fluid and air heater were 105^{o}C and 110 ^{o}C respectively under the automatic control mode. The controller were set to a higher temperature than the required as it was observed that the final temperature was always a few degrees (4-5 ^{o}C) lower than the set temperature on the controller. The liquid would reach the saturation temperature (i.e. 100 ^{o}C) after a while, once the data acquisition system record the saturation temperature, the bulk fluid heater would then switched to the manual control and set to 50 % of the full power. At this point the inlet condensing water valve would be opened at a flow rate 900 cm^{3}/min. The inlet condensing water temperature would be raised by switching on the heart at the inlet pipe. The inlet condensing temperature recorded was between 33 ^{o}C to 35 ^{o}C. The liquid would then continue boiling under these settings for 15 minutes. It is believed that this duration is enough to remove any non-condensable gases as well as to bring the whole vessel to a temperature close to the liquid's saturation temperature.

After the 15 minutes, the bulk fluid heater controller would be switched back to automatic control setting mode and the inlet condensing flow rate would be adjusted at 300 cm^3/min. The inlet condensing water temperature would be about 53 ^oC to 56 ^oC, which ensured that the liquid is not experiencing any sub-cooling during the experiment.

At this time the vessel is almost at the same temperature as the liquid and the main heaters in the copper block would then switched on using the manual control mode. The input to the copper block heater would be increased incrementally to attain higher heat flux. The input was not increased till the copper block thermocouples temperatures reach steady-state. It was assumed that the steady-state achieved when the copper block temperature would remain within 0.1 ^oC for 30 seconds (i.e. 6 data points).

The above mentioned procedure was repeated by increasing the input to the copper block heaters by 5% and the temperatures values were recorded and then the average temperature was used to calculate the surface temperature and the heat flux values.

The calculation of the surface temperature and the heat flux values will be explained in section3.6.

3.5. Post-Experiment Procedure

After each experiment, the fluid inside the vessel either pure water or nanofluid is cooled down using the cooling coil until it reaches a safe temperature to be drained out of the boiling vessel . As the nanofluid is drained, a film of nanofluid would remain on the surface. This film was washed away with a weak water jet to avoid any air-dry to additional nanoparticles to assure that the only deposition layer on the heater surface is only due to the boiling phenomena.

The copper block was then removed from the boiling vessel and an image of the surface was taken to compare different deposition patterns of the nanoparticles. The surface image was processed using MATLAB. The percentage of the surface area covered by nanoparticles has been determined and used to quantify the uniformity of nanoparticle deposition on the heater surface.

As the deposition was not easily washed away using a water jet, so the surface had to be polished after each experiment to completely remove the nanoparticles deposition layer.

3.6. Determination of the surface Heat Flux (q”) and Surface Temperature (T_s)

In order to determine the surface temperature and the heat flux through the copper surface, three thermocouples were located at the radial center of the copper block at different axial distances from the surface (see figure 3.2). Assuming that the radial heat losses are negligible, a linear best fit of the recorded temperatures was carried out. Equations 3.3 and 3.4 were used to apply the linear best fit and obtain the heat flux (q”) and surface temperature (T_S) of the copper block.

$$q" = k \frac{\sum_{i=1}^{N} x_i T_i - \sum x_i \sum T_i}{N \sum\left(x_i^2\right) - \left(\sum x_i\right)^2} \qquad (3.3)$$

$$T_s = \frac{N \sum_{i=1}^{N} x_i^2 \sum T_i - \sum x_i \sum x_i T_i}{N \sum\left(x_i^2\right) - \left(\sum x_i\right)^2} \qquad (3.4)$$

Where: N = number of temperature readings

í = i^{th} readings

x = Thermocouple axial distance from the surface

T = Temperature recorded at each thermocouple position

3.7. The Uncertainty Analysis

Each measured parameter has a certain uncertainty associated with it. The uncertainty of any calculated parameter is a function of the uncertainty of all parameters used to carry out its calculation. The uncertainty of the calculated parameter can be determined using Equation 3.5

$$u\ (R) = \sqrt{\left[(u\ (w_1) \frac{\partial R}{\partial w_1})^2 + \ (u\ (w_2) \frac{\partial R}{\partial w_2})^2 + \cdots + \ (u\ (w_n) \frac{\partial R}{\partial w_n})^2 \right]} \qquad (3.5)$$

Where: u (…) = uncertainty in (), R = any calculated parameter, and W_n = the n^{th} parameters that R depends on.

3.8. The Uncertainty in Thermocouples Readings and Axial Location

The uncertainty in the Temperature recorded by the thermocouples is ± 0.8 ^{o}C. As mentioned previously the three thermocouples used to measure the temperature across the copper block were 1.0 mm diameter, and the holes were 1.1 mm diameter. This gives an uncertainty of $\pm$ 0.05 mm in the thermocouple location.

3.9. The Uncertainty in Surface Temperature (Ts)

Applying Equation 3.5, the uncertainty in the surface temperature was found to be $\pm$0.91 ^{o}C. For an intermediate surface temperature of 117 ^{o}C, the uncertainty in the surface temperature would be $\pm$0.78%.

3.10. The Uncertainty in Liquid Saturation Temperature (Tsat)

Both pure water and nanofluids were boiled at saturation temperature under atmospheric pressure. However, it was noticed that the saturation temperature varied from one experiment to another. This variation is due to the change in the room pressure.

Two thermocouples were used to record the bulk fluid temperature during the boiling experiment; the average of the two temperatures was calculated and used as the saturation temperature. The minimum recorded saturation temperature was 99.43 ^{o}C, while the highest was 100.23 ^{o}C.

Considering the error in each thermocouple as ± 0.8 ^{o}C, and applying Equation 3.5, the uncertainty in the liquid saturation temperature is ± 0.97 ^{o}C. For an average liquid saturation temperature of 100 ^{o}C, the uncertainty in the liquid saturation temperature is $\pm$0.97%.

3.11. The Uncertainty in Surface Superheat (Ts-Tsat)

The uncertainty in the surface superheat is due to the uncertainty in the surface temperature and the liquid saturation temperature. Using Equation 3.5, to combine the effect of both uncertainties resulted in an uncertainty in the surface superheat of ± 1.33 ^{o}C. The maximum superheat temperature recorded was 30.58 ^{o}C, while the minimum was 12.40 ^{o}C. For an average superheat temperature of 21.49 ^{o}C, the uncertainty in the surface superheat is ±6.18 %.

3.12. The Uncertainty in The Surface Heat Flux (q")

The uncertainty in the surface heat flux is due to the uncertainty in the temperature gradient measured in the copper block. It was assumed that the uncertainty in the copper thermal conductivity is negligible. Using Equation 3.5, the uncertainty in the surface heat flux is about 11% at an average heat flux value.

3.13. Setup Validation Using the Boiling Curve of Pure Water.

In order to validate the experimental setup, a set of pure water experiments was performed on each surface roughness and each experiment was compared against the Rohsenow's correlation, Equation 3.5. The constants used in the Rohsenow's correlation were s=1 and r = 0.33. Regarding the experimental constant C_{sf}, it was calculated for each experiment separately. It was observed that the values of this constants were still within the range of 0.0068 – 0.0128, which complies with the values recommended by Rohsenow.

$$q'' = \mu_l h_{lv} \left[\frac{\sigma}{g(\rho_l - \rho_v)}\right]^{-1/2} \mathrm{Pr_l}^{-s/r} \left[\frac{C_{pl}}{h_{lv} C_{sf}} (T_s - T_{sat})\right]^{1/r} \quad (3.5)$$

The boiling curves of pure water obtained for the three prepared surfaces are shown in Figure 3.12,Figure 3.13 and Figure 3.14. The experimental results are in good agreement with the Rohsenow correlation. The uncertainty in the heat flux and the superheat temperatures is represented by the error bars. The boiling curves deviated from the correlation at superheat temperature above 11^{o}C in case of surface roughness of 420 nm. For the 80 nm and 20 nm surfaces, the boiling curves deviated from the correlation at superheat temperatures above 13^{o}C and 12^{o}C, respectively.

Also, experiments repeatability was checked for both pure water and nanofluids experiments. The boiling curves obtained for experimental repeatability are shown in Appendix A.

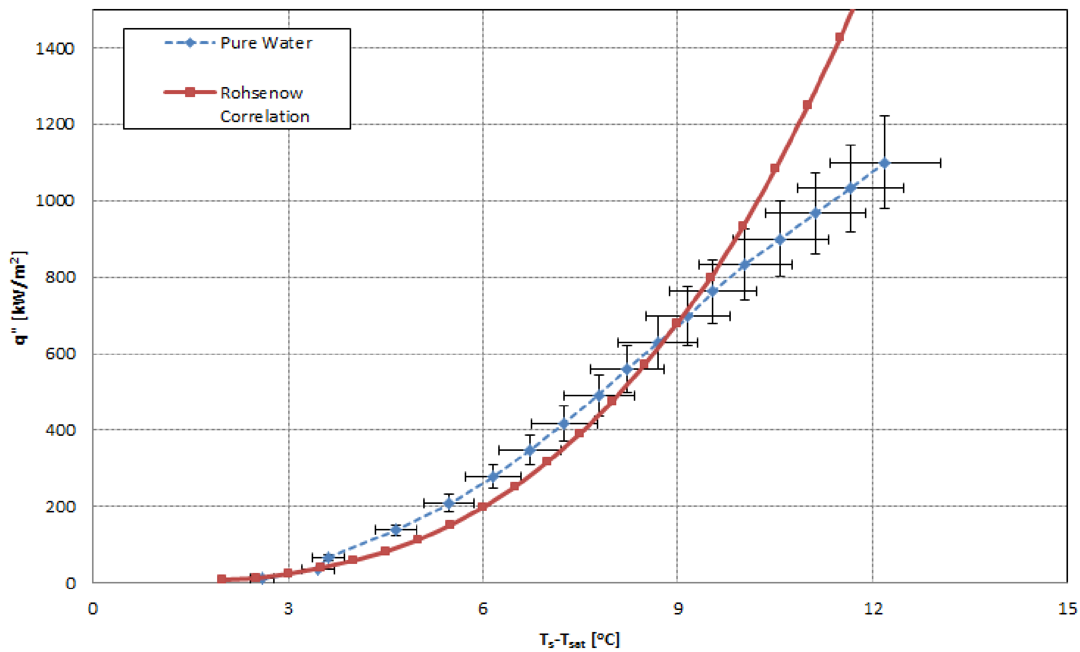

Figure 3.12 Setup Validation for Ra = 420 nm surface

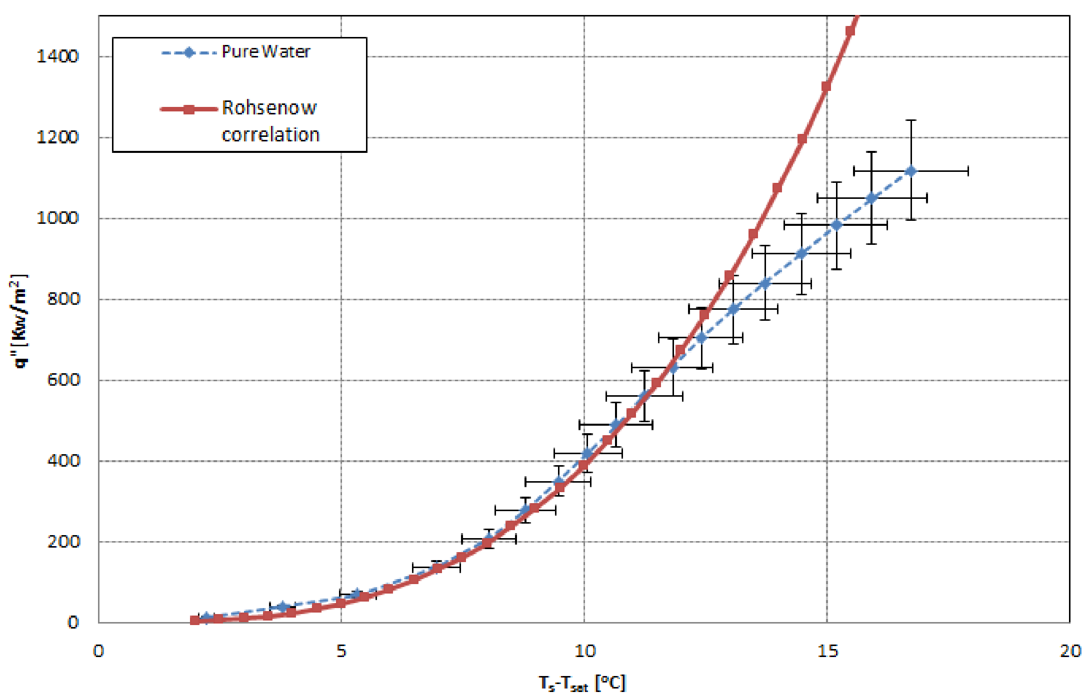

Figure 3.13 Setup Validation for Ra = 80 nm surface

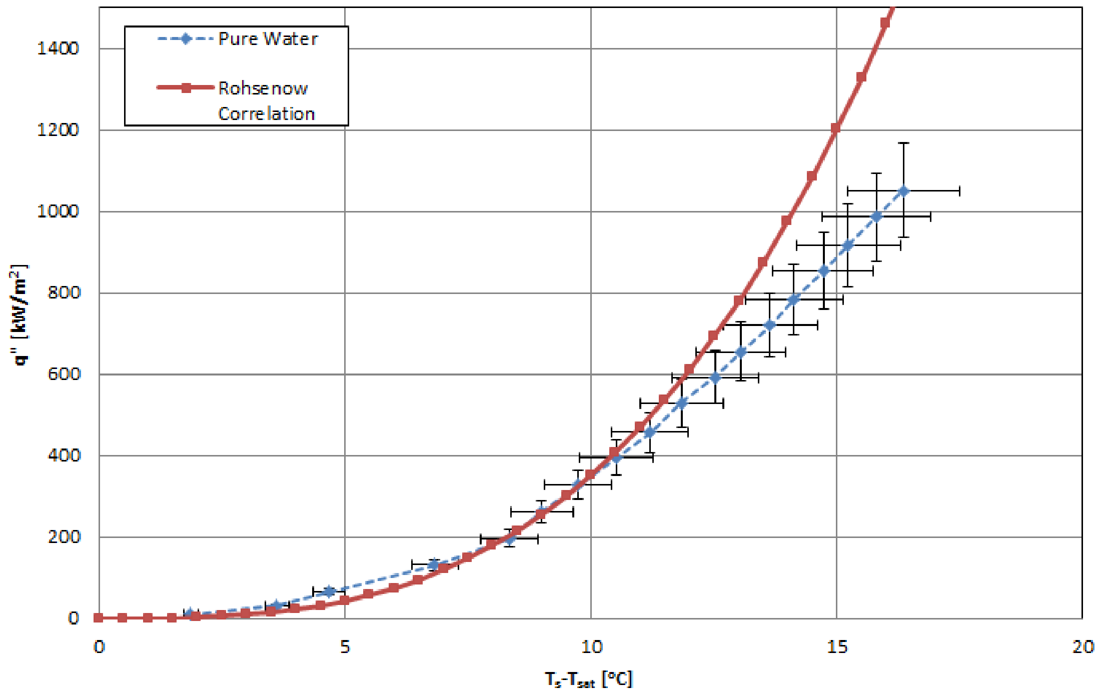

Figure 3.14 Setup Validation for Ra = 20 nm surface

Chapter 4
Pool Boiling Results and Discussion

The experimental work in this study was carried out in four stages. Each stage will be discussed and explained separately. The focus of the first stage was to investigate the effect of surface conditions, represented in this study by the average surface roughness (Ra), on the pool boiling of Aluminum Oxide (Al_2O_3) and Copper Oxide (CuO) nanofluids. The second stage focused on the effect of nanoparticles concentration on the pool boiling of Aluminum Oxide (Al_2O_3) and Copper Oxide (CuO) nanofluids .In the third stage the effect of changing the nanoparticles material (i.e., Al_2O_3 to CuO) on the pool boiling of nanofluids. In the fourth stage, the effect of Aluminum Oxide nanoparticles size on the pool boiling behavior was investigated.

4.1. Effect of Surface Initial Conditions

4.1.1. Pool Boiling of Aluminum Oxide (Al_2O_3) Nanofluid

The effect of the surface conditions was investigated during stage 1. As it was mentioned previously; three different surfaces were prepared using different emery sand papers grid sizes to obtain an average surface roughness of 420, 80 and 20 nm. The supplied Al_2O_3 nanoparticles size was 40-50 nm however, as mentioned in Chapter 3, the actual average cluster size after preparing the nanofluid sample was examined using the Malvern Instrument. It was found that the actual size range is between 190-200 nm, which is almost 4 times the initial particle size provided by the supplier. The nanoparticles concentration was 0.01% vol. In order to investigate the effect of the surface initial conditions (Ra), for each surface roughness value three separate experiments were performed. After polishing the surface a pure water boiling experiment was carried out. Then the experiment using the nanofluid was performed and in order to examine the effect of nanoparticles deposition on the heater surface, another pure water boiling experiment was performed on the nanoparticle deposited surface (NPD).

The boiling curves of pure water were obtained for the three different initial surface conditions are shown in Figure 4.1. As expected, the heat transfer rate increased with the increase in the surface roughness value from 20 nm to 420 nm. This is due to the fact that the higher surface roughness, the high the number of the active nucleation sites on the surface. Which leads to more heat transfer rate compared to low surface roughness surface. The bubble generation during the pure water boiling experiments was monitored using a high speed camera, both on the initial surface and on the NPD surface after the nanofluids boiling experiments. Images for water boiling on a clean surface are shown in Figure 4.3 for surface roughness of 20 nm, 80 nm and 420 nm, respectively. The images show that the number of active nucleation sites is higher for the rougher surface. It was hard to quantify the difference in the number of nucleation sites due to bubbles coalescence.

As each surface has different surface roughness, the onset of nucleation temperature (ONB) changes. It was observed that the nucleation was started earlier in the case of boiling pure water on the surface of 420 nm average surface roughness compared to the case of 20 nm average surface roughness.

Before performing the nanofluids boiling, the average surface roughness of each surfaces was checked before and after the water boiling experiment and no significant changes in the surface roughness after the pure water boiling experiments were found.

The boiling curves obtained from the Al_2O_3 nanofluids experiments are shown in Figure 4.2. The trend is opposite to the case of pure water. The heater with the highest surface roughness (Ra =420 nm) showed the lowest heat transfer rate. It was also observed that the rate of heat transfer in the case of average surface roughness of 80 nm was slightly higher that the case of 20nm. The main reason behind this – as it will be explained in more details in the following sections- is the effect of nanoparticles deposition. The rate of nanoparticles deposition increases with surface roughness.

A slight enhancement in the rate of heat transfer in the case of the Ra= 80 nm was observed compared to the case of the Ra= 20 nm. This was believed to be because of the deposition ratio. The deposition ration is higher in the latter case (see Table 4.2)

In the following section more experimental results obtained for each surface roughness will be discussed in details and a proposed hypothesis will be presented.

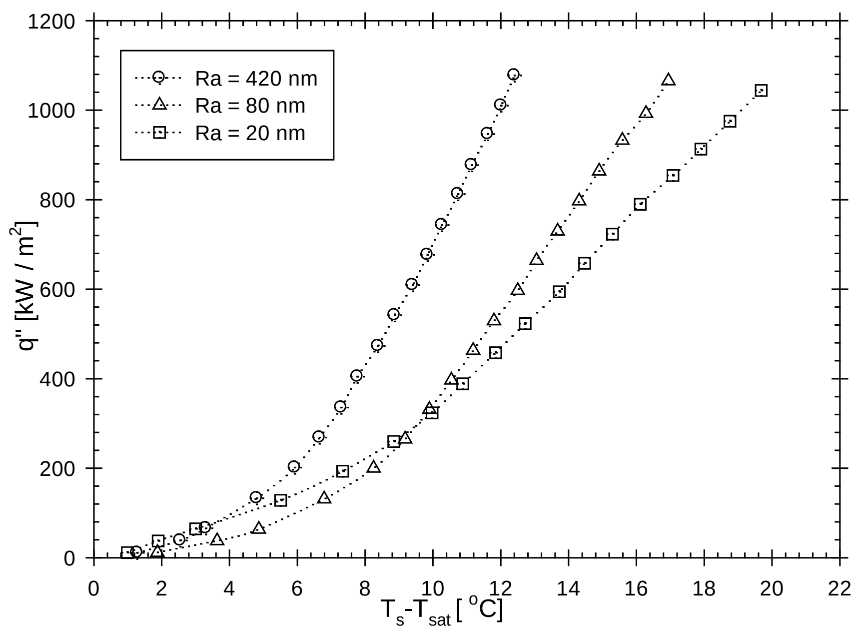

Figure 4.1 Effect of surface condition on pool boiling curves of pure water

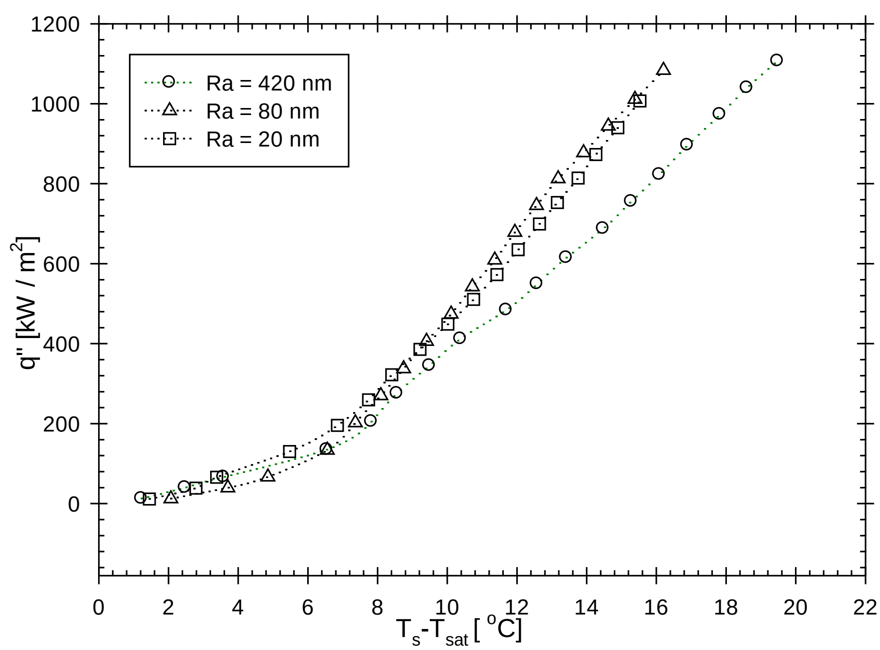

Figure 4.2. Effect of surface condition (Ra) on pool boiling curves of 0.01 vol. % AL_2O_3 nanofluid

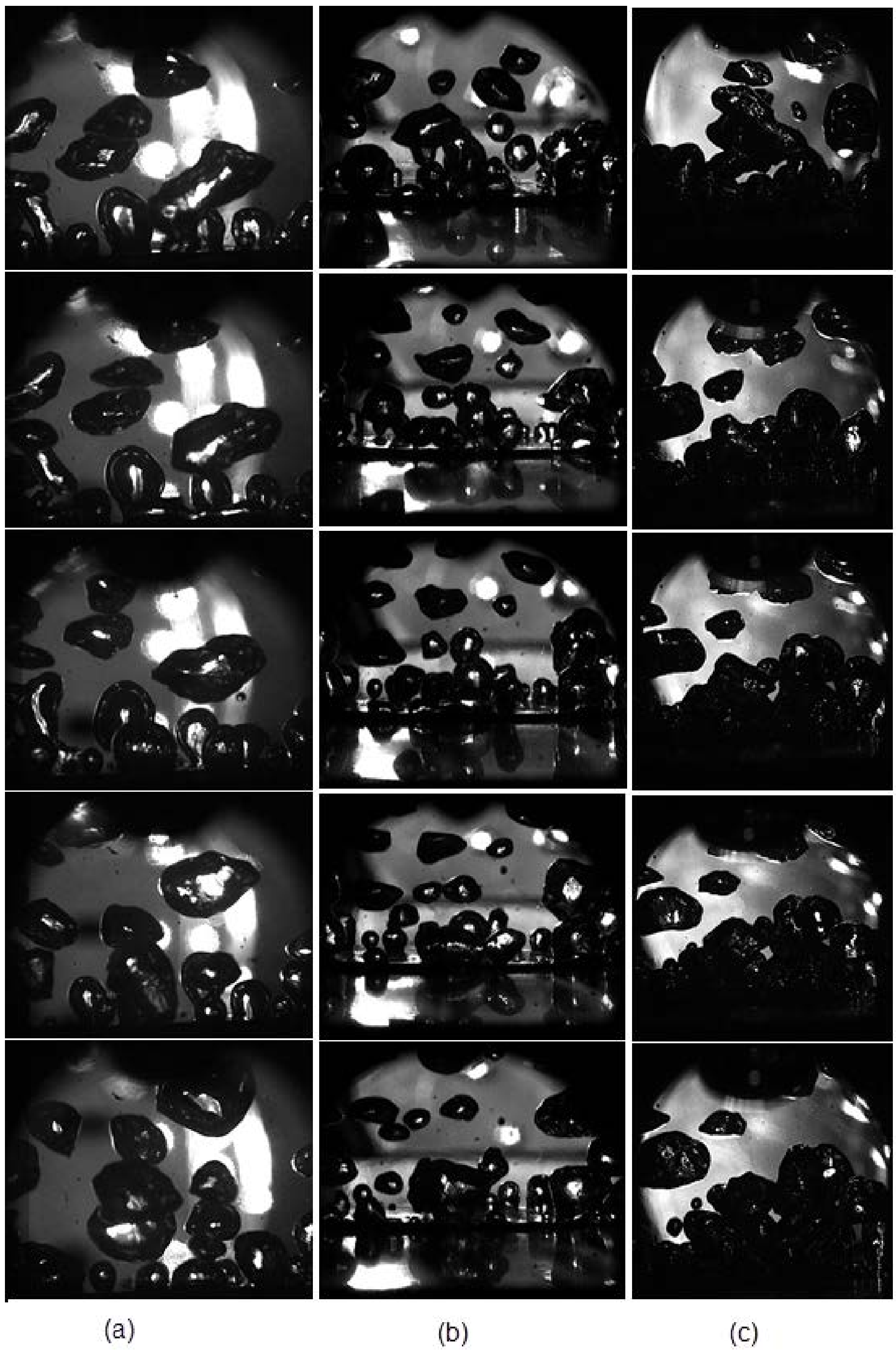

Figure 4.3 Images of pure water boiling from a clean surface (a) Ra=20 nm (b) Ra=80 nm (c) Ra=420 nm

4.1.1.1. Initial Surface Condition with Ra = 420 nm

As indicated previously, three boiling experiments were carried out for each surface condition; pure water, nanofluid on a clean surface and pure water on the nanoparticle deposited surface (NPD). Figure 4.4 shows the boiling curves obtained for three boiling experiments for the case of Ra = 420 nm. The rate of heat transfer using the nanofluid deteriorated compared to pure water. In order to quantify this deterioration the heat transfer rate ratio of the nanofluids and pure water at 11^{o}C surface superheat was calculated.

As shown in Table 4.1, the pure water heat flux was 877 kW/m2 while Al2O3 nanofluid heat flux was 440 kW/m2 .In other words, in this case the heat transfer rate deteriorated by about 49 %. The main reason behind this deterioration is the deposition of nanoparticles on the heater surface. As shown in Figure 4.7(b), the deposition pattern occurred in this case is uniform and covered almost the entire surface. The deposition layer works as an insulation on the surface that prevented the liquid from accessing the nucleation sites. It also might reduce the surface wettability as evident from the increase in the onset of nucleation temperature (ONB) from 6.5 oC in the case of pure water on a clean surface to 10.7 oC in the case of pure water on the nanoparticle deposited surface (see Table 4.1).

The effect of nanoparticles deposition on the deactivating of the nucleation sites has been examined using high speed imagining of the bubble growth process on the surface during boiling of pure water on the clean surface and boiling pure of water on the nanoparticle deposited surfaces (NPD). The number of active nucleation sites was lower in the latter case.

Images for 0.01 % vol. of Al_2O_3 nanofluid boiling on a clean surfaces are shown in Figure 4.9 for surface roughness of 20 nm, 80 nm and 420 nm, respectively. The images show that the number of active nucleation sites is higher for the roughest surface

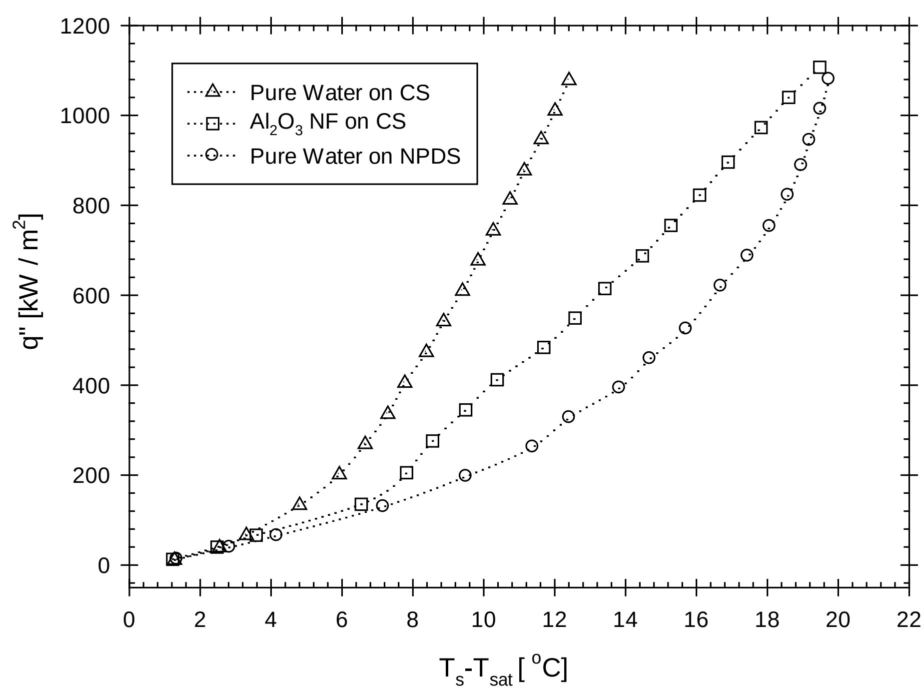

Figure 4.4 Boiling Curves obtained for the pure water on clean surface, 0.01% vol. AL_2O_3 nanofluid and pure water on NPD surface for the Ra=420 nm surface

4.1.1.2. Initial Surface Condition with Ra = 80 nm

Figure 4.5 shows the three boiling curves obtained for the Ra = 80 nm surface. In this case, there is a 41% enhancement in the rate of heat transfer when using the nanofluids compared to pure water at 11oC surface super heat (see Table 4.1).

As shown in Figure 4.7(c), the deposition pattern in this case is less uniform compared to the Ra= 420 nm case. It is assumed that the non-uniform deposition layer allowed the liquid to access some of the nucleation sites on the surface. It is also believed that the surface wettability might was enhanced as evident from the decreasing in the ONB temperature from 9 ^{o}C in the case of pure water on the clean surface to 7.25 ^{o}C in the case of pure water on NPD surface.

High speed imaging during the boiling of pure water on the clean surface experiment indicated an increase in the number of active nucleation sites compared to the boiling of pure water on NPD surface experiment (see Figure 4.9).

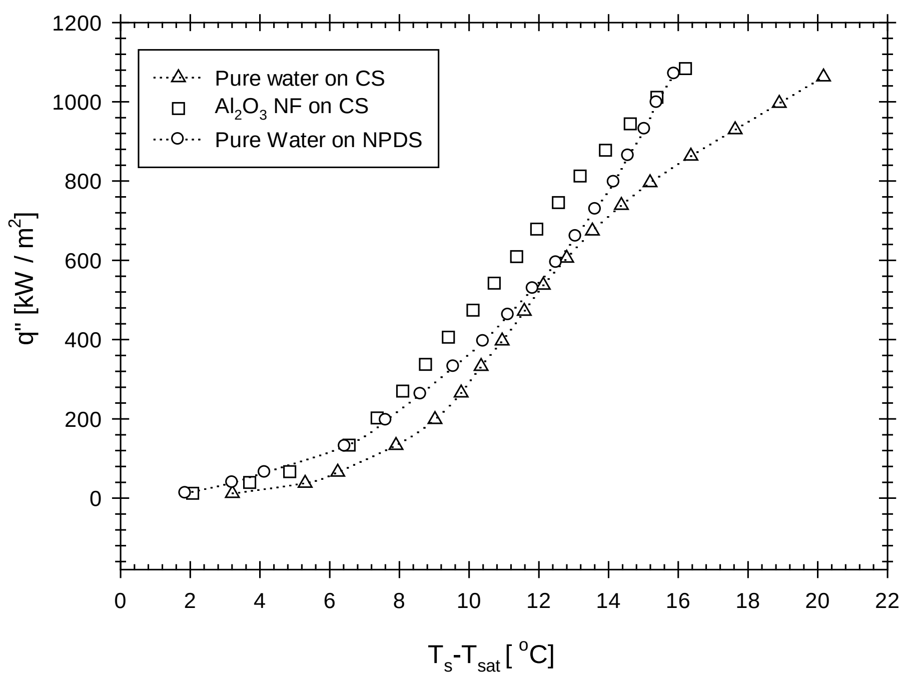

Figure 4.5 Boiling Curves obtained for the pure water on clean surface, 0.01% vol. AL_2O_3 nanofluid and pure water on NPD surface for the Ra=80 nm surface

4.1.1.3. Initial Surface Condition with Ra = 20 nm

Figure 4.6 shows the three boiling curves obtained for the Ra = 20 nm surface. In this case, there is a 34% enhancement in the rate of heat transfer when using the nanofluids compared to pure water at 11^{o}C superheat (see Table 4.1).

As shown in Figure 4.7(d) that the deposition pattern in this case is less uniform compared to the Ra = 420nm case. It is assumed that the non-uniform deposition layer allowed the liquid to access some of the nucleation sites on the surface. It is also worth to notice here that the surface wettability was enhanced as evident from the decrease in the ONB temperature from 8.8 ^{o}C in the case of pure water on the clean surface to 7.1 ^{o}C in the case of pure water on the NPD surface.

High speed imaging during the boiling of pure water on the clean surface experiment indicated an increase in the number of active nucleation sites compared to the boiling of pure water on NPD surface experiment (see Figure 4.9).

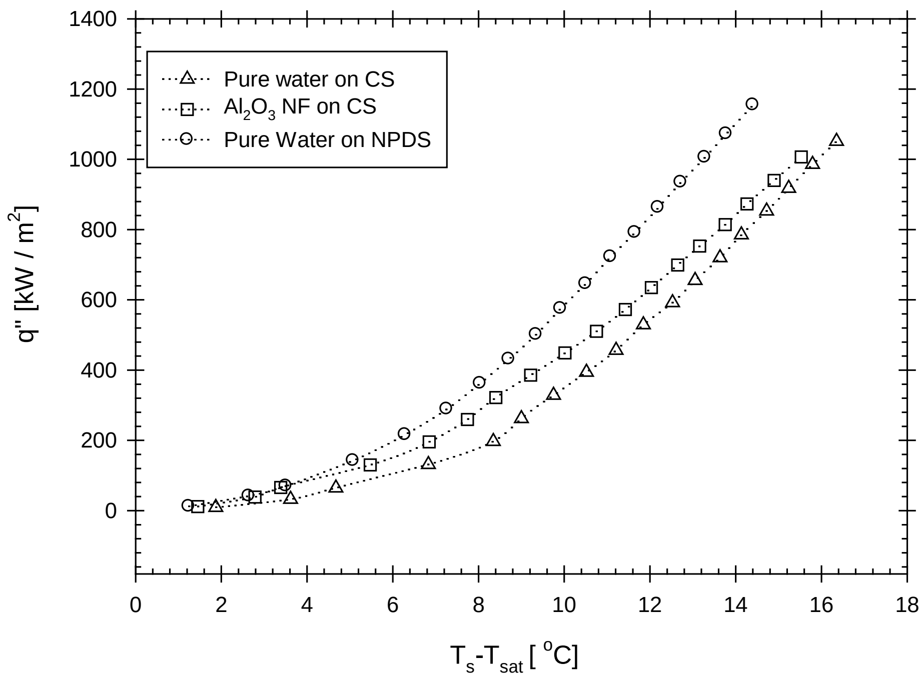

Figure 4.6 Boiling Curves obtained for the pure water on clean surface, 0.01% vol. AL_2O_3 nanofluid and pure water on NPD surface for the Ra=20 nm surface

Table 4.1 Heat Flux values at 11 °C surface superheat

Ra (nm)	**Pure water - Heat Flux (kW / m2)**	**AL_2O_3 - Heat Flux (kW / m2)**	**% of Enhancement or Deterioration**
420	877	440	-49 %
80	396	561	+41 %
20	392	532	+ 34%

Table 4.2 Experimental results summary for the boiling of 0.01 vol. % AL_2O_3 nanofluid

D_p (nm)	193	193	193
Ra (nm)	420	80	20
SPIP	2.176	0.414	0.104
Deposition Ratio	99.2%	79.2%	82.8%
Deposition Pattern	uniform	non-uniform	non-uniform
ONB for Pure Water on clean surface	6.5 ^oC	8.7 ^oC	8.8 ^oC
ONB for Pure Water on NPD surface	10.7 ^oC	7.25 ^oC	7.1 ^oC

As can be noticed from Table 4.2 and Figure 4.8 the enhancement in the heat transfer is related to the non-uniformity of the deposition layer. The threshold of the uniformity in this study is defined by 90% deposition ratio. It worth noting that for all cases where enhancement in the rate of heat transfer was observed, the deposition ratio was always less than 90% and for all cases where deterioration was observed, the deposition ratio was always above 90%.

Also, as shown in Table 4.2 the SPIP was evaluated for the three surface roughnesses. It was observed that in the case of the enhancement in the rate of heat transfer, the values of SPIP were less than 1 (SPIP<1). However, in the case of deterioration the values of SPIP was more than 1 (SPIP>1).

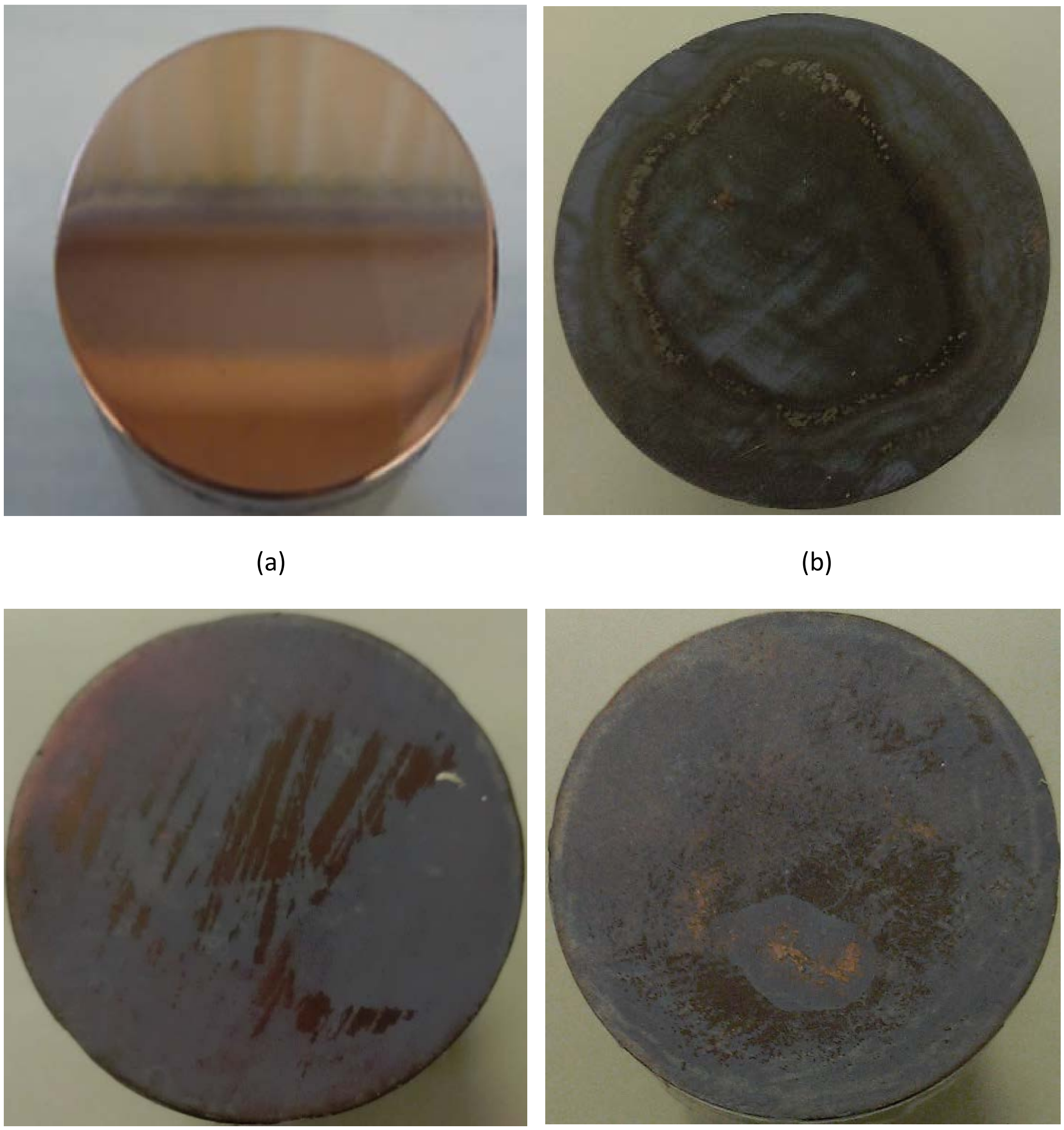

(a) (b) (c) (d)

Figure 4.7 Images of the heater surface before and after the 0.01% vol. AL_2O_3 nanofluid boiling experiments (a) clean surface (b) Ra = 420 nm (c) Ra = 80 nm (d) Ra = 20 nm

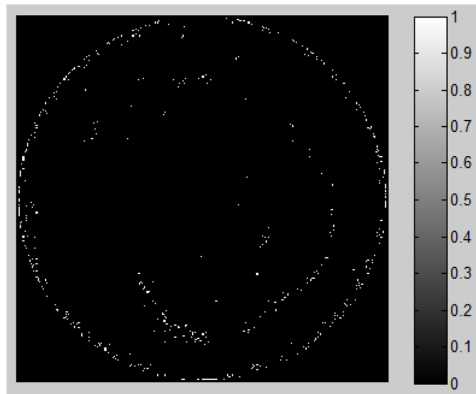

(a)

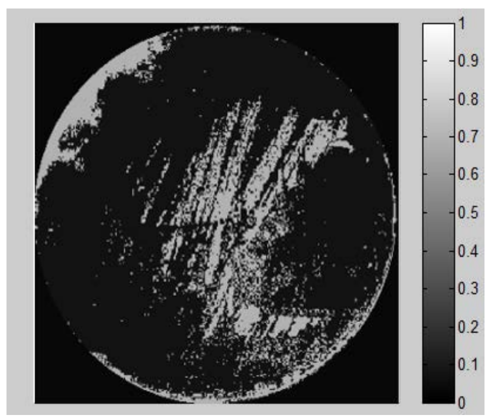

(b)

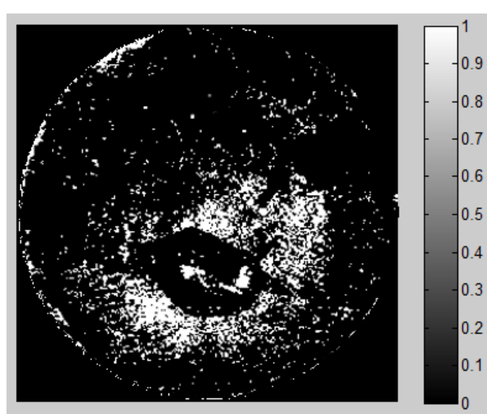

(c)

Figure 4.8 MATLAB processed images of the heater surface after the 0.01% vol. AL_2O_3 nanofluid boiling experiments (a) Ra = 420 nm (b) Ra = 80 nm (c) Ra = 20 nm

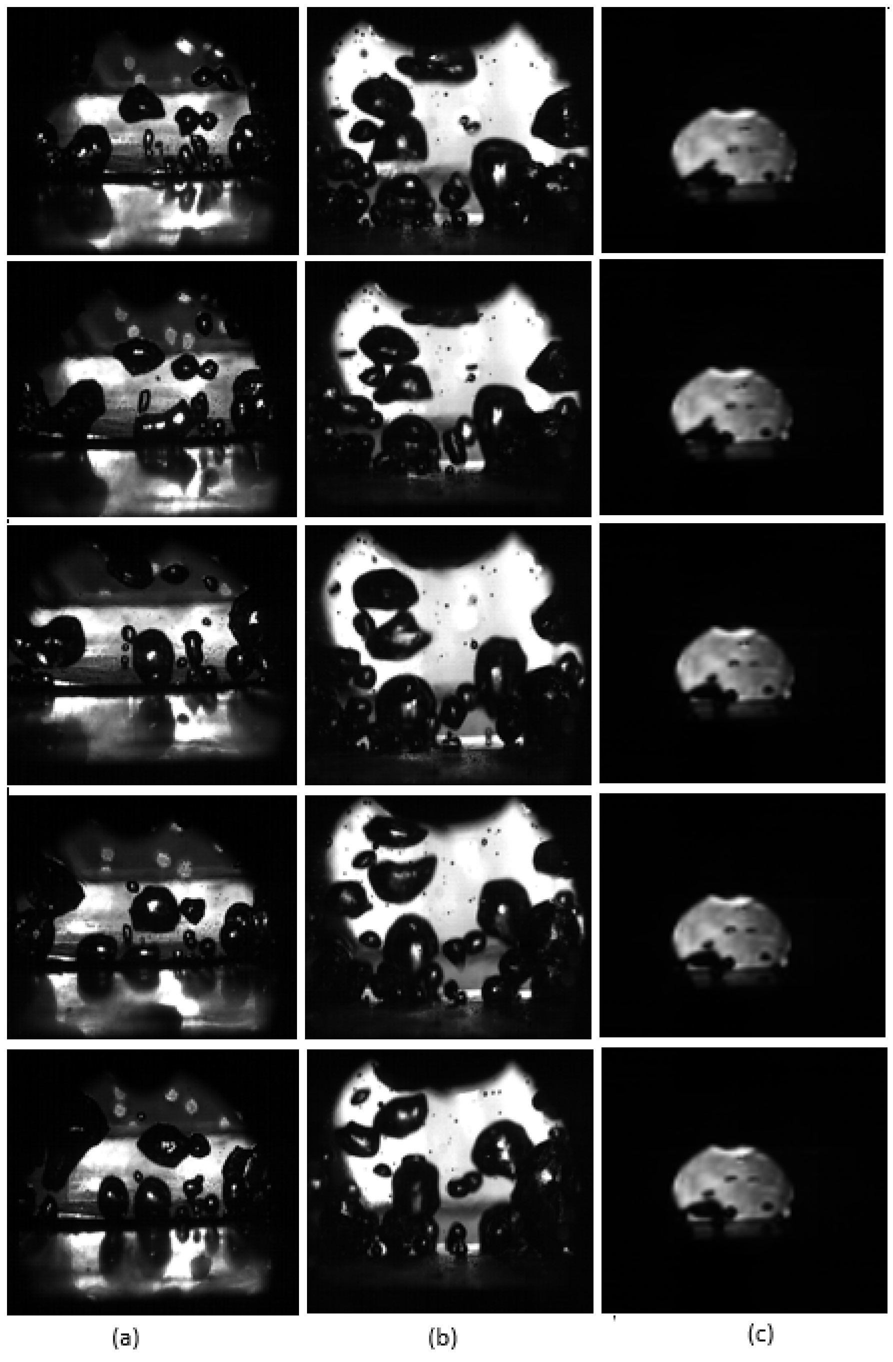

Figure 4.9 Images of 0.01 % vol. of Al_2O_3 boiling from a clean surface (a) Ra =20 nm (b) Ra =80 nm (c) Ra =420 nm

4.1.2. Pool Boiling of Copper Oxide (CuO) Nanofluids

The effect of the surface initial conditions in term of its Ra on the pool boiling of copper oxide (CuO) nanofluids will be discussed in this section. The thermal conductivity of Al_2O_3 (40 W/m.K) is about three times that of CuO (13.5 W/m.K) at room temperature as shown in Figure 4.10.

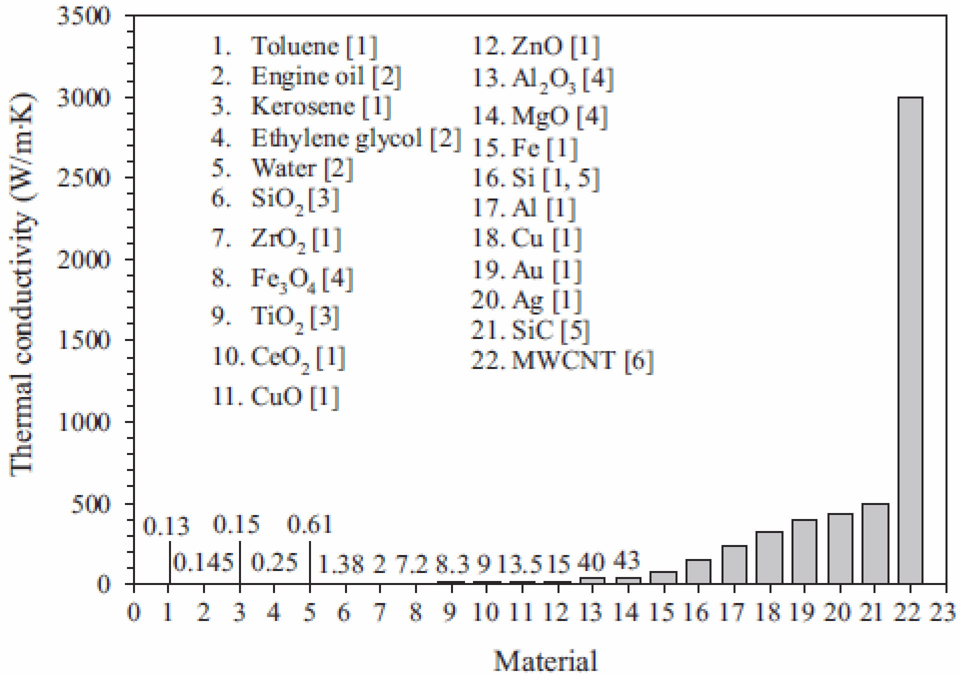

Figure 4.10 Thermal conductivities of commonly used liquids and materials at room temperature [27]

The same procedure was followed; three different surfaces were prepared using different emery sand paper grit sizes to obtain an average surface roughness of 420, 80 and 20 nm. The supplied CuO nanoparticles size was 40-50 nm, which is the same as the Al_2O_3 nanoparticles. However as mentioned in Chapter 3, the actual average cluster size after preparing the nanofluid sample was measured using the Malvern Instrument and was found to be 550 nm, which is almost 2.9 times the actual average Al_2O_3 cluster size. The concentration of the nanofluids used in these experiments was kept constant at 0.01% vol.

The boiling curves obtained for the CuO nanofluids on the three surfaces are shown in Figure 4.11. The experimental results showed an opposite trend compared with the case of Al_2O_3 nanofluid. The surface with the highest average surface roughness (Ra = 420 nm) resulted in the highest heat flux values, while the surface with the lowest average surface roughness (Ra = 20 nm) gave the lowest heat flux values. The change in the heat flux can be attributed to the nanoparticles deposition pattern on the heater surface, as will be explained in details below. It is believed that the change in the results trend is due to the difference in the actual particle size of CuO compared to Al_2O_3.

In the same way as was done for the Al_2O_3 experiments, for each surface three experiments were performed. After preparing the surface, an experiment with pure water was carried out on the clean surface, followed by an experiment using the nanofluid. The third experiment was carried out using pure water on the nanofluid deposited surface (NPD).

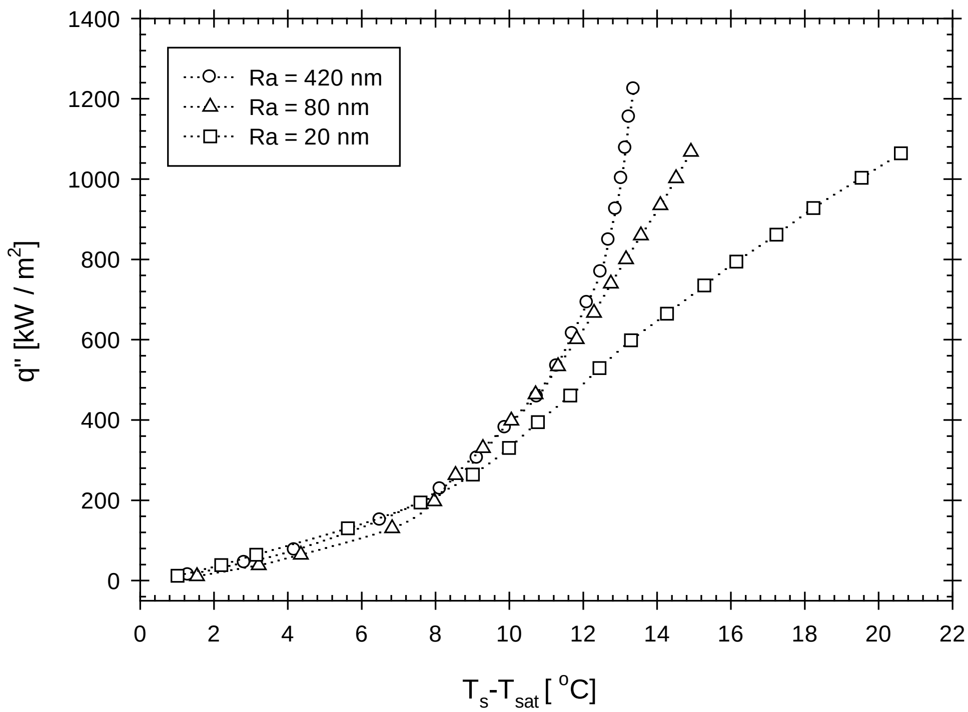

Figure 4.11 Surface condition effects (Ra) on the pool boiling of 0.01 vol. % CuO nanofluid

A visual inspection of the surface after the experiments showed a deposited layer of nanoparticles which was easily recognized by the naked eye. The layer was not easily washed away using a water jet, so the surface had to be polished after each experiment to completely remove the nanoparticles deposition layer.

In the following section more experimental results obtained for each surface roughness will be discussed in details and a proposed hypothesis will be presented.

4.1.2.1. Initial Surface Condition with Ra =420 nm

As indicated before, three boiling experiments were carried out for each surface condition; pure water on a clean surface, nanofluid on a clean surface and a pure water on the NPD surface. Figure 4.12 shows the three boiling curves obtained for three boiling experiments for the case of Ra = 420 nm. The rate of heat transfer using the nanofluid deteriorated compared to pure water. In order to quantify this deterioration the heat transfer rate ratio of the nanofluids and pure water at 11oC surface superheat was calculated. As shown in Table 4.3, the pure water heat flux was 877 kW/m2 while the CuO nanofluid heat flux was 518 kW/m2. In other words, in this case the rate of heat transfer deteriorated by about 40 %. The main reason behind this deterioration is the deposition of nanoparticles on the heater surface. As shown in Figure 4.16(b), the deposition pattern occurred in this case is uniform and covered almost the entire surface. The deposition layer prevented the liquid to access the nucleation sites also, as evident from the increase in the ONB temperature from 6.5 ^{o}C in the case of pure water on a clean surface to 9.2 ^{o}C in the case of pure water on a NPD surface (See Table 4.4), surface wettability might was reduced.

The effect of nanoparticles deposition on the deactivating of the nucleation sites has been examined using high speed imaging of bubble growth process on the surface during boiling of pure water on the clean surface and boiling pure water on the NPD surface. The number of active nucleation sites was lower in the latter case.

High speed imaging during the boiling of pure water on the clean surface experiment indicated an increase in the number of active nucleation sites compared to the boiling of pure water on NPD surface experiment (see Figure 4.17)

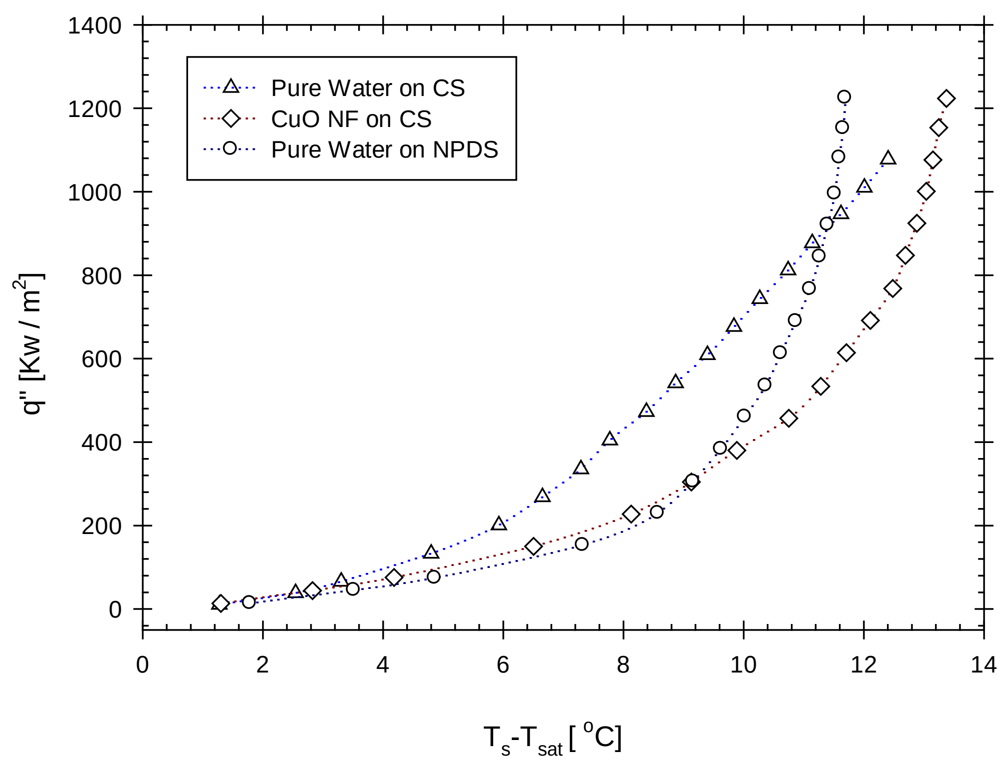

Figure 4.12 Boiling Curves obtained for the pure water on clean surface, 0.01% vol. CuO nanofluid and pure water on NPD surface for the Ra=420 nm surface

4.1.2.2. Initial Surface Condition with Ra =80 nm

As indicated before, three boiling experiments were carried out for each surface condition; pure water on a clean surface, nanofluid on a clean surface and a pure water on the NPD surface. Figure 4.12, shows the three boiling curves obtained for three boiling experiments for the case of Ra = 80 nm. The rate of heat transfer using the nanofluid enhanced compared to pure water. In order to quantify this deterioration the heat transfer rate ratio of the nanofluids and pure water at 11oC surface superheat was calculated. As shown in Table 4.3, the pure water heat flux was 396 kW/m2 while the CuO nanofluid heat flux was 506 kW/m2. In other words, in this case the rate of heat transfer deteriorated by about 27 %. The main reason behind this enhancement is the deposition of nanoparticles on the heater surface. As shown in Figure 4.16(c), the deposition pattern occurred in this case is less uniform compared to the case of Ra= 420nm. The non-uniformity in the deposition layer allowed the liquid to access the nucleation sites. Although, the surface wettability might was reduced as evident from the increase in the ONB temperature from 8.8 ^{o}C in the case of pure water on a clean surface to 9.6 ^{o}C in the case of pure water on a NPD surface (See Table 4.4) however, the difference between the two temperatures is within the uncertainty limits and it might been enhanced in this case.

The effect of nanoparticles deposition on the activating of the nucleation sites has been examined using high speed imaging of bubble growth process on the surface during boiling of pure water on the clean surface and boiling pure water on the NPD surface. The number of active nucleation sites was more in the latter case.

High speed imaging during the boiling of pure water on the NPD surface experiment indicated an increase in the number of active nucleation sites compared to the boiling of pure water on clean surface experiment (see Figure 4.17)

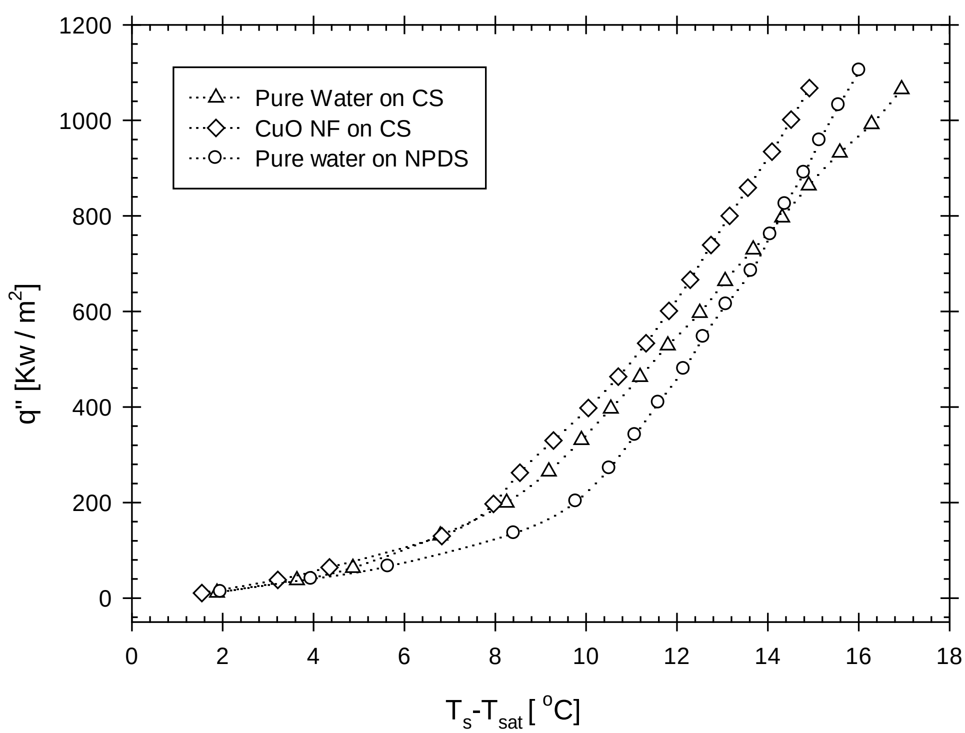

Figure 4.13 Boiling Curves obtained for the pure water on clean surface, 0.01% vol. CuO nanofluid and pure water on NPD for the Ra=80 nm surface

4.1.2.3. Initial Surface Condition with Ra = 20 nm

Figure 4.14 shows the three boiling curves obtained for the Ra = 20 nm surface. In this case, there is a 5% enhancement in the rate of heat transfer when using the nanofluids compared to pure water at 11^{o}C superheat (see Table 4.1).

It was observed that the trend in this experiment is opposite to the rest of the experiments. As shown in Figure 4.16(d) that the deposition pattern occurred in this case is uniform and covered almost the entire surface. The deposition layer prevented the liquid to access the nucleation sites also, reduced the wettability as evident from the increase in the ONB temperature from 8.8 ^{o}C in the case of pure water on a clean surface to 12.2 oC in the case of pure water on a NPD surface (See Table 4.4).

High speed imaging during the boiling of pure water on the clean surface experiment indicated an increase in the number of active nucleation sites compared to the boiling of pure water on NPD surface experiment (see Figure 4.17and Figure 4.9).

Although an enhancement in the rate of heat transfer was observed, this enhancement is within the uncertainty limits. And according to the high speed imaging records, the deposition ratio and the increase in the ONB temperature it is believed that this case showed deterioration in the rate of heat transfer.

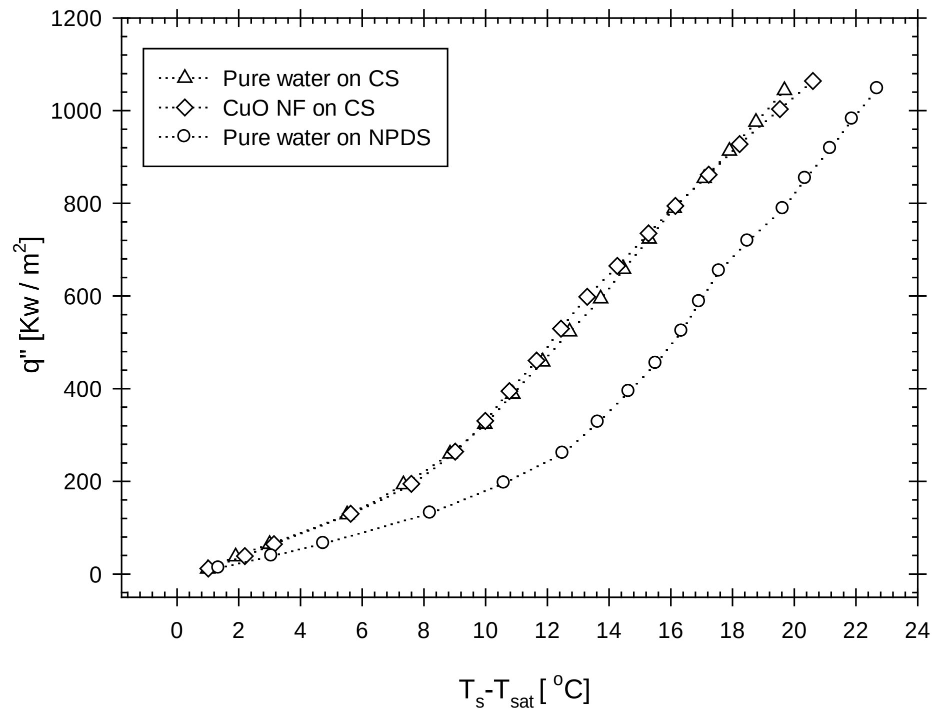

Figure 4.14 Boiling Curves obtained for the pure water on clean surface, 0.01% vol. CuO nanofluid and pure water on NPD for the Ra=20 nm surface

Table 4.3 Heat Flux values at 11 °C surface superheat

Ra (nm)	Pure water - Heat Flux (kW / m^2)	CUO - Heat Flux (kW / m^2)	% of Enhancement or Deterioration
420	877	518	-40 %
80	396	506	+27 %
20	392	412	+5 %

Table 4.4 Experimental results summary for 0.01 vol. %CuO nanofluid.

Dp (nm)	**550**	**550**	**550**
Ra (nm)	420	80	20
SPIP	0.764	0.145	0.036
Deposition Ratio	99.8%	86.0%	97.5%
Deposition Pattern	uniform	non-uniform	uniform
ONB for Pure Water on clean surface	6.5 ^{o}C	8.8 ^{o}C	8.8 ^{o}C
ONB for Pure Water on NDS surface	9.2 ^{o}C	9.6 ^{o}C	12.2 ^{o}C

As can be noticed from Table 4.4 and Figure 4.15 ; the enhancement in the heat transfer is related to the non-uniformity of the deposition layer. The threshold of the uniformity in this study is defined by 90% deposition ratio. It worth noting that for all cases where enhancement in the rate of heat transfer was observed, the deposition ratio was always less than 90% and for all cases where deterioration was observed, the deposition ratio was always above 90%.

Also, as shown in Table 4.4 the SPIP was evaluated for the three surface roughnesses. It was observed that in all cases the value of the SPIP was less than 1 (SPIP<1) and both enhancement and deterioration were observed.

.

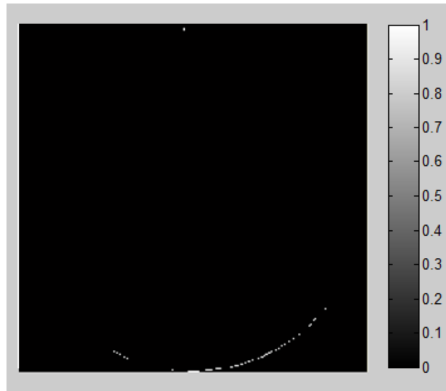

(a)

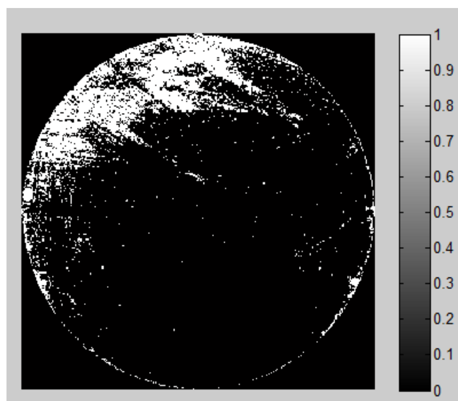

(b)

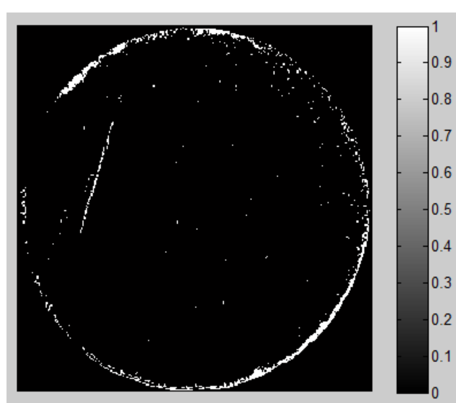

(c)

Figure 4.15 MATLAB processed images of the heater surface after 0.01 vol. % CuO nanofluid (a) Ra = 420 nm (b) Ra = 80 nm (c) Ra = 20 nm

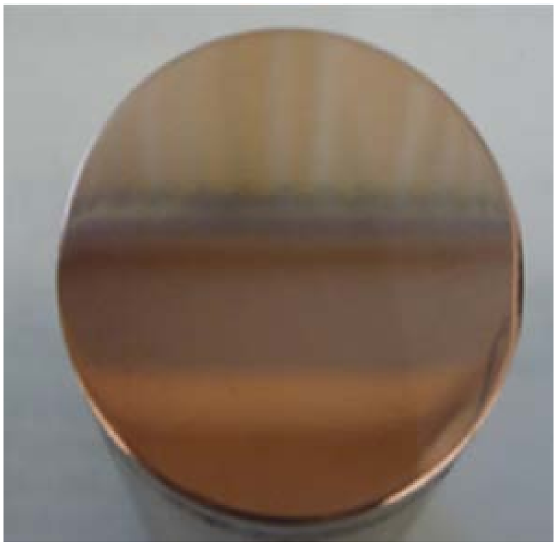

(a)

(b)

(c)

(d)

Figure 4.16 Images of the heater surface before and after 0.01% vol. CUO nanofluid (a) clean surface (b) Ra = 420 nm (c) Ra = 80 nm (d) Ra = 20 nm

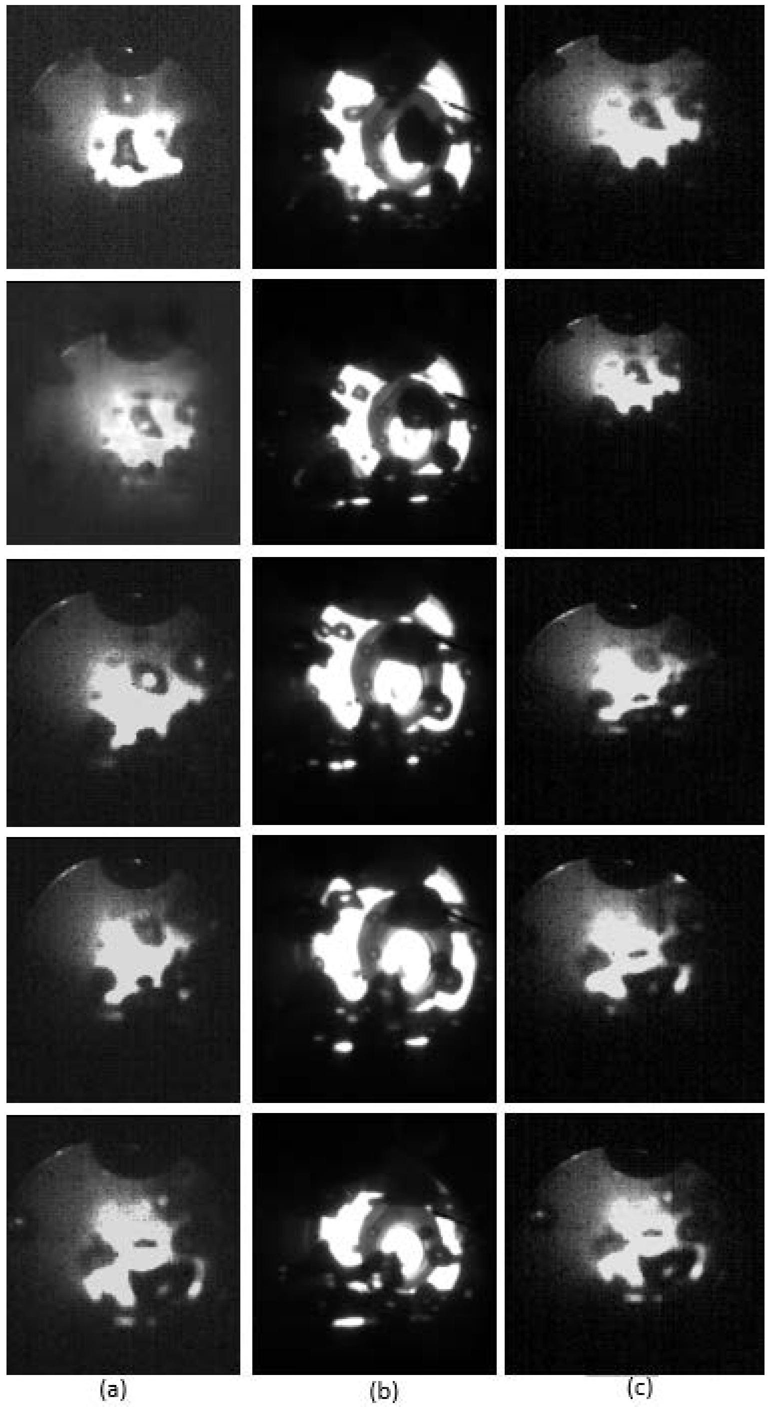

Figure 4.17 Images of 0.01 % vol. of CuO boiling from a clean surface (a) Ra = 20 nm (b) Ra = 80 nm (c) Ra = 420 nm

4.2. Effect of Nanoparticles Material (Al_2O_3 vs. CuO)

The effect of changing the nanoparticles material from aluminum oxide (Al_2O_3) to copper oxide (CuO) is discussed in this section. As been mentioned previously, the thermal conductivity of CuO is 13.5 W/m.K and for Al_2O_3 is 40 W/m.K, at room temperature. Considering that the nanofluids concentration was kept constant at 0.01% vol., one would expect the heat transfer rate in the case of Al_2O_3 to be higher than the heat transfer rate in the case of CuO.

4.2.1. Initial Surface Condition with Ra = 420 nm

Figure 4.18 shows the boiling curves obtained for the case of Ra = 420 nm. Results show deterioration in the heat flux when using both CuO and Al_2O_3 nanofluids compared to pure water. At 11^{o}C surface superheat, the Al_2O_3 showed more deterioration than CuO by 9%.

For better understanding of these results, one should consider the following three factors. The first factor, which is a major one – is the rate of deposition, referring to Figure 4.7(b) and Figure 4.16(b) one can see that the rate of deposition was higher in the case of Al_2O_3. The second factor is the SPIP, which represents the ratio between the surface roughness and the particle diameter. The effect of this parameter will be discussed in details in the discussion of the effect of nanoparticles size presented in section 4.4.

Considering the actual cluster sizes measured for the Al_2O_3 (193 nm) and CuO (550 nm), the values of the SPIP calculated for Al_2O_3 and CuO, are 2.2 and 0.76, respectively.

Considering the hypothesis proposed by Narayan et.al. [14], Al_2O_3 particles have a better chance to show block or split the nucleation sites.

The third factor is the thermal conductivity of the nanoparticles material. The thermal conductivity of CuO is about one third that of Al_2O_3 .Results shown in Figure 4.18 support that the effect of deposition dominated the effect of the SPIP and the thermal conductivity.

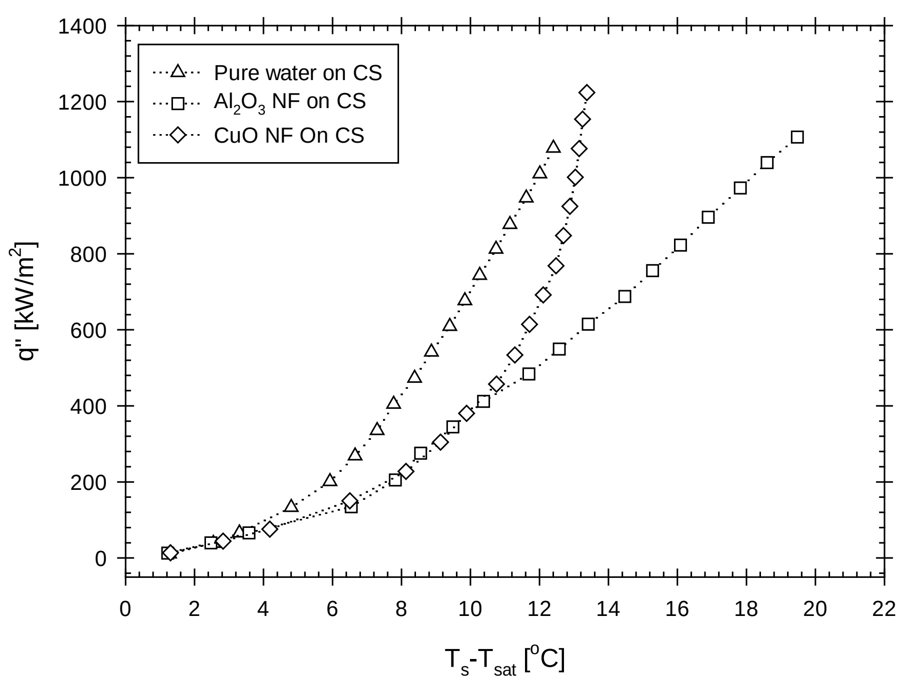

Figure 4.18 Effect of nanofluids material on boiling curves obtained using Ra = 420 nm surface

4.2.2. Initial Surface Condition with Ra = 80 nm

Figure 4.19 shows the boiling curves obtained for the case of Ra = 80 nm. Results show enhancement in the heat flux when using both CuO and Al_2O_3 nanofluids compared to pure water. At 11^{o}C surface superheat, the Al_2O_3 showed more enhancement than CuO by 14%.

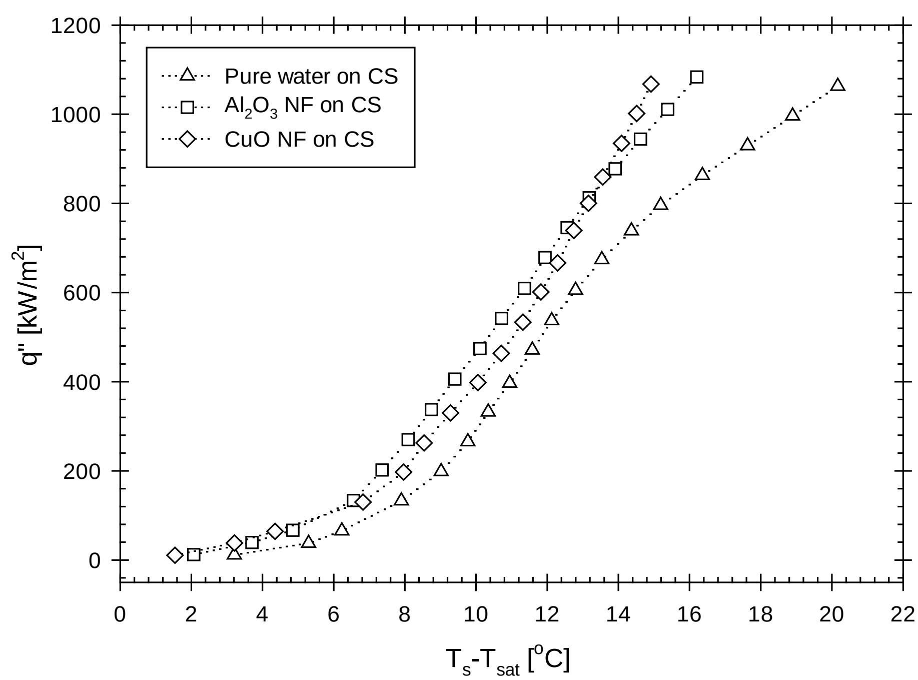

Figure 4.19 Effect of nanofluids material on boiling curves obtained using Ra = 80 nm surface

Considering the three factors mentioned previously, Figure 4.7(c) and Figure 4.16(c) show that the rate of deposition was higher is the case of CuO. Considering the calculated SPIP for Al_2O_3 and CuO are 0.4 and 0.15, respectively, both particles have a good chance to either block or split the nucleation sites. It was observed that the number of nucleation sites was increased in both cases. Results shown in Figure 4.19 suggest that the effect of deposition and the effect of SPIP dominated the effect of the thermal conductivity in this case.

4.2.3. Initial Surface Condition with Ra = 20 nm

Figure 4.20 shows the boiling curves obtained for the case of Ra = 20 nm. Results show enhancement in the heat flux when using both CuO and Al_2O_3 nanofluids compared to pure water. At 11^oC surface superheat the Al_2O_3 showed more enhancement than CuO by 29%.

Considering the three factors mentioned previously, Figure 4.7(d) and Figure 4.16(d); we can see that the deposition rate was less uniform in the case of Al_2O_3. Considering the calculated SPIP for Al_2O_3 and CuO are 0.1 and 0.04, respectively, both particles have a good chance to either block or split the nucleation sites. It was observed that the number of nucleation sites was increased in the case of Al_2O_3.

Results shown in Figure 4.20 suggest that the effect of deposition and thermal conductivity dominated the effect of the SPIP in this case.

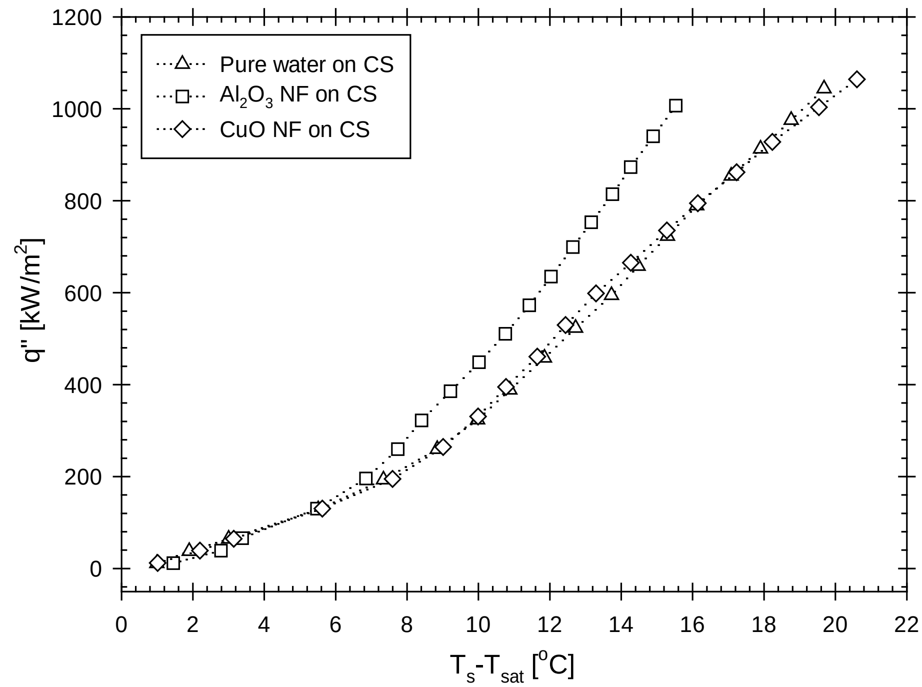

Figure 4.20 Effect of nanofluids material on boiling curves obtained using Ra = 20 nm surface

As seen from figures 4.18, 4.19 and 4.20, in the single phase region, the effect of using nanofluids either Al_2O_3 or CuO has insignificant effect on the rate of heat transfer however, it affected the ONB temperature. As nucleate boiling developed, the effect of using nanofluids became more observable and depending on the rate of deposition either enhancement or deterioration in the rate of heat transfer was observed.

To conclude what has been investigated in the previous two sections, Figure 4.21 presented the effect of surface initial condition (Ra) on the thermal behavior of pool boiling of pure water CuO and Al_2O_3 nanofluids with 0.01 % vol. concentration.

In the case of pure water, the heat transfer rate increased with the increase in the surface roughness value from 20 nm to 420 nm. This is due to the fact that the higher surface roughness surface has more active nucleation sites. In case of nanofluids, it was found that the heat transfer rate decreased with the increase in the surface roughness in case of Al_2O_3. In case of CuO, the heat transfer rate increased with the increase in the surface roughness.

Using nanofluids has a significant effect on the pool boiling rate of heat transfer. Both enhancement and deterioration was observed, and generally the effect of the rate of deposition dominated the effect of the SPIP and the thermal conductivity.

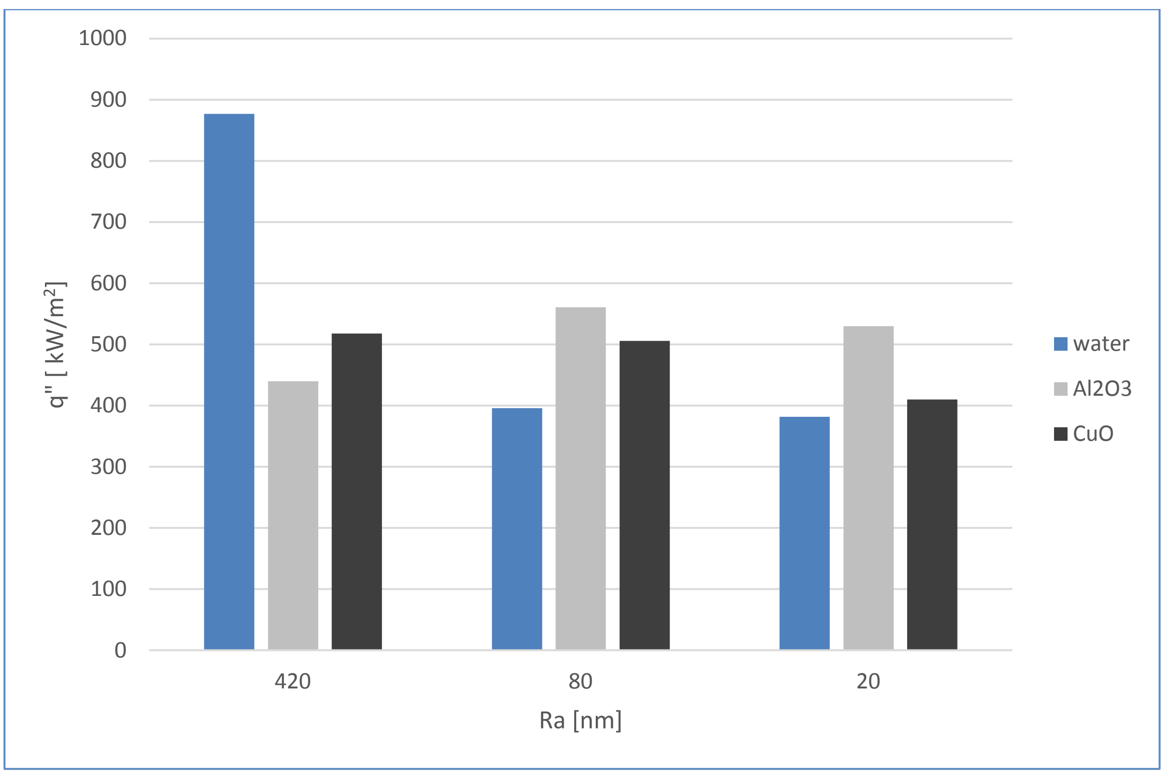

Figure 4.21 Effect of surface roughness and nanoparticles material on heat flux

4.3. Effect of Nanoparticles Concentration

The effect of nanoparticles concentration was investigated by performing another set of experiments using the three surfaces (Ra = 420 nm, Ra = 80 nm and Ra = 20 nm) and both CuO and Al_2O_3 nanofluids at a lower volumetric concentration of 0.005 vol. %.

4.3.1. Effect of Al_2O_3 Nanoparticles Concentration

By reducing the concentration to 0.005 vol. %, deterioration in the heat transfer with respect to pure water was still observed for the three surfaces. This deterioration was confirmed by filming the rate of nucleation happening on the surface during pure water boiling experiment on a clean surface and comparing it with the rate of nucleation during boiling pure water on the NPD surfaces. The number of active nucleation sites was lower when boiling occurred on the NPD surfaces (see Figure 4.3and Figure 4.27)

The boiling curves showing the concentration effect on pool boiling of Al_2O_3 nanofluids in the case of the Ra= 420 nm surface are shown in Figure 4.22. Concentrations, 0.01 vol. % and 0.005 vol. resulted in deterioration in the rate of heat transfer with respect to pure water. However, the deterioration is lower at the case of 0.005 vol. % .For example, at a surface superheat temperature of 11^{o}C, the level of deterioration recorded at the 0.01 vol. % and 0.005 vol. % concentrations was 49% and 36.4%, respectively. Which indicates that the heat flux obtained at the 0.005 vol. % concentration is about 13% higher than the one obtained at the 0.01 vol. % concentration.

By taking a closer look at the deposition layer for these two cases, Figure 4.26 (b) and Figure 4.7 (b), shows that both surfaces had a uniform deposition pattern, it is believed that the surface wettability was affected by the deposition layer and the contact angle was increased. The onset of nucleation temperature changed from 5.7 ^{o}C for the boiling of pure water on a clean surface to 11.8 ^{o}C for the case of boiling pure water on the NPD surface. The deposition ratio decreased from 99.2 in the case of 0.01 vol. % to 97.5% at 0.005 vol. %. The case with lower deposition ratio showed resulted in lower deterioration (see Figure 4.25 (a) and Table 4.6).

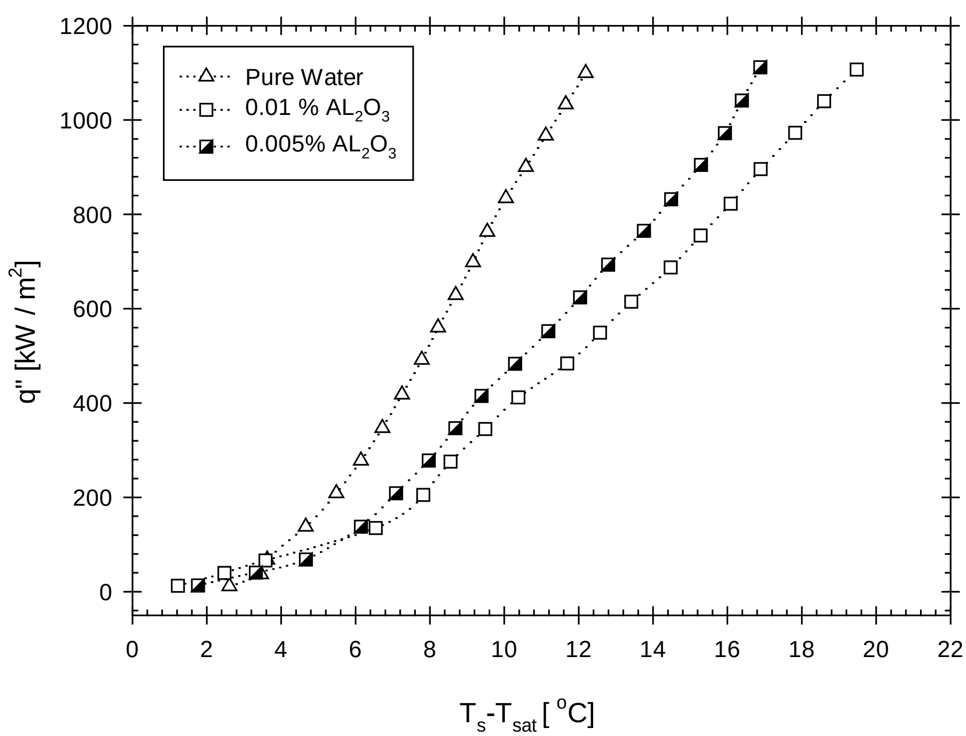

Figure 4.22 Effect of concentration of Al_2O_3 nanofluid in the case of Ra = 420nm surface

The boiling curves showing the concentration effect on pool boiling of Al_2O_3 nanofluids in the case of the Ra = 80 nm surface are shown in Figure 4.23. On the contrary to the case of 0.01 vol. %, deterioration in the rate of heat transfer was recorded at 0.005 vol. %. For example, at a surface superheat temperature of 11^{o}C, the level of enhancement recorded at the 0.01 vol. % concentrations and the deterioration recorded at the 0.005 vol. % concentration is 41% and 24.2%, respectively. Which indicates that the heat flux obtained at the 0.01 vol. % is about 65% higher than the one obtained at the 0.005 vol. %, concentration.

By taking a closer look at the deposition layer for these two cases, Figure 4.26 (c) and Figure 4.7 (c), shows that each surfaces has a different deposition pattern, it is believed that the surface wettability was affected by the deposition layer and the contact angle was increases in the case of 0.005 vol. %, and was reduced in the case of 0.01 vol. %.

The onset of nucleation temperature changed from 8.3 ^{o}C for boiling of pure water on a clean surface to 13.3 ^{o}C for boiling of pure water on NPD surface and the deposition ratio increased from 79.2 % in the case of 0.01 vol. % to 98.8% in the case of 0.005 vol. %. The case with lower deposition ratio resulted in enhancement in the rate of heat transfer (see Figure 4.25 (b) and Table 4.6).

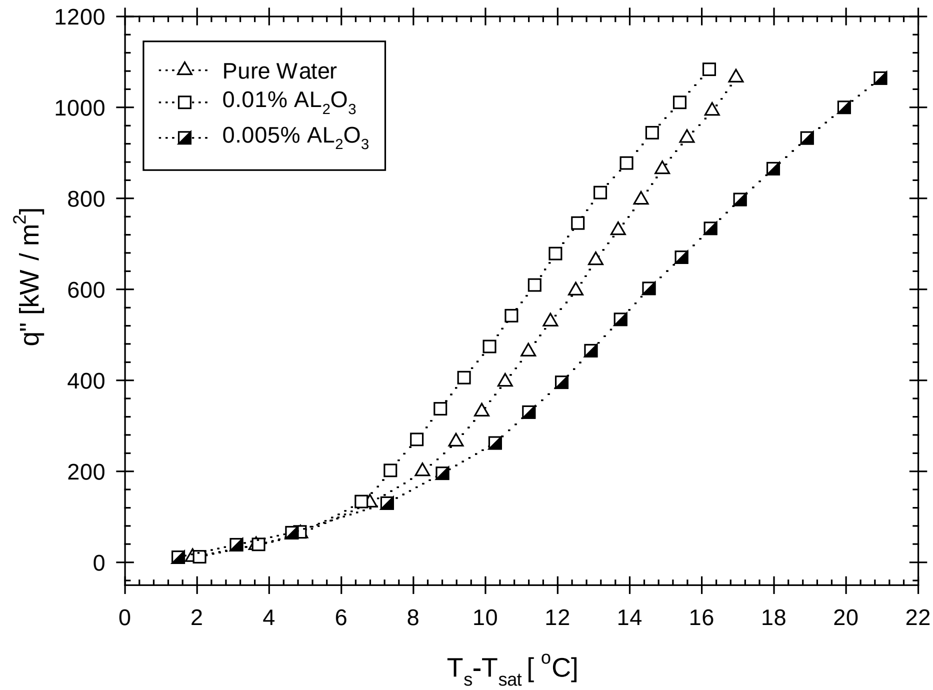

Figure 4.23 Effect of concentration of Al_2O_3 nanofluid in the case of Ra = 80nm surface

The boiling curves showing the concentration effect on pool boiling of Al_2O_3 nanofluid in the case of Ra=20 nm surface are shown in Figure 4.24. On the contrary to the case of 0.01 vol. % concentration, deterioration in the rate of heat transfer was recorded at 0.005 vol. % concentration.

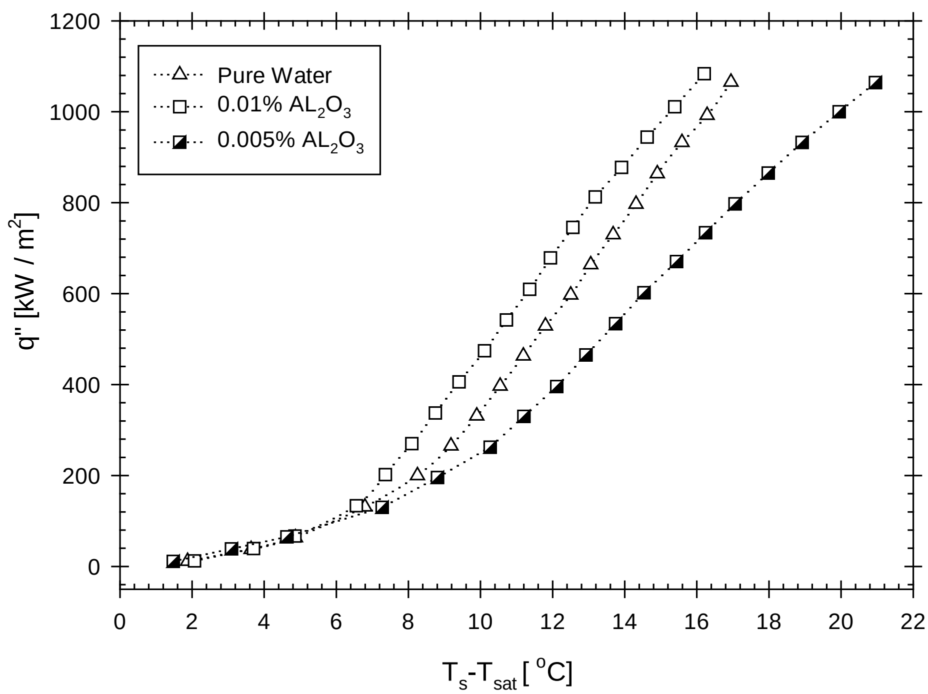

Figure 4.24 Effect of concentration of Al_2O_3 nanofluid in the case of Ra = 20nm surface

For example, at a surface superheat temperature of 11^oC, the level of enhancement recorded at the 0.01 vol. % concentration and the deterioration recorded at the 0.005 vol. % concentration is 34% and 13%, respectively. Which indicates that the heat flux obtained at the 0.01 vol. %, is about 47% higher than the one obtained at the 0.005 vol. %, concentration.

By taking a close look at the deposition layer for these two case, Figure 4.26 (d) and Figure 4.7 (d) show that each surfaces has a different deposition pattern, it is believed that the surface wettability was affected by the deposition layer and the contact angle was increases in the case of 0.005 vol. %, and was reduced in the case of 0.01 vol. %.

The onset of nucleation temperature changed from 8.3 ^{o}C for boiling of pure water on a clean surface to 13.3 ^{o}C for boiling of pure water on NPD surface and the deposition ratio increased from 82.8 % in the case of 0.01 vol. % to 96.8% in the case of 0.005 vol. %. The case with lower deposition ratio resulted in enhancement in the rate of heat transfer (see Figure 4.25 (c) and Table 4.6).

From the previous set of experiments it can be concluded that reducing the nanoparticles concentration showed both enhancement and deterioration in the rate of heat transfer of pool boiling of nanofluids. The effect of deposition rate dominated the effect of concentration.

Table 4.5 Heat Flux values at 11 ^oC for 0.005 vol. % Al_2O_3 nanofluid

Ra (nm)	Pure water - Heat Flux (KW / m^2)	Al_2O_3- Heat Flux (KW / m^2)	% Of Enhancement or Deterioration
420	877	558	-36.4 %
80	425	322	-24.2 %
20	417	362	-13.2 %

Table 4.6 Experimental results summary for 0.005 vol. % Al_2O_3 nanofluid

D_p (nm)	193	193	193
Ra (nm)	420	80	20
SPIP	2.176	0.414	0.104
Deposition Ratio	97.5%	98.8%	96.9%
Deposition Pattern	uniform	Uniform	Uniform
ONB for pure water on clean surface	5.7 ^oC	8.3 ^oC	8.5 ^oC
ONB for pure water on NPD surface	11.8 ^oC	13.3 ^oC	14 ^oC

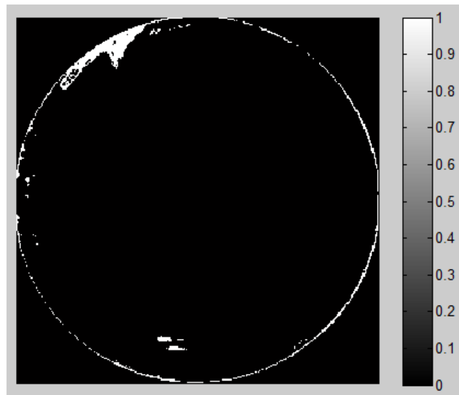

(a)

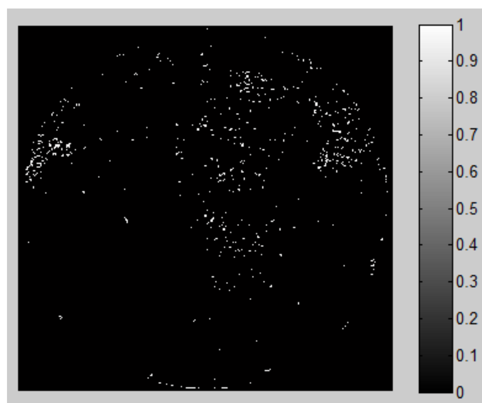

(b)

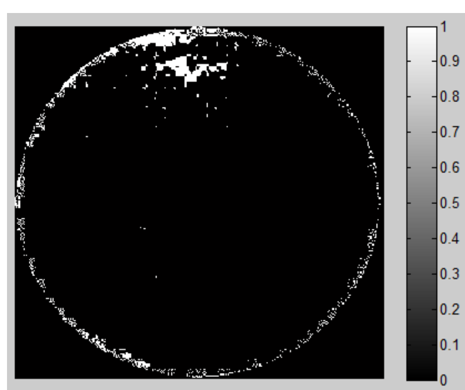

(C)

Figure 4.25 MATLAB processed images of the heater surface after 0.005 vol. % Al_2O_3 nanofluid boiling experiments (a) Ra = 420 nm (b) Ra = 80 nm (c) Ra = 20 nm

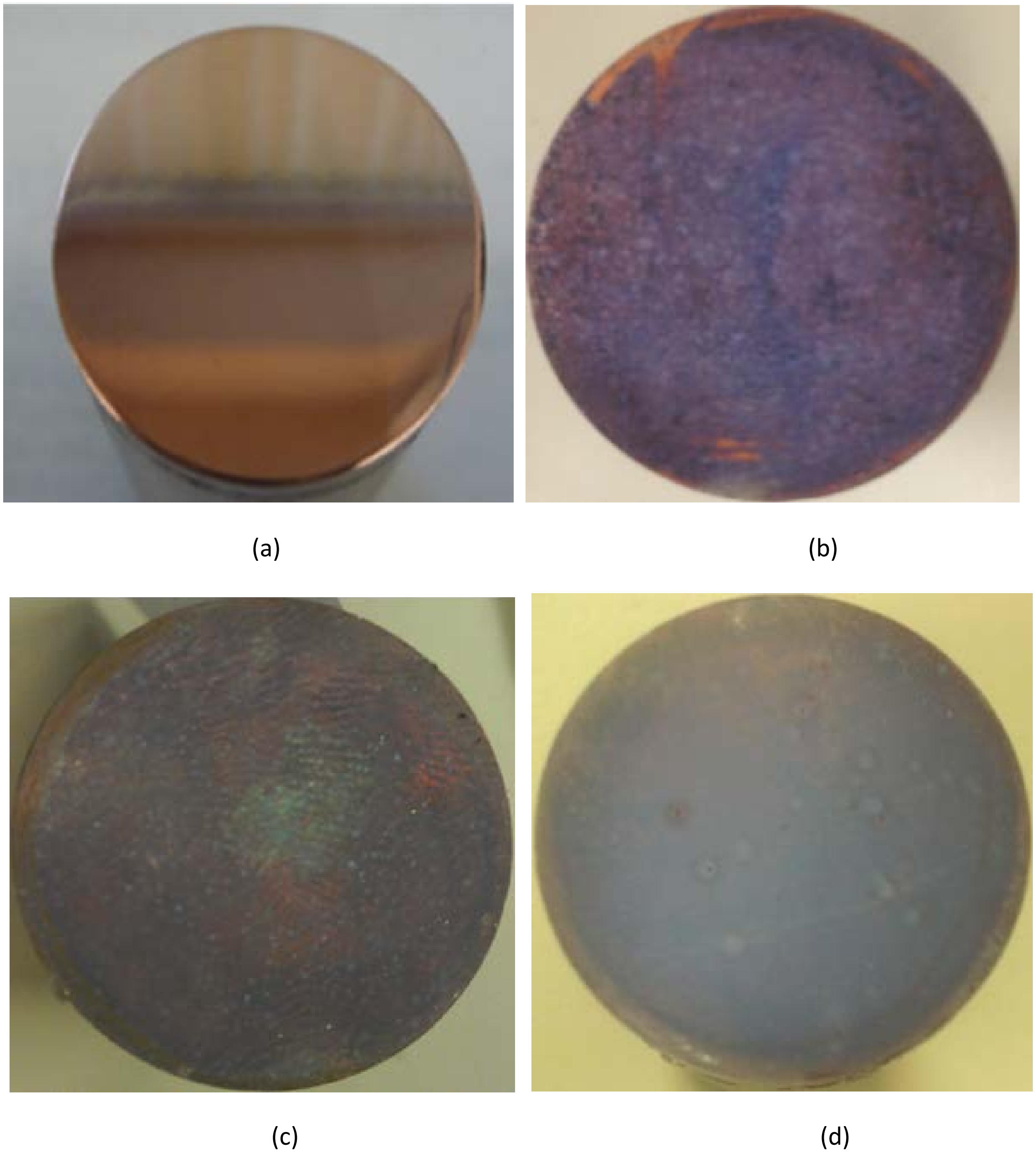

Figure 4.26 Images of the heater surface before and after 0.005% vol. Al_2O_3 nanofluid boiling experiments (a) clean surface (b) Ra = 420 nm (c) Ra = 80 nm (d) Ra = 20 nm

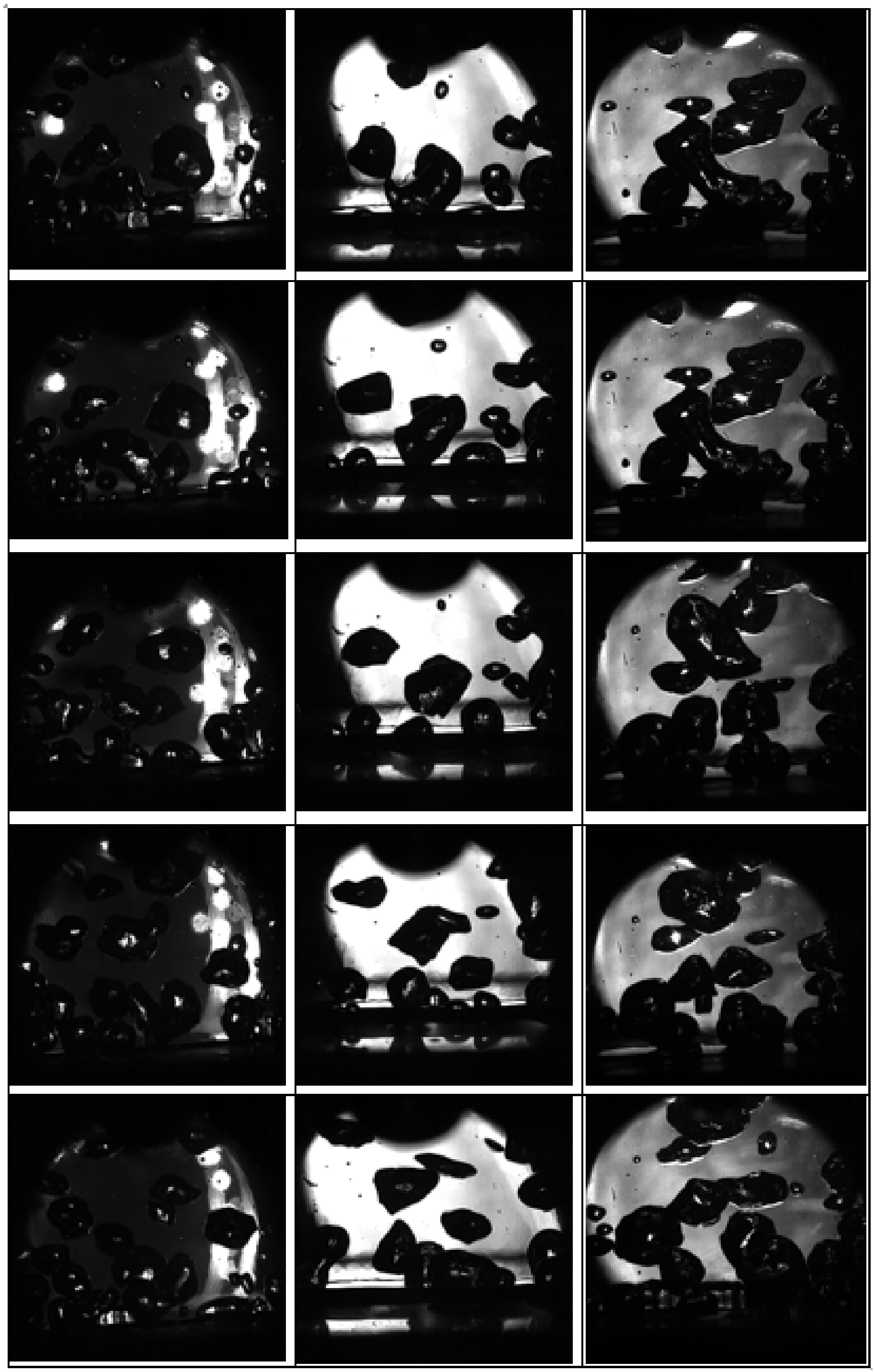

Figure 4.27 Images of 0.005 % vol. of Al_2O_3 boiling from a clean surface (a) Ra =20 nm (b) Ra= 80 nm (c) Ra= 420 nm

4.4. Effect of Particles Size

The last investigated parameter that affects the rate of heat transfer of pool boiling of nanofluids is the effect of particles size with respect to the surface condition. Alumina Oxide nanoparticles of 10 nm nominal initial particle size was used to perform another set of experiments. The same surface conditions of 420, 80 and 20 nm average surface roughness were prepared. The concentration was kept constant at 0.005 vol. %.

The boiling curves obtained for the 10nm and the 50 nm cases are shown in Figure 4.28, Figure 4.29 and Figure 4.30 .For the cases of boiling 10 nm Al_2O_3 nanofluid, results obtained for the three surface conditions showed deterioration in the rate of heat transfer when boiling nanofluid compared to boiling pure water. Also, for the three surface conditions, using the 10 nm Al_2O_3 particle size resulted in more deterioration in the rate of heat transfer compared to the case of using the 50 nm Al_2O_3 nanoparticles.

For example, in the case of Ra = 420 nm surface at surface super heat of 11^oC, deterioration rate about 85% was recorded using 10 nm particles compared to deterioration rate about 36% using 50 nm particles. Also, it is believed that the surface wettability was affected by the uniform deposition pattern occurred in both cases, as evident from the increase in the onset of nucleation temperature (ONB) by 8.5 ^oC and 6.1 ^oC for the case of using 10 nm and 50 nm particles, respectively. (See Table 4.7)

It worth noting that, the highest deterioration in the rate of heat transfer was observed in the case of Ra=420nm surface, which had the highest deposition ratio of 95.4% and 97.5% ^{o}C for the case of using 10 nm and 50 nm particles, respectively.

In the case of Ra = 80 nm surface at surface super heat of 11^{o}C, deterioration rate about 49% was recorded using 10 nm particles compared to deterioration rate about 24% using 50 nm particles. Also, it is believed that the surface wettability was affected by the uniform deposition pattern occurred in both cases, as evident from the increase in the onset of nucleation temperature (ONB) by 6.5 ^{o}C and 5 ^{o}C for the case of using 10 nm and 50 nm particles, respectively. (See Table 4.7).

In the case of Ra = 20 nm surface at surface super heat of 11^{o}C, deterioration rate about 26% was recorded using 10 nm particles compared to deterioration rate about 13% using 50 nm particles. Also, it is believed that the surface wettability was affected by the uniform deposition pattern occurred in both cases, as evident from the increase in the onset of nucleation temperature (ONB) by 2.8 ^{o}C and 5.5 ^{o}C for the case of using 10 nm and 50 nm particles, respectively. (See Table 4.7).

By using MATLAB, the processed images of the heater surface after boiling 10 nm Al_2O_3 nanofluids are shown in Figure 4.31.

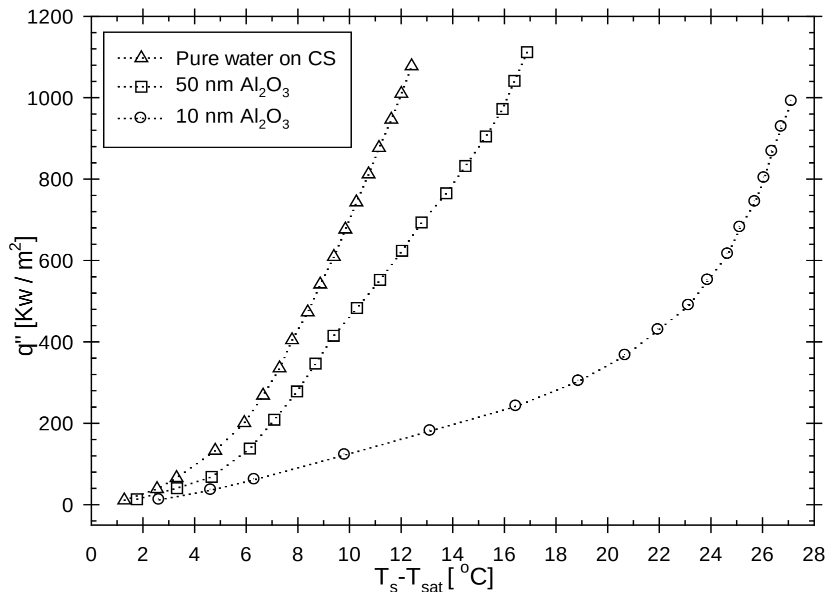

Figure 4.28 Boiling Curves obtained for boiling of pure water , 50 nm and 10 nm of Al_2O_3 nanofluid on a surface with Ra = 420 nm

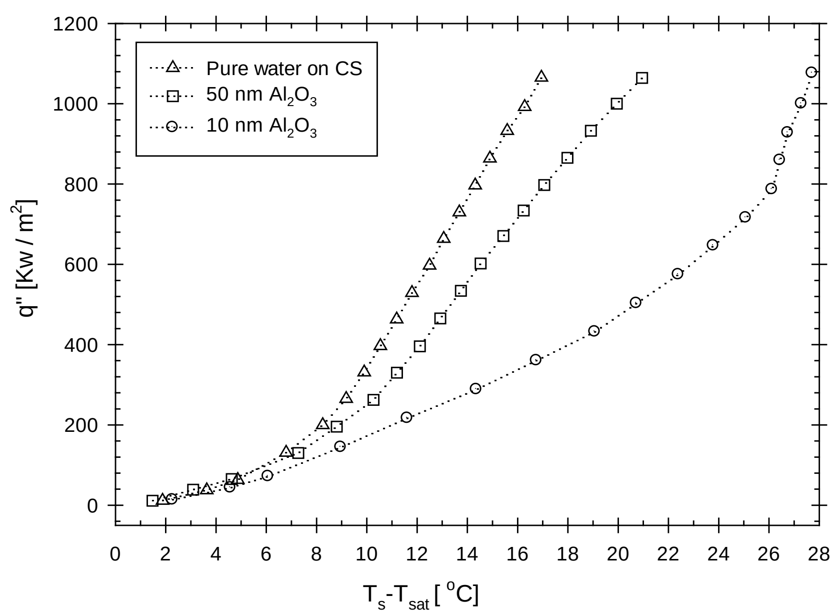

Figure 4.29 Boiling Curves obtained for boiling of pure water , 50 nm and 10 nm of Al_2O_3 nanofluid on a surface with Ra = 80 nm

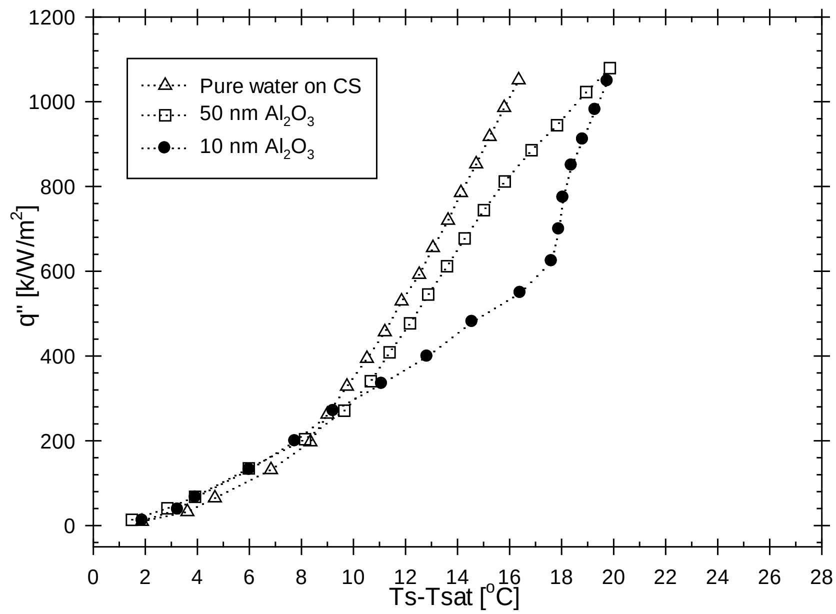

Figure 4.30 Boiling Curves obtained for boiling of pure water , 50 nm and 10 nm of Al_2O_3 nanofluid on a surface with Ra = 20 nm

Table 4.7 Experimental results summary for10 nm Al_2O_3

D_p (nm)	**30.58**	**30.58**	**30.58**
Ra (nm)	420	80	20
SPIP	13.734	2.616	0.654
Deposition Pattern	uniform	uniform	uniform
% of Enhancement or Deterioration	-85%	-49%	-26%
Deposition Ratio	95.4%	92.8%	93.4%
ONB for pure water on clean surface	6.7 ^{o}C	9.2 ^{o}C	9.3 ^{o}C
ONB for pure water on NPD surface	15.2 ^{o}C	15.7 ^{o}C	12.1 ^{o}C

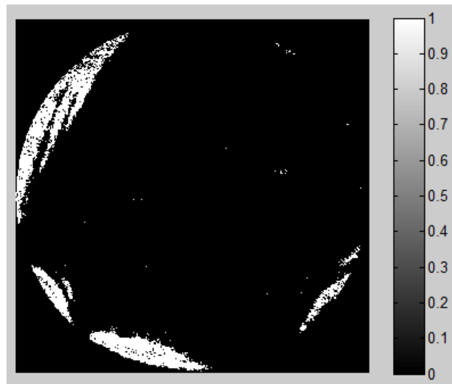

(a)

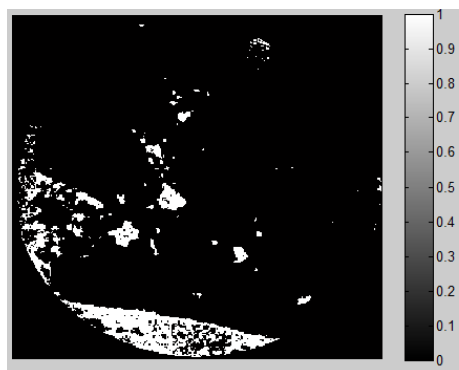

(b)

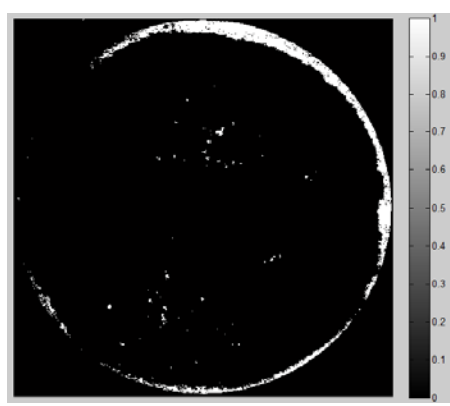

(C)

Figure 4.31 MATLAB processed images of the heater surface for 10 nm Al_2O_3 nanofluid boiling experiments (a) Ra = 420 nm (b) Ra = 80 nm (c) Ra = 20 nm

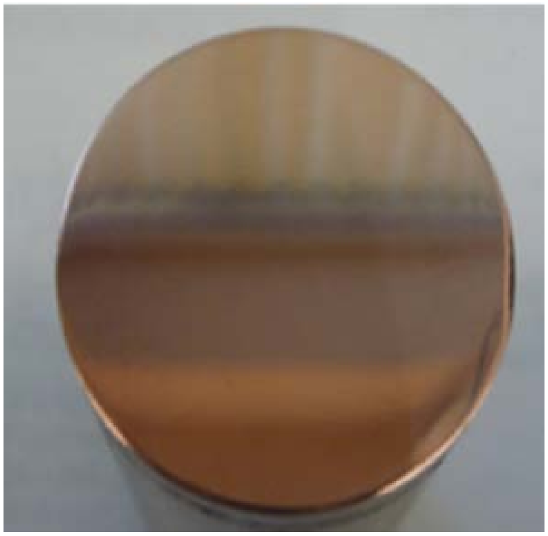

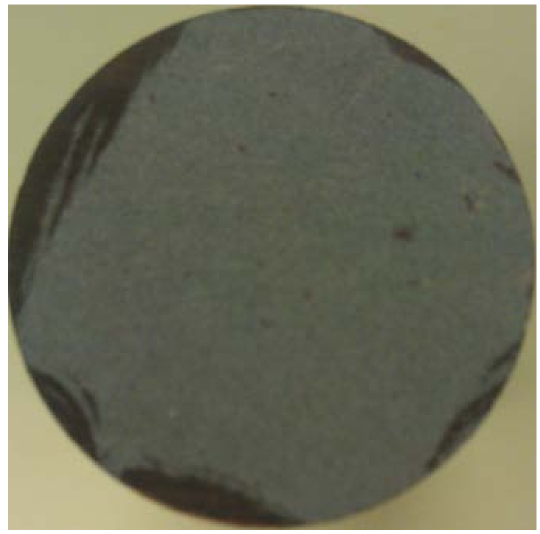

(a) (b)

(c) (d)

Figure 4.32 Images of the heater surface before and after the 10 nm Al_2O_3 nanofluid boiling experiments (a) clean surface (b) Ra = 420 nm (c) Ra = 80 nm (d) Ra = 20 nm

In order to investigate the effect of the SPIP on the pool boiling of nanofluids, both the 10 nm and 50 nm Al_2O_3 initial particle size experimental results for the 0.01 vol.% and 0.005 vol.% concentrations were analyzed. Considering the three surface roughness of 420nm, 80 nm and 20 nm and both the measured particle size and initial particle size, the calculated SPIP values ranged 0.1 to 13.7.

It worth noting that, the highest deterioration in the rate of heat transfer was observed at the highest SPIP values. While, the lowest deterioration in the rate of heat transfer was observed at the lowest SPIP values for the case of using 10 nm and 50 nm particles, respectively.

The experimental results showing the effect of the SPIP on the rate of heat transfer is shown Figure 4.33 and 4.34. It can be concluded that SPIP is not a major parameter that affects the heat transfer, as for the same SPIP value both deterioration and enhancement in the rate of heat transfer were observed. So by changing the particle size to a smaller size no enhancement was observed and it is now clear that the particles size has no significant effect on the heat transfer of the pool boiling of nanofluids. Also, surface roughness was changed during the experiment due to deposition; as deposition accumulated during the experiment on the heater surface. The SPIP is believed to be moving target and cannot be evaluated by using the initial surface roughness value and initial particle diameter.

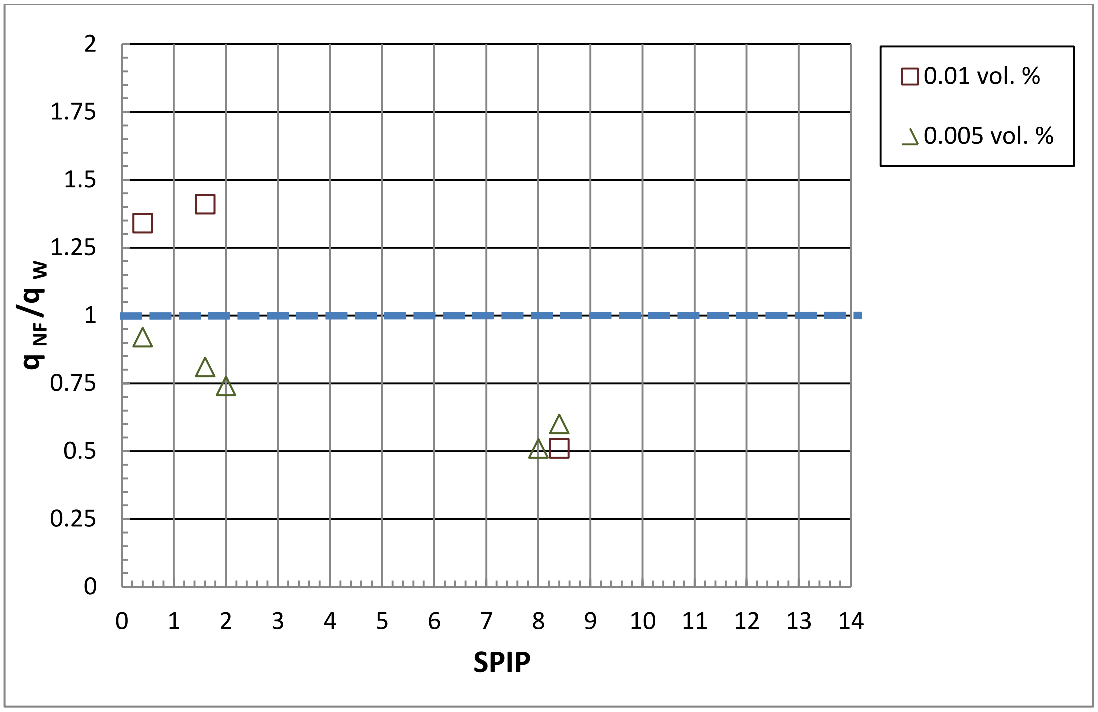

Figure 4.33 Variation of heat flux with SPIP (Al_2O_3) considering the average particles measured diameter

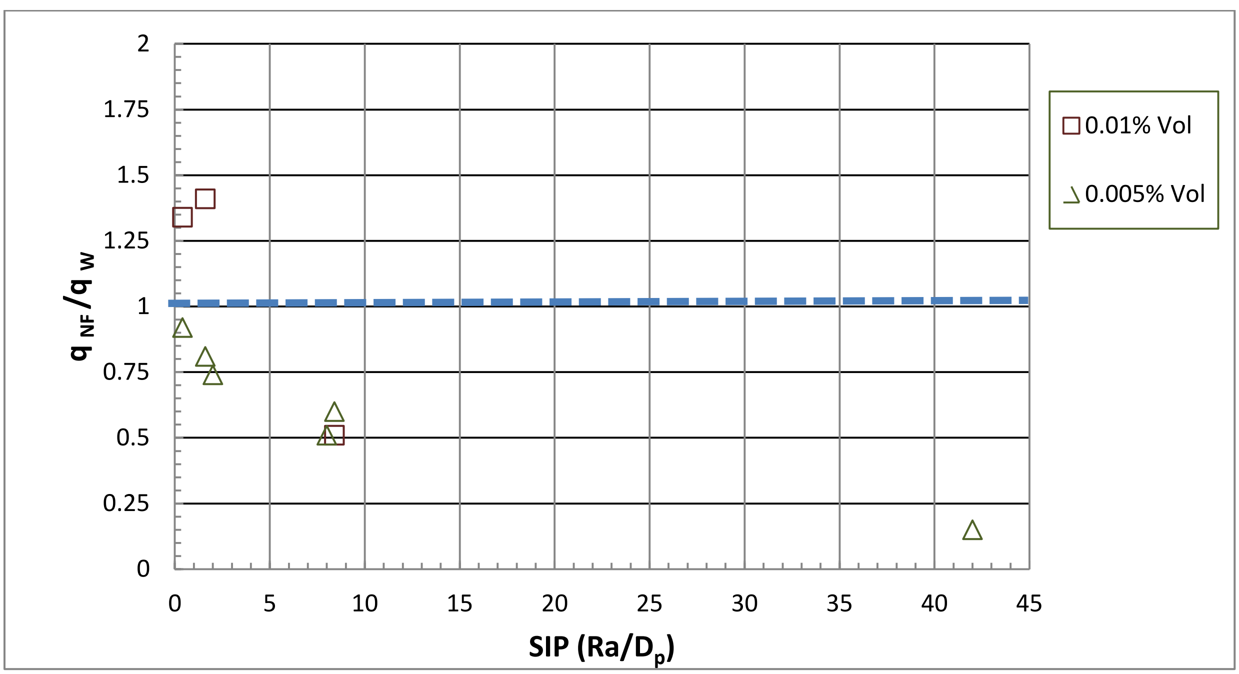

Figure 4.34 Variation of heat flux with SPIP (Al_2O_3) considering the initial particle diameter

Chapter 5
Boiling Under Submerged Impinging Jet

In this chapter a brief introduction of the concept of using submerged impinging jets is presented followed by a summary of the previous work carried out on boiling of nanofluids with submerged impinging jets. Then the modification of the experimental setup will be discussed. Finally, results of the jet impingement boiling (JIB) experiments will be presented and discussed. The JIB experiments have been carried out in three stages. Each stage will be discussed separately. In the first stage the effect of submerged impinging jet on the rate of heat transfer of pure water was investigated. The effect of submerged impinging jet using Al_2O_3 nanofluids was considered and the comparison between pool boiling and boiling under submerged impinging jets was conducted in the third stage of the investigation.

5.1. Introduction

Results presented in chapter 4 clearly indicated that nanoparticles deposition has a significant effect on the rate of heat transfer in pool boiling of nanofluids. It is, therefore, expected that the relative motion of nanofluids with respect to the heater surface could have an effect on the nanoparticles rate of deposition.

Impinging jets are widely used where high rates of heat transfer are required. Compared to other heat transfer methods, jet impingement boiling results in higher heat transfer rates. That is because of the effect of jet momentum on the flow boundary layer and the induced turbulence and mixing. Figure 5.1shows the development of a jet impinging on a heated surface. The flow field can be divided into three main regimes; (I) free jet region, (II) impingement zone and (III) wall jet zone.

In region (I) the surrounding fluid is entrained into the jet, thus reducing the jet velocity. This regime surrounds a core where the fluid velocity at the nozzle centerline is almost equal to the nozzle exit velocity. In the impingement zone near the surface a rapid decrease in the axial velocity and a corresponding increase in the static pressure take place. The wall jet zone is the zone where the velocity reaches its maximum value near the wall, then decreases along the wall.

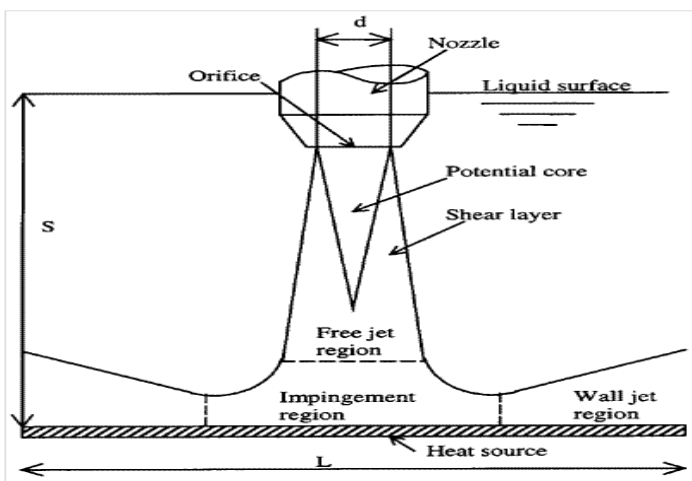

Figure 5.1 Schematic of the development of a submerged impinging jet [http://www.electronics-cooling.com]

Frost and Rüdel [28] carried out an experimental study to visualize the thermal and hydrodynamic development of a submerged water jet impinging on a flat surface.

De-ionize water seeded with 0.08 vol. % thermo-chromic microencapsulated liquid crystals was used for the visualization purpose. Initially, the temperatures of the heated surface and the surrounding water were 27 ^{o}C. The jet was isothermal as water at 34 ^{o}C.

They were able to visualize the shear layer. Flow characteristics typical to turbulent impinging jets were visualized; vortices, initiated at the edge of the jet are transported to the stagnation region, a wall jet develops, which rolls back and changes direction.

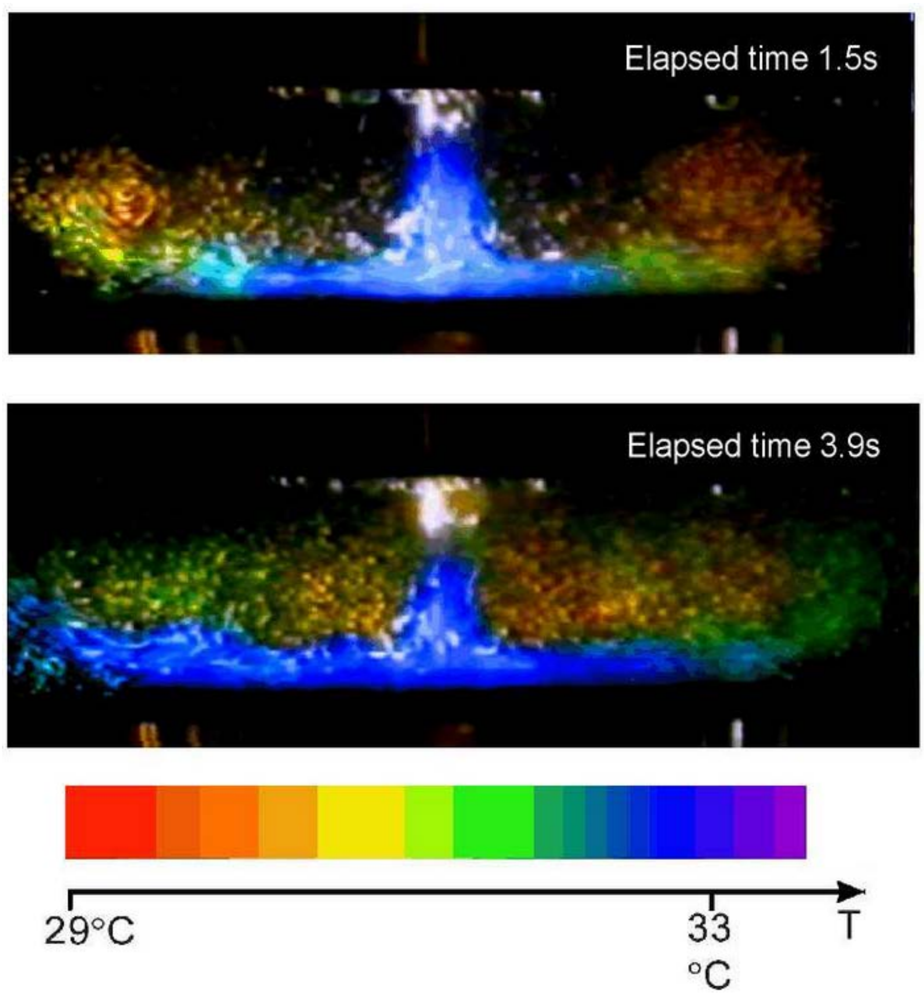

Figure 5.2 Visualization of flow and thermal fields of a water jet impinging on a flat surface [28]

A very limited work has been carried out using nanofluids with submerged impinging jets. Only two studies are relatively comparable to the current study. Nguyen et.al. [29] carried out an experimental investigation of boiling under confined and submerged Al_2O_3-water nanofluid jets impinging on a 30 mm diameter circular aluminum surface , the average surface roughness value was not reported. They used 36 nm Al_2O_3 particles size with volumetric concentration ranging from 0 to 6 %. The nozzle diameter was 3mm. The flow Reynolds number varied between 3800 and 88000, and Prandtl number varied from 5 to 10. The experimental setup consisted of a closed fluid circuit composed of a 10 liter open reservoir and a high head, all plastic, magnetically driven centrifugal pump. The vertical distance between the nozzle and the heated surface was adjusted using three precision mechanical guides and was adjusted at 2, 5 and 10 mm.

They reported both enhancement and deterioration in the heat transfer coefficient by using nanofluids compared to the case of pure water. The highest heat transfer rate was obtained at the intermediate nozzle to surface distance of 5 mm and concentration of 2.8%. At the same nozzle to surface distance and 6% concentration, the heat transfer rate deteriorated. At 2 mm and 10 mm nozzle to surface distances, the rate of heat transfer was deteriorated for both 2.8% and 6% concentrations. They also mentioned that due to the confinement of the jet, a large recirculation fluid zone was observed on the top of the heated surface (see Figure 5.3), which had a significant effect on the heat transfer rate and the thickness of this zone depends on the nozzle to surface distance. In the case of small nozzle to surface distance, this zone expected to be large. And as the nanoparticles are entrapped inside this zone, an unfavorable effect could occur when interacting with the radial flow near the reservoir bottom, which may explain the decrease in the heat transfer in the case of 6% vol. concentration.

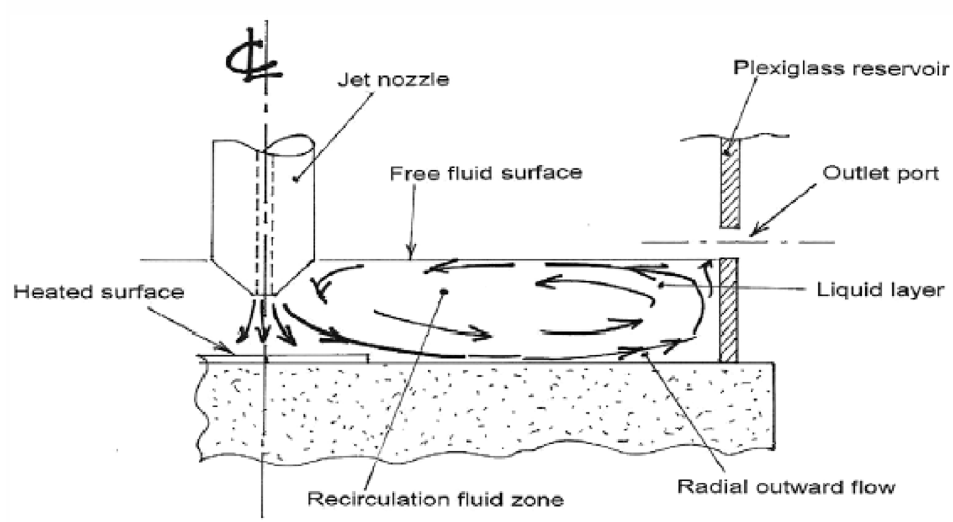

Figure 5.3 An illustrative view of the internal flow structure inside the reservoir [29].

Qiang Li et. al. [30] carried out an experimental investigation of boiling under confined and submerged Cu-water nanofluid jets impinging. Copper particles with 25 nm and 100 nm diameter were used with pure water as base fluid. Four different particle volume concentrations of 1.5%, 2.0%, 2.5% and 3.0% were investigated in this study. The flow Reynolds number varied between 2000 and 12000. The heating surface was a circular copper disk with 16 mm diameter and 4 mm height with an average surface roughness of 20 nm and 100nm. The nozzle had a 2 mm diameter. The vertical distance between the nozzle and the heated surface was adjusted at 2, 4 and 6 mm.

They concluded that, using Cu –water nanofluids increased the rate of heat transfer compared to using pure water. The heat transfer coefficient for Cu-water nanofluid was much higher compared to pure water at the same Reynolds number. They observed an increase in the rate of heat transfer by increasing the concentration. For example, in the case of 3.0% concentration, the rate of heat transfer was 52% higher by using nanofluids compared to pure water Also, considering the particles nominal size, it was observed that the heat transfer coefficient with 25 nm was higher than that with 100 nm Cu nanoparticles.

They proposed a new heat transfer correlation considering the effect of using nanofluids as well as the impinging jet, Equation (5.1).

$$Nu_{nf} = C_1(1.0 + C_2\emptyset^{m_1}Pe^{m_2})Re_{nf}^{m_3}\,Pr_{nf}^{1/3}[1.0 + a_1(H/D) + a_2(H/D)^2 + a_3(H/D)^3] \qquad (5.1)$$

All correlation coefficients, as well as all exponents, were found from data reduction.

Where: $C_1 = 0.2464$ $C_2 = 2.2061$ $m_1 = 0.8464$

$m_2 = 0.2715$ $m_3 = 0.5375$ $a_1 = 0.3923$

$a_2 = 0.0086$ $a_3 = 0.0259$

It worth noting here that the discrepancy between the experimental results and the values obtained using Equation 5.1 was found to be within $\pm 2\%$

5.2. The Present Impinging Jet Experimental Setup

The pool boiling experimental setup was modified to perform submerged impinging jet experiments. In order to have the fluid flowing through a complete closed circuit with indirect contact with the pump, a peristaltic pump was chosen to transport the fluid from the boiling vessel to the nozzle via a platinum cured silicon tubing system.

Both the pump head and the digital drive are shown in Figure 5.4. The high performance pump head consists of three rollers to squeeze the silicon tube. Rollers, bearings, rotor plates, and rotor shaft are made of stainless steel (SS) which offers high durability and long operating life. The digital drive offers a controllable flow rate from 0.001 to 3400 mL/min. The value of the flow rate depends on the drive rpm and tubing size. The brushless motor offers ±0.1% speed control accuracy, which indicates how accurate the flow rate delivered through the system.

Figure 5.4 Master flex Pump head and Digital Drive

The pump flow rate as a function of the pump speed and tubing sizes is shown in Figure 5.5. The tubing size used in this study is L/S 36 which gives a maximum flow rate of 3400 mL/min, and can be used with a maximum temperature of 230°C. Figure 5.6 shows the specifications of the L/S 36 silicon tubing.

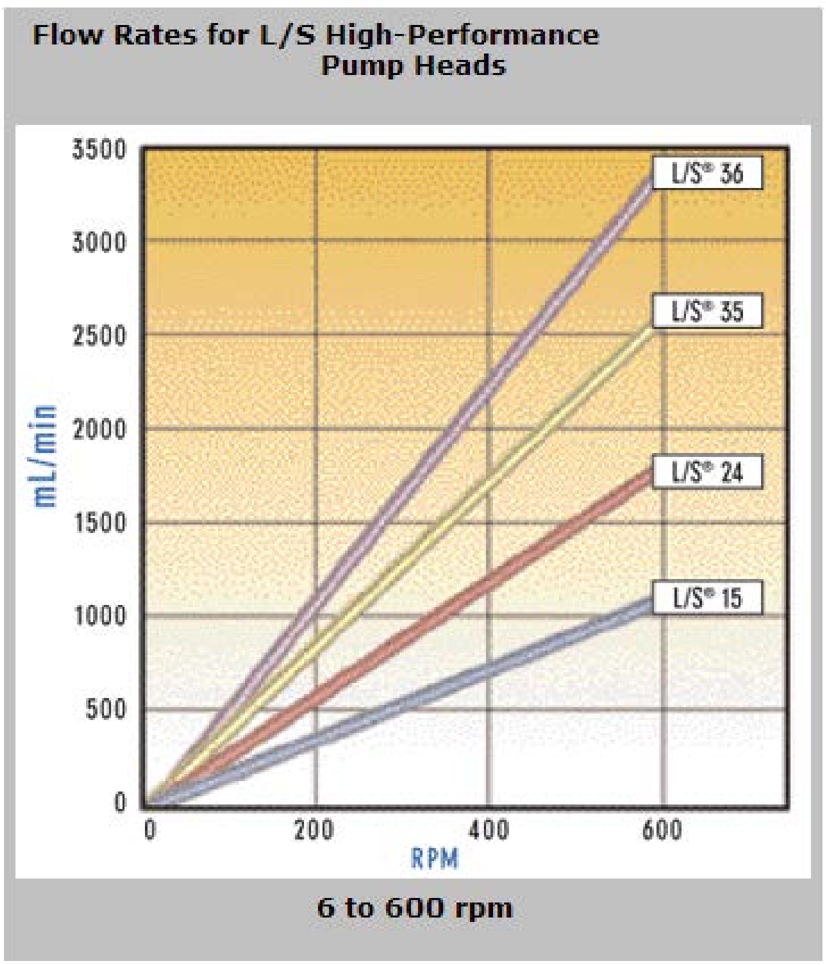

Figure 5.5 Pump flow rate curve

Specifications	
Product Type	Pump Tubing
Pump Series	L/S
Tubing formulation	Silicone
Sterilization Method	Autoclave
Min temperature (° F)	-58
Min temperature (° C)	-50
Max temperature (° F)	446
Max temperature (° C)	230
Masterflex tubing size (L/S)	36
Tubing ID (mm)	9.5
Tubing ID (in.)	0.38
Max pressure (psi)	20
Max pressure (bar)	1.4
Suction lift (ft H_2O)	27
Suction lift (m H_2O)	8.3
Flow range with 6 to 600 rpm drive with high performance head (ml/min)	34.8 to 3400

Figure 5.6 Master flex® platinum-cured silicone tubing, L/S® 36 Specifications

The modified experimental setup is shown in Figure 5.7. The boiling vessel was kept the same, except that the top window was removed to install a 1inch stainless steel fluid inlet pipe (5).

The system was then assembled and the silicon tube was connected to a 3 mm diameter nozzle via a hose barb. The silicon tube was braced by a 1inch stainless steel pipe to avoid nay unfavorable bends and also to maintain the nozzle in the same location.

In addition to all the thermocouples installed for pool boiling experiments, a new thermocouple was installed just before the nozzle (21) to measure the fluid temperature.

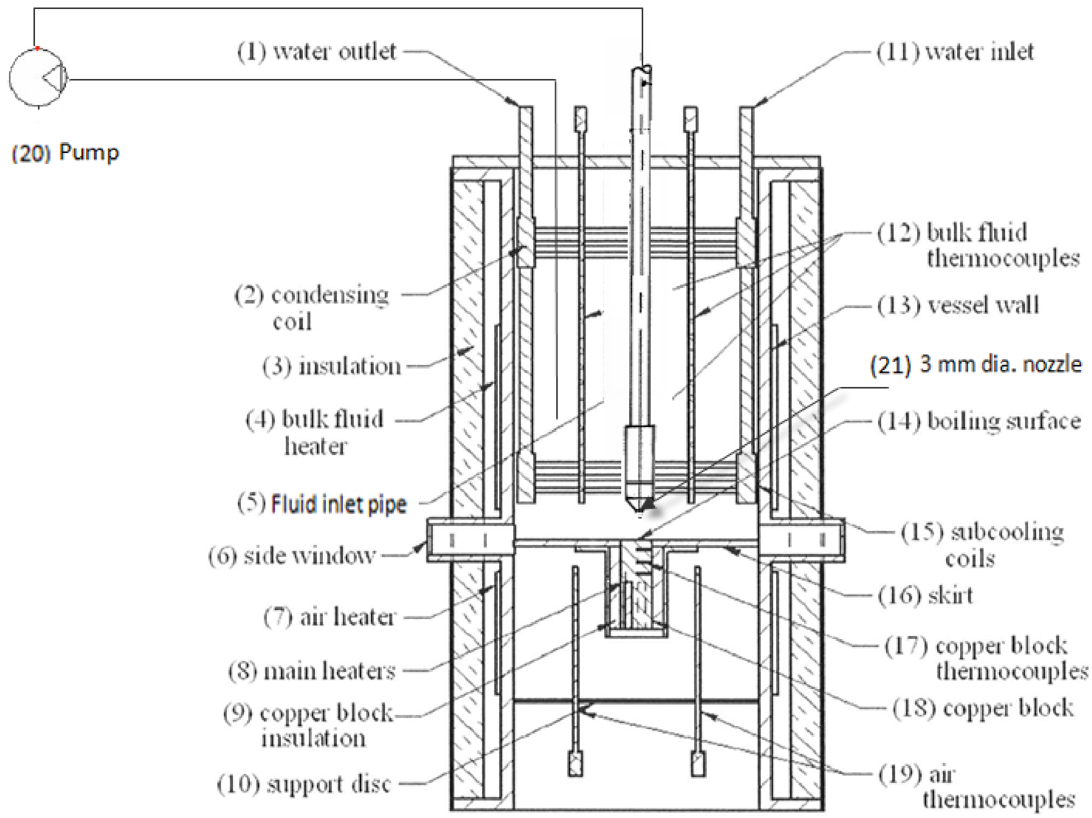

Figure 5.7 impinging jet experimental setup schematic

The same experimental procedure used for the pool boiling experiments was followed. When the bulk fluid temperature reached the saturation temperature, the bulk fluid heater was switched to the manual control and set to 50 % of the full power. At this point, the inlet condensing water valve was opened at a flow rate of 900 cm^3/min. The pump was then switched on to circulate the fluid. The liquid was allowed to continue boiling under these settings for 15 minutes in order to bring the whole vessel to a temperature close to the liquid saturation temperature. After the 15 minutes, the bulk fluid heater controller was switched back to the automatic control mode and the inlet condensing flow rate was adjusted to 300 cm^3/min. Then, the same procedure mentioned previously in Chapter 3 was followed.

5.3. Comparing Boiling under Submerged Jet with Pool Boiling

5.3.1. Boiling Under Submerged Impingement Jet

A set of experiments using the submerged jet was performed under the following conditions: nanoparticles concentration of 0.005%, heated surface roughness of 80nm, jet to surface vertical distance of 3 mm (i.e. $\frac{L}{D} = 1$) and pump flow rate of 0.054 Kg/s, which corresponds to Reynolds number of 101311.

Figure 5.8 shows the boiling curves obtained from the submerged impinging jet experiments. The use of nanofluids resulted in deterioration in the heat transfer performance compared with pure water. A 19% deterioration in the rate of heat transfer at surface superheat of 14 ^{o}C was observed.

Figure 5.11(b) shows an image of the heater surface after the JIB experiments. No deposition layer could be easily identified by visual inspection. However, it was assumed that a very thin layer of nanoparticles was deposited on the heated surface. This assumption was proofed by performing an experiment using pure water on the NPD surface. The boiling curves for these two pure water experiments are shown in Figure 5.8.

✓ Effect of SPIP

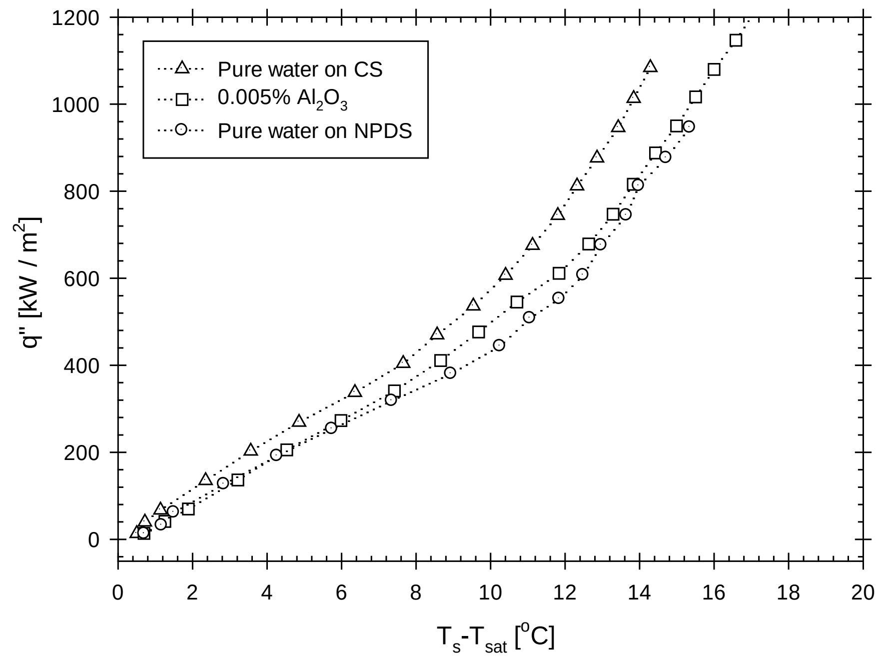

Figure 5.8 Boiling curves obtained from the JIB experiments at 0.005% Vol. AL_2O_3, Ra = 80 nm, L/D=1 and m = 0.054 Kg/s.

The deterioration in the rate of heat transfer of pure water under submerged impinging jet is believed to be due to the deactivation of nucleation sites because of the nanoparticles deposition. Also, as mentioned previously in the pool boiling case discussed in Chapter 4, it is believed that nanoparticles deposition reduces the wettability of the heated surface which affects the onset of nucleate boiling temperature. The ONB temperature increased from 9.7 ^{o}C in the case of pure water on a clean surface to 11.4 ^{o}C in the case of pure water on the NPD surface.

5.3.2. Comparison between Pool Boiling JIB

Figure 5.10 shows the boiling curves obtained for both pool boiling and JIB experiments of 0.005% Al_2O_3 nanofluids. Results show an enhancement in the rate of heat transfer in the case of JIB compared to the pool boiling experiment. As shown in Table 5.2, the ONB occurred by surface superheat of 8.3^{o}C and 9.7^{o}C for pool boiling and JIB, respectively.

As expected, the heat transfer rate in the case of boiling under submerged jet is much higher compared to the pool boiling of pure water. This could be observed from the higher heat flux value that was achieved by using submerged impinging jet. In case of natural convection at 6^{o}C superheat, the heat flux value 92.46 kW/m^2. However, in case of submerged impinging jet, the heat flux value at the same superheat 314.6 kW/m^2. That indicates a 240 % enhancement in the heat transfer performance.

For region II (Two-phase), at 14 ^{o}C superheat it is still observable that using the JIB resulted in enhancement in the rate of heat transfer. However, the question now is, between the forced conviction and the nucleate boiling, which mechanism is dominated In order to try to answer this question, few assumptions were made for the following analysis:

- All water thermal properties were evaluated at the saturation temperature
- Bubbles dynamics were neglected.

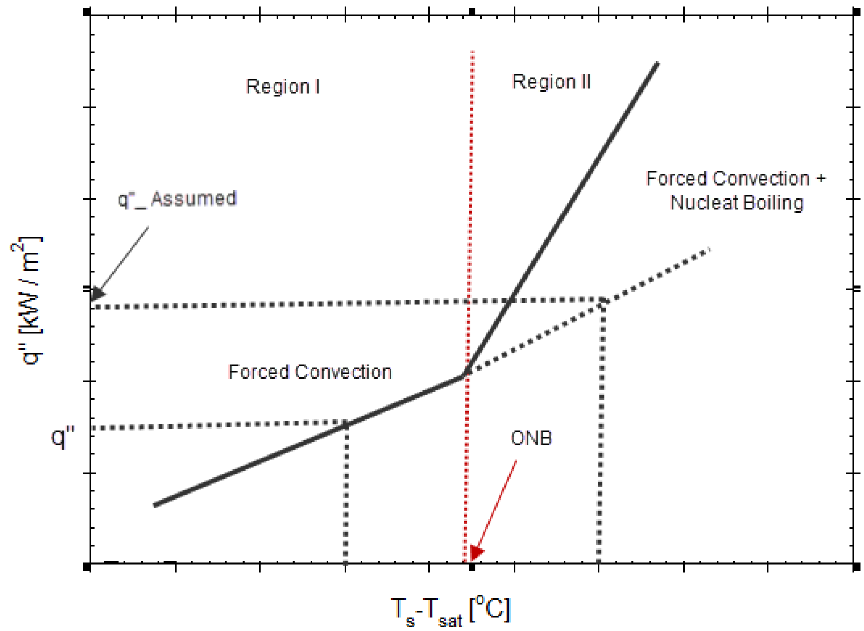

Figure 5.9 Illustrative graph showing Region I and Region II for boiling under submerged jet

Web et al [31] proposed a correlation to calculate the Nusselt number for single phase liquid submerged impinging jet (Equation 5.2) which is basically a function of jet 's Reynolds number ,Prandtl number and the ratio between the nozzle to heater surface and nozzle diameter.

$$Nu = C\, Re^{0.5}\, Pr^{1/3}\, [a \left(\frac{H}{D}\right) + b \left(\frac{H}{D}\right)^2 + d \left(\frac{H}{D}\right)^3] \tag{5.2}$$

This correlation was used to calculate the value of forced convection heat transfer coefficient in region I and compare it with the experimental value. Then assuming no phase change, the forced convection heat transfer coefficient was calculated at 14 ^{o}C superheat and the difference between the total heat transfer coefficient and the calculated forced convection heat transfer coefficient was assumed to be the nucleate boiling contribution to the heat transfer performance.

At 14 ^{o}C superheat, the heat transfer coefficient 74.285 $kW/m^2.K$, Equation 5.2 was used to predict the single phase forced convection heat transfer coefficient at the same superheat temperature. As mentioned previously all the properties in this equation were calculated at water saturation temperature. Nusselt number value 441.398, hence the forced convection heat transfer coefficient value 46.857 $kW/m^2.K$. subtracting this value from the heat transfer coefficient to get the nucleate boiling heat transfer coefficient separately as 27.428 $kW/m^2.K$. That means that the heat transfer is approximately 36% due to the nucleate boiling and 64% due to the forced convection heat transfer formed by the submerged jet.

The same analysis concept was implemented to compare the case of using nanofluids instead of pure water. In this case we have to accommodate for the change in the nanofluids properties. The models proposed in Table 2:1 were used to calculate the thermal properties in Table 5.1.

Table 5.1 Nanofluid properties as function of particle volume concentration

Properties	Water	0.005% Al_2O_3	Units
μ	0.0002275	0.0002278	Ns/m^2
K	0.6725	1.00014	W/m.K
ρ	958.3	958.4	Kg/m^3
C_p	4219.0	4218.8	J/Kg k
α	1.66334E-07	9.21586E-08	m^2/s
Pe	306172.95	489211.16	N/A
Pr	1.4303	0.9599	N/A

In the case of nanofluids, Figure 5.10 shows the boiling curves obtained for booth pool boiling and JIB experiments using Al_2O_3 nanofluid. Equation 5.1 was used to calculate the Nusselt number for single phase forced convection heat transfer assuming to phase change.

In the case of submerged impinging jet at 14 ^oC superheat, the total heat transfer coefficient 59.7 kW/m^2 .K, Nusselt number value 197.5, hence the forced convection heat transfer coefficient value 20.9 kW/m^2 .K. subtracting this value from the total heat transfer coefficient to get the nucleate boiling heat transfer coefficient separately as 38.8 kW/m^2 .K. That means that the heat transfer is approximately 65% due to the nucleate boiling and 35% due to the forced convection heat transfer formed by the submerged jet.

Equation 2.1 was used to calculate the Nusselt number and implicitly the nucleate boiling heat transfer coefficient for the pool boiling experiment. The Nusselt value is 336 and hence the heat transfer coefficient value 35.6 $kW/m^2.K$. It was observed that the nucleate heat transfer coefficient in case of submerged jet is 8% higher than the pool boiling case, which believed to be due to the jet effect on the nanoparticles deposition pattern. As shown in Figure 5.11(b), the deposition layer was hardly observed by visual inspection.

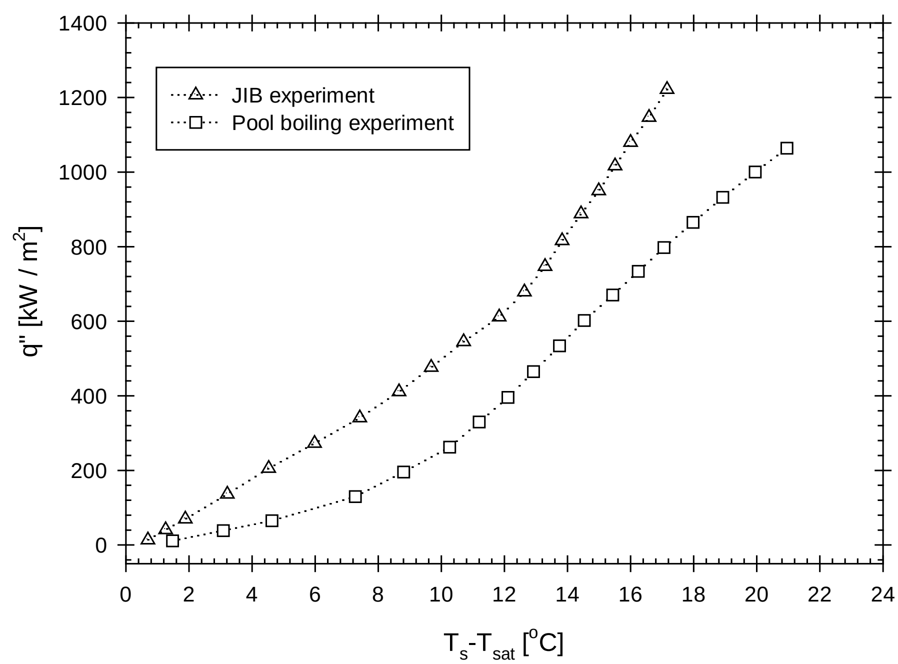

Figure 5.10 Boiling curves obtained for pool boiling and JIB of 0.005% Vol. AL_2O_3

The heat transfer performance of using Al_2O_3 nanofluid under submerged impinging jet of a flat surface , was found to be more effective than just adding the nanoparticles in a quiescent liquid (i.e. pool boiling). The rate of heat transfer was enhanced due to the contribution of the forced convection with the nucleate boiling.

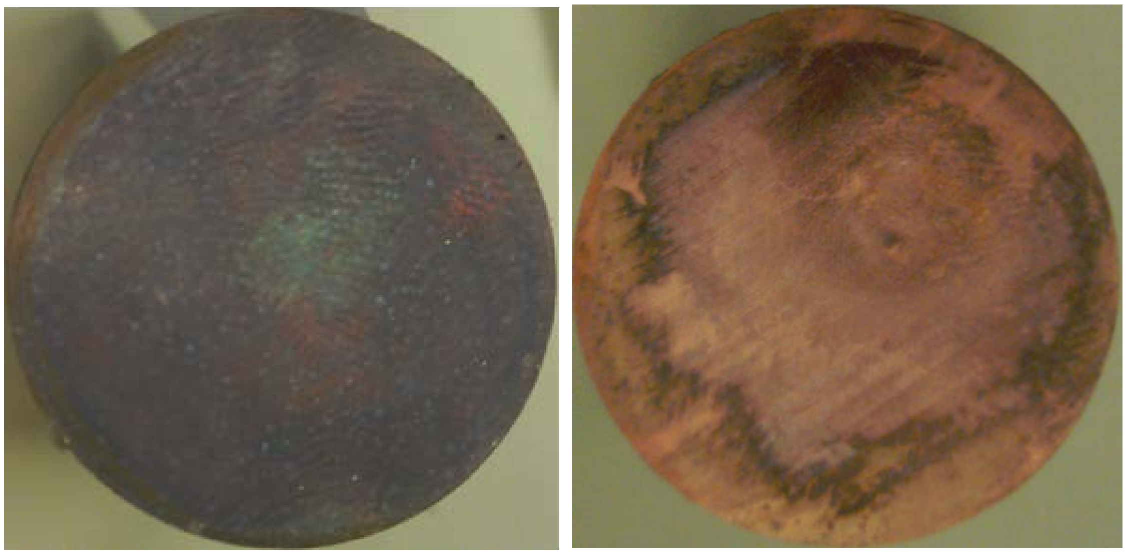

Figure 5.11 Images of the heater surface after 0.005% vol. AL_2O_3 nanofluids (a) Pool Boiling (b) JIB

Table 5.2 Experimental results comparing the pool boiling of nanofluids to JIB

	Pool Boiling	**Submerged Impinging Jet**
D_p (nm)	193	193
Ra (nm)	80	80
SPIP	0.414	0.414
pH Level	6.5	6.5
% of Enhancement or Deterioration	- 25%	- 19 %
ONB for pure water on CS	8.3 ^oC	9.7 ^oC
ONB for pure water on NPD Surface	13.3 ^oC	11.4 ^oC

Chapter 6
Summary, Conclusions and Recommendations for Future Work

This chapter summarizes the salient results of this study. A comparison with the findings in the literature review is presented for each set of experiments

6.1. Summary and Conclusions

6.1.1. Pool Boiling of Nanofluids

An experimental study characterizing the effect of surface initial conditions, nanoparticles material, nanoparticles concentration, and nanoparticles size on the pool boiling of nanofluids was carried out.

Three flat copper surfaces were prepared and polished using emery sand papers. The resulted surface roughness values were 20, 80,420 nm. Both Aluminum Oxide (Al_2O_3) and Copper Oxide (CuO) nanoparticle materials were used in this study. Three different volumetric concentrations (pure water, 0.01, 0.005 vol. %), were investigated. Two different Al_2O_3 particles initial sizes of 10 nm and 50 nm were used in this study.

It was found that, in case of pure water, the heat transfer rate increased with the increase in the surface roughness value from 20 nm to 420 nm. This is believed to be due to the fact that the higher surface roughness surface has more active nucleation sites. The same trend was observed in the case of boiling CuO nanofluids. However, in the case of boiling Al_2O_3 nanofluids, the trend was contrary to pure water experiments, as the surface with the highest surface roughness (Ra =420 nm) showed the lowest heat transfer rate.

The nanoparticles material was changed from Al_2O_3 to CuO in order to investigate the effect of nanoparticles material on the rate of heat transfer of pool boiling of nanofluids. Using Al_2O_3 nanofluid showed enhancement in both cases of initial surface condition of Ra = 80 nm and Ra = 20 nm with respect to CuO nanofluid, however for the case of initial surface condition of Ra = 420 nm the CuO nanofluid showed more enhancement than Al_2O_3 nanofluid.

Nanoparticles concentration was investigated and it was concluded that, reducing the concentration deteriorated the rate of heat transfer. For both Ra = 80 nm and Ra = 20 nm surfaces, boiling 0.01 vol. % of Al_2O_3 resulted in enhancement in the rate of heat transfer. However, in the case of boiling 0.005 vol. % of Al_2O_3, deteriorated the rate of heat transfer. In the case of Ra = 420 nm, both concentrations resulted in deteriorated the rate of heat transfer.

The effect of nanoparticles size represented by the SPIP =Ra / dp was investigated. It was found that SPIP is not to be the major parameter that can be used to describe the trends obtained using nanofluids. The nanoparticles deposition was found to be the dominated factor that can be used to define either an enhancement or a deterioration trend. In all carried out experiments, surfaces with deposition ration less than 90 % showed enhancement in the rate of heat transfer .And, deterioration trend was observed for surfaces with deposition ratio more than 90%. So, the threshold for the enhancement /deterioration was found to be 90% deposition ratio.

Few studies were found to be comparable with the current study, as mentioned previously, the main reason for the contradicting results found in the literature review is the difference in the experimental conditions used in each study. Table 6.1 gives a summary of the previous studies comparable with the current study.

Most of the previous investigations used high nanoparticles concentrations and hence the main trend was deterioration in the heat transfer coefficient. That was the motivation to consider lower nanoparticles concentrations in this study.

Although the main trend in the previous investigations was deterioration, in the current study both enhancement and deterioration were observed. It is believed that the observed trends in the current study are in good agreement with the previous investigations showed in Table 6.1. All previous investigators observed less deterioration in the heat transfer coefficient as the concentration was lowered. Hence, it is expected to have enhancement in the heat transfer by reducing the concentration.

Finally, a new quantifying parameter was proposed and investigated in the current study. This parameter is the nanoparticles deposition. All previous studies concluded that the deposition was a major factor that affected the heat transfer; however no one tried to quantify the deposition effect. In the current study, MATLAB was used to calculate the deposition percentage on the heated surface and it was found that deterioration was consistently occurred when the ratio of the surface deposition was more than 90% of the heater surface.

Table 6.1 Previous Studies Comparable with current study

Investigator	Nanofluid	Heated surface	Investigated parameters	Remarks
Abdelhady (2013)	Al_2O_3–water dp = 40-50nm CuO -water dp =40-50 nm	Horizontal Copper Flat surface Ra= 20 , 80 and420 nm	Particles volume concentration 0.01% and 0.005 % Nanoparticles Stability pH=6.5 (Neutral) and pH=4.5 (Acid)	Deterioration and Enhancement
Bang and Chang [13]	Al_2O_3–water dp = 47nm	Horizontal Flat surface Ra= 37 nm	Particles volume concentration 0.5 % and 4.0 %	Deterioration
Das et al [15]	Al_2O_3–water dp = 20-50nm	cylindrical stainless steel Ra= 0.38-1.12µm	High particles weight concentration of 4-16 wt. %	Deterioration
Hassan et al [4]	Al_2O_3–water dp = 40-50nm	Horizontal Copper Flat surface Ra= 20-425 nm	Particles volume concentration 0.1 %	Deterioration
Osama et al [13]	Al_2O_3–water dp = 40-50nm	Horizontal Copper Flat surface Ra= 50-150 nm	Particles volume concentration 0.01 vol %, 0.1 vol % and 0.5 vol %.	Deterioration
Osama et al [14]	Al_2O_3–water dp = 40-50nm	Horizontal Copper Flat surface Ra= 100-150 nm	Nanoparticles Stability pH=6.5 (Neutral) and pH=5.5 (Acid)	Enhancement
Harish et al [15]	Al_2O_3–water dp < 50nm	Aluminum disk Ra=308 nm & 53 nm	Particles volume concentration 0.5%, 1% and 2%	Deterioration

In the current study, the mechanisms of enhancements in pool boiling of nanofluids are as following:

- The enhancement in the thermal conductivity due to using nanofluids
- Increasing the number of active nucleation sites
- The deposition layer non-uniformity
- The deposition ratio is less than 90%

6.1.2. Submerged Impingement Jet

An experimental study characterizing the effect of using nanofluids with a submerged impingement jet was carried out under the following conditions: nanoparticles concentration of 0.005%, heated surface roughness of 80nm, jet to surface vertical distance of 3 mm and Reynolds number of 101311.

The conclusion out of these experiments is, a deterioration in the rate of heat transfer is still observable by using nanofluids compared to pure water. However, comparing pool boiling with impingement jet showed an enhancement in the rate of heat transfer in the latter case. It is believed that, the rate of heat transfer was enhanced in the case of jet impingement due to the contribution of the forced convection with the nucleate boiling.

A very limited work was carried out using nanofluids with submerged impinging jets. Two studies were found to be relatively comparable to our study. Table 6.2 summarizes the previous studies that comparable with the current study.

As this research area still developing, we can see that both enhancement and deterioration trends by using nanofluids were reported .However, some studies reported additional enhancement when increasing the nanoparticles concentration (Qiang Li et al [30]) up to particles volume fraction of 2.8%. While Nguyen et al [29] observed deterioration in the heat transfer coefficient with increasing the nanoparticles concentration to 6% particles volume fraction.

That means that there is an agreement that an enhancement in the heat transfer coefficient is most likely to occur with low concentration, which contradict with the current study. It is believed that the main reason for this contradiction is due to the difference in the applied heat flux in each study. As in the current study the heated surface subjected to a variable heat flux, while other studies reported constant heat flux. This would affect the experiment duration and in turn affecting the rate of deposition.

Table 6.2 Previous Studies Comparable with current study

Investigator	Abdelhady(2013)	Nguyen et al [29].	Qiang Li et al [30]
Nanofluid	Al_2O_3–water dp = 40-50nm	Al_2O_3–water dp = 36 nm	CuO–water dp = 25 & 100 nm
Heated surface	Horizontal Copper Flat surface Ra= 80 nm	Horizontal Aluminum Flat surface Ra= N/A	Horizontal Aluminum Flat surface Ra= N/A
Jet Configuration	Submerged jet D_{noozle} = 3 mm L=3	Submerged jet D_{noozle} = 3 mm L=2,5 and 10	Submerged jet D_{noozle} = 2 mm L=2,4 and 6
Flow range	Mass flow rate 0.056 Kg/sec. Reynolds number 101,311.	Mass flow rate 0.002 to 0.2 Kg/sec. Reynolds number from 3,800 to 88,000.	Mass flow rate 0.0007 to 0.005 Kg /sec. Reynolds number from 2,000 to 14,000.
Investigated parameters	Concentration of 0.005 % Nanoparticles Stability pH=6.5 (Neutral)	Concentration of 2.8% and6.0 % Nanoparticles Stability pH=6.5 (Neutral)	Concentration of 1.5% ,2.0%,2.5% and3.0 % Nanoparticles Stability pH=6.5 (Neutral)
Remarks	Deterioration	Deterioration and Enhancement	Enhancement

6.2. Recommendations for Future Work

To better understand the effect of using nanofluids under pool boiling in the future, the deposition phenomenon should be investigated deeply. As surface roughness is random, it would be efficient to eliminate the ambiguity of those factors. It is recommended to use the laser texturing technique or EDM to engineer the heated surface so that it contains only defined number of nucleation sites with specific dimensions. Also, for the deposition, it is recommended to investigate the effect of the deposition layer thickness and how it varies among experiments.

For boiling under submerged jet, continued work is required to expand upon the work presented in this study to further understanding of the heat transfer characteristics of submerged jet impingement boiling. Investigating different nanoparticles materials with different nominal sizes and higher nanoparticles concentrations and compare the results with the previous studies. Investigating the effect of using different surface conditions, different nozzle diameter and different nozzle to heated surface vertical distances is also recommended.

Finally, in this study a preliminary approach to impose the contribution of both forced convection and nucleate boiling heat transfer coefficient was initiated. More experiments need to be carried out and an experimental correlation could be developed to explain which heat transfer mechanism dominating and hence an extended study would be required to investigate how to maximize the effect of the dominated heat transfer mechanism.

References

[1] I.L.Pioro, W.Rohsenow and S.S.Doerffer., "Nucleate pool boiling heat Transfer. I:Review of parametric effects of boiling surface.," *International Journal of Heat and Mass Transfer.,* vol. 47, pp. 5033-5044, 2004.

[2] X. Wang, X. Xu and S. U. S. Choi, "Thermal Conductivity of Nanoparticles-Fluid Mixture," *J. Thermophys. Heat Transfer,* vol. 13, no. 4, pp. 474-480, 1999.

[3] G. P. Narayan, K. Anoop, G. Sateesh and S. K. Das, "Effect of surface orientation on pool boiling heat transfer of nanoparticle suspensions," *International Journal of Multiphase Flow,* vol. 34, pp. 145-160, 2008.

[4] A. A. Hassan, M. S. Hamed, H. S. Baraich and A. Abdelhady, "Effect of surface condition on pool boiling of nanofluids on horizontal flat surfaces," in *ECI 8th International Conference on Boiling and Condensation Heat Transfer*, Lausanne, Switzerland, 2012.

[5] Y. H. Jeong, W. J. Chang and S. H. Chang, "Wettability of heated surfaces under pool boiling using surfactant solutions and nano-fluids," *International Journal of Heat and Mass Transfer,* vol. 51, pp. 3025–3031, 2008.

[6] O. Ahmed and M. S. Hamed, "Experimental investigation of the effect of particle deposition on pool boiling of nanofluids," *International Journal of Heat and Mass Transfer,* vol. 55, pp. 3423–3436, 2012.

[7] W. Yu and H. Xie, "A Review on Nanofluids: Preparation, StabilityMechanisms,and Applications," *Journal of Nanomaterials,* 2012.

[8] O. Ahmed and M. S. Hamed, "Experimental techniques to investigate the boiling of nanofluids," in *7th International Conference on Heat Transfer, Fluid Mechanics and Thermodynamics*, Antalya, Turkey, 2010.

[9] W. Rohsenow, "A method of correlating heat-transfer data for surface boiling of liquids," *ASME Journal of Heat Transfer,* vol. 74, pp. 969-976, 1952.

[10] P.J.Berenson, "Experiments on pool boiling heat transfer," *International Journal of Heat and Mass Transfer,* vol. 5, pp. 985-999, 1962.

[11] C. S.K. and W. R.H., "Surface effects in pool boiling," *International Journal of Heat and Mass Transfer,* vol. 28, pp. 1881 - 1889., 1985.

[12] K. Myeong-Gie, "Effect of surface roughness on pool boiling heat transfer," *International Journal of Heat and Mass Transfer,* vol. 43, pp. 4073-4085, 2000.

[13] I. C. Bang and S. H. Chang, "Boiling heat transfer performance and phenomena of Al2O3–water nano-fluids from a plain surface in a pool," *International Journal of Heat and Mass Transfer,* vol. 48, pp. 2407–2419, 2005.

[14] G. P. Narayan, K. B. Anoop and S. K. Das., "Mechanism of enhancement/deterioration of boiling heat transfer using stable nanoparticle suspensions over vertical tubes," *JOURNAL OF APPLIED PHYSICS,* vol. 102, pp. 074317-1 -074317-17, 2007.

[15] S. k. Das, N. Putra and W. Roetzel, "Pool boiling characteristics of nanofluids," *International Journal of Heat and Mass Transfer ,* vol. 46,pp. 851–862, 2003.

[16] G.Harish, V.Emlin and V.Sajith, "Effect of surface particle interactions during pool boiling of nanofluids," *International Journal of Thermal Sciences 50,* vol. 50, pp. 2318-2327, 2011.

[17] P. Vassallo, R. Kumar and S. D'Amico, "Pool boiling heat transfer experiments in silica–water nano-fluids," *International Journal of Heat and Mass Transfer,* vol. 47, pp. 407–411, 2004.

[18] D. Wen and Y. Ding, "Experimental investigation into the pool boiling heat transfer of aqueous based $_{\gamma}$-alumina nanofluids," *Journal of Nanoparticle Research,* vol. 7, pp. 265–274, 2005.

[19] D. K. Sarit, P. Nandy and R. Wilfried, "Pool boiling of nano-fluids on horizontal narrow tubes," *International Journal of Multiphase Flow,* vol. 29, pp. 1237-1247, 2003.

[20] S. M. Kwark, R. Kumar, G. Moreno, J. Yoo and S. M. You, "Pool boiling characteristics of low concentration nanofluids," *International Journal of Heat and Mass Transfer ,* vol. 53, pp. 972-981, 2010.

[21] V. P. Carey, Liquid Vapor Phase-Change Phenomena, Taylor and Francis Group, 2008.

[22] R. A. Taylor and P. E. Pahlan, "Pool boiling of nanofluids: Comprehensive review of existing and limited new data," *International Journal of Heat and Mass Transfer ,* vol. 52 , pp. 5359 –

5347, 2009.

[23] K. Sven, K. Rahmatollah, O. Lothar and P. Bjorn, "Heat Transfer Characteristics of nanofluids in two-phase boiling," in *ECI International Conference on Boiling Heat Transfer*, Florianopolis -SC- Brazil, 2009.

[24] A. Osama, *A study of the effect of experimental techniques on pool boiling of nanofluida,* Hamilton: Department of Mechanical Engineering , McMaster University, 2010.

[25] A. Suriyawong, A. S. Dalkilic and S. Wongwises, "Nucleate Pool Boiling Heat Transfer Correlation for TiO2-Water Nanofluids," *Journal of ASTM International,* vol. 9, no. 5, 2012.

[26] B. Pak, B. and Y. Cho, , "Hydrodynamic and Heat Transfer Study of Dispersed Fluids with Submicron Metallic Oxide Particles," *Exp. Heat Transfer,* vol. 11, no. 2, pp. 151-170, 1998.

[27] R. Hamilton and O. Crosser, "Thermal Conductivity of Heterogeneous Two-Component systems," *Ind. Eng. Chem. Fundam,* vol. 1, no. 3, pp. 187-191, 1962.

[28] F. Ashforth and W. Rüdel, "Thermal and Hydrodynamic Visualisation of a Water Jet Impinging on a Flat Surface using Microencapsulated Liquid Crystals," *International Journal of Fluid Dynamics,* 2003.

[29] C. T. Nguyen, N. Galanis, G. Polidori, S. Fohanno, C. V. Popa and A. L. Bechec, "An experimental study of a confined and submerged impinging jet heat transfer using Al2O3-water nanofluid," *International Journal of Thermal Sciences,* vol. 48, pp. 401-411, 2009.

[30] L. Qiang, X. Yimin and Feng Yu, "Experimental investigation of submerged single jet impingement using Cu-water nanofluid," *Applied Thermal Engineering,* vol. 36, pp. 426-433, 2012.

[31] B.W.Webb and C.F.Ma, "Single -phase liquid jet impingement heat transfer," *Advances in Heat tarnsfer,* vol. 26, pp. 105-217, 1995.

[32] H.M.Kurihara and J.E.Myers., "The effects of superheat and surface roughness on boiling coefficients," *J.AIChE 6,* vol. 1, pp. 83-86, 1960.

[33] J. BERENSON., "EXPERIMENTS ON POOL-BOILING HEAT TRANSFER," *Int. J. Heat Mass Transfer,* vol. 5, pp. 985-999, 1962.

[34] R.J.Benjamin and R. A, "Nucleate pool boiling of pure liquids at low to moderate heat flux.," *International Journal of Heat and Mass Transfer,* vol. 39, no. 12, pp. 2495-2504, 1996.

[35] S. M. You and J. H. Kim, "Effect of nanoparticles on critical heat flux of water in pool boiling heat transfer," *Applied physics letter,* vol. 83, no. 16, pp. 3374 – 3376, 2003.

Appendix A
Experiments Repeatability

Few experiments were repeated to examine the repeatability of the experimental setup. Both pure water and nanofluids experiments were repeated. The repeatability was checked for pool boiling experiments.

Results of the pool boiling of pure water and nanofluids experiments on the Ra= 80 nm surface are shown in figure A.1 and figure A.2 respectively. The boiling curves lie within the experimental error bars and hence a trustable repeatability is confirmed for both pure water and nanofluids experiments.

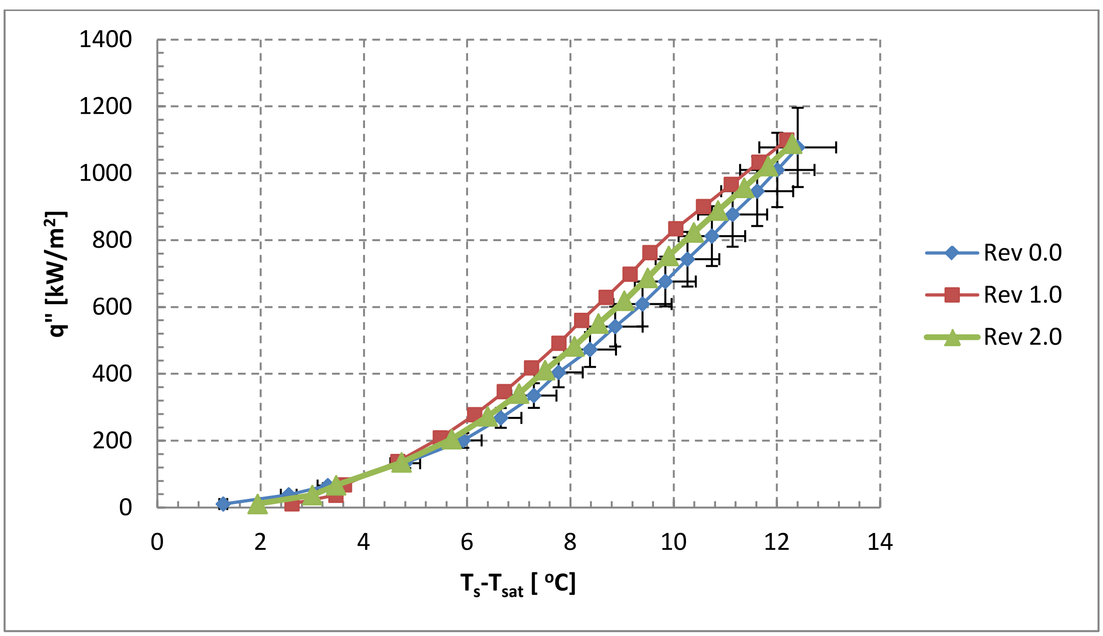

Figure A.1 Repeatability of water pool boiling experiments

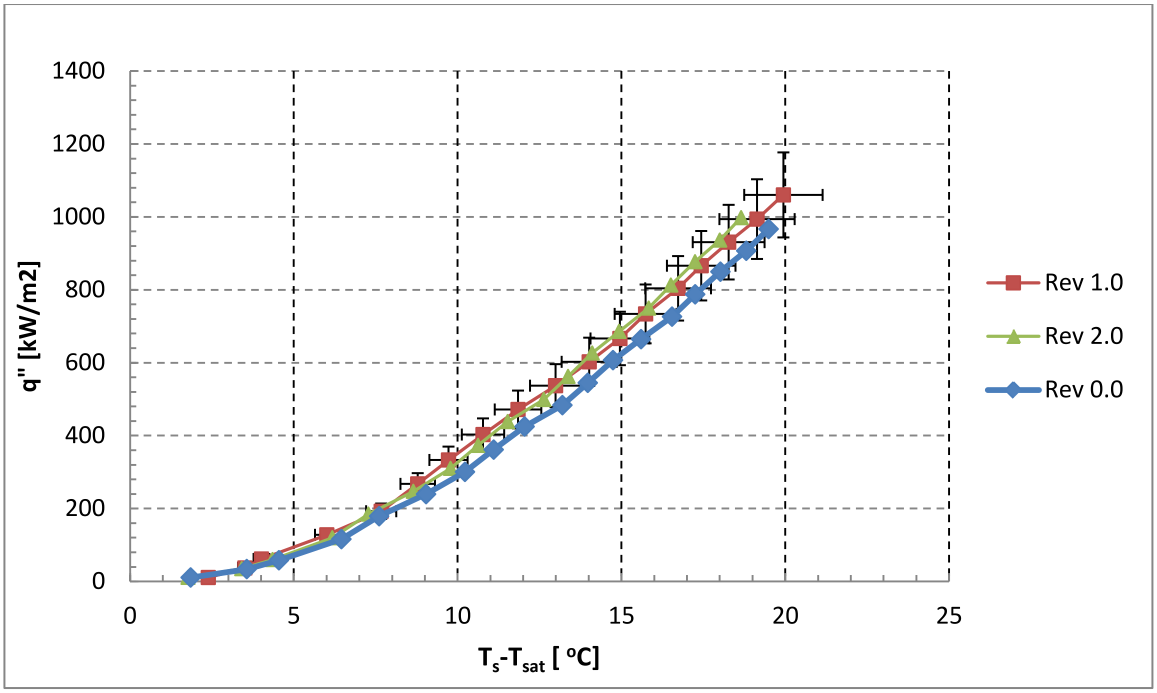

FigureA.2 Repeatability of 0.005 %Al_2O_3 pool boiling